AD

USAAVLABS TECHNICAL REPORT 68-10

PRELIMINARY EVALUATION OF GAS TURBINE REGENERATORS EMPLOYING HEAT PIPES

By

Calvin C. Silverstein

April 1968

U. S. ARMY AVIATION MATERIEL LABORATORIES
FORT EUSTIS, VIRGINIA

CONTRACT DAAJ02-67-C-0053
CALVIN C. SILVERSTEIN
ENGINEERING CONSULTANT
BALTIMORE, MARYLAND

Disclaimers

The findings in this report are not to be construed as an official Department of the Army position unless so designated by other authorized documents.

When Government drawings, specifications, or other data are used for any purpose other than in connection with a definitely related Government procurement operation, the United States Government thereby incurs no responsibility nor any obligation whatsoever; and the fact that the Government may have formulated, furnished, or in any way supplied the said drawings, specifications, or other data is not to be regarded by implication or otherwise as in any manner licensing the holder or any other person or corporation, or conveying any rights or permission, to manufacture, use, or sell any patented invention that may in any way be related thereto.

Disposition Instructions

Destroy this report when no longer needed. Do not return it to the originator.

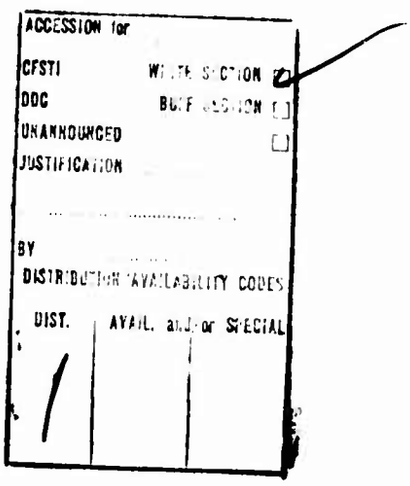

DEPARTMENT OF THE ARMY
U. S. ARMY AVIATION MATERIEL LABORATORIES
FORT EUSTIS, VIRGINIA 23604

The object of this contractual effort was to conduct a design study and analysis of an advanced gas turbine heat exchanger based on the heat pipe principle. The analysis included comparison of the heat pipe concept with a state-of-the-art regenerator concept.

The results indicate that cost and weight of the heat pipe design are significantly higher than those of conventional regenerators. However, it is recognized that the concept is technically feasible and that economic considerations are subject to developmental improvements.

The conclusions and recommendations contained herein are concurred in. Results will be used to establish the potential of heat pipe heat exchangers for future propulsion systems and to determine developmental efforts required.

Task 1G121401D14413
Contract DAAJ02-67-C-0053
USAAVLABS Technical Report 68-10
April 1968

PRELIMINARY EVALUATION OF GAS TURBINE REGENERATORS EMPLOYING HEAT PIPES

Final Report

By

Calvin C. Silverstein
Engineering Consultant
Baltimore, Maryland

for

U.S. ARMY AVIATION MATERIEL LABORATORIES
FORT EUSTIS, VIRGINIA

SUMMARY

A preliminary investigation of gas turbine regenerators employing heat pipes as the active heat transport elements has been carried out. The study was performed in order to evaluate heat pipe regenerators with respect to other regenerator types and to the requirements of U.S. Army advanced gas turbine powerplants for aircraft application.

Included in the study were: a review of current heat pipe technology, a design study of heat pipe regenerator characteristics, and an evaluation of heat pipe regenerator feasibility.

The regenerator core best suited for Army requirements appears to be a radial-heat-pipe, two-zone core operating at 60 percent effectiveness. A core with a mass flow rate of 5 lb/sec would utilize 1/4-inch-diameter cesium-titanium heat pipes in regions of the core below 1000°F and 1/8-inch-diameter cesium-Hastelloy X heat pipes in the core zone with temperatures greater than 1000°F. The core would have an overall diameter of 27 to 31.4 inches, a length (in the flow direction) of 5.6 to 7.0 inches, and a total heat pipe weight of 65 pounds.

Primary advantages of the radial heat pipe regenerator are ready integrability with the gas turbine and reduced exhaust gas duct losses. Weight is comparable to or in excess of that for other core types. Development and fabrication costs are likely to be high.

TABLE OF CONTENTS

TABLE OF CONTENTS (Continued)

LIST OF ILLUSTRATIONS

LIST OF ILLUSTRATIONS (Continued)

LIST OF ILLUSTRATIONS (Continued)

LIST OF TABLES

LIST OF SYMBOLS

DIMENSIONAL VARIABLES

A	core heat transfer surface area, ft^2
A_c	core free-flow area, ft^2
A_f	core frontal area, ft^2
C	specific heat at constant pressure, Btu/lb-°F
d	outer heat pipe diameter, in.
E	elastic modulus, psi
g	acceleration due to gravity, 32.2 ft/sec^2
G	flow rate per unit area, $lb/sec\text{-}ft^2$
h	heat transfer coefficient, $Btu/hr\text{-}ft^2\text{-}°F$
H	core module height, in.
k	thermal conductivity, Btu/hr-ft-°F
K	reciprocal of permeability, ft^{-2}
L	length, in.
N_s	specific number of heat pipes, heat pipes/lb/sec
P	pressure, psi
ΔP	pressure drop, psi
Q	heat transport rate through heat pipe, Btu/hr
r	outer heat pipe radius, in.; radius of curvature, microns
$\bar{r}$	mean radius of heat pipe wall, in.
r_h	hydraulic radius, in.

LIST OF SYMBOLS (Continued)

DIMENSIONAL VARIABLES

r_p	mean radius of capillary wick pores in axial direction, microns
r_{pn}	mean radius of capillary wick pores in radial direction, microns
r_v	inner radius of capillary wick, in.
r_w	outer radius of capillary wick, in.
R	gas constant, (lb-ft)/(lb-°R)
t	heat pipe wall thickness, mils
t_w	capillary wick thickness, mils
T	temperature, °F
U	overall thermal conductance, Btu/hr-ft^2-°F
$\bar{V}$	mean specific volume, ft^3/lb
V	core volume, ft^3
W	flow rate, lb/sec
W_c	core weight, lb
β	fluid parameter, (Btu-hr)$^{1/2}$/ft^2 = 12 $(P_v \kappa / \nu_v)^{1/2}$
κ	heat of vaporization of heat pipe liquid, Btu/lb
μ	absolute viscosity, lb/hr-ft
ν	kinematic viscosity, ft^2/hr
ρ	density, lb/ft^3
σ	surface tension of heat pipe liquid, lb/ft
σ_c	compressive stress, psi

LIST OF SYMBOLS (Continued)

DIMENSIONAL VARIABLES

Ω	heat pipe weight per unit surface area, lb/ft^2

DIMENSIONLESS VARIABLES

b	tortuosity of capillary wick
C_h	coefficient for evaluating heat transfer coefficient
C_f	coefficient for evaluating friction factor
f	friction factor
n	vertical acceleration, number of g's
NTU	number of heat transfer units, $(UA_s)/(3600C)$
p	r_{pn}/r_{pu}
q	r_p/r_{pu}
X_ℓ	longitudinal heat pipe spacing parallel to flow direction, number of diameters
X_t	transverse heat pipe spacing normal to flow direction, number of diameters
α	acceleration parameter, $(1 + n)\rho_\ell\, r_{pn} L_p \sin\theta/(2\sigma)$
ϵ	regenerator effectiveness
ω	Poisson's ratio
ϕ	porosity of capillary wick, void volume/total volume
θ	angle between heat pipe axis and horizontal, with condenser end at apex of angle, deg

LIST OF SYMBOLS (Continued)

SUBSCRIPTS

a	air
b	buckling
c	condenser section of heat pipe
e	evaporator section of heat pipe
g	gas
h	static pressure head
i	inner or inlet; also, maximum value for isothermal heat pipe operation
ℓ	heat pipe liquid
m	maximum
min	minimum
o	optimum or maximum value for uniform pore, horizontal heat pipe with $L_e/L_c >> 1$ and optimum wick thickness; also, outer or outlet
p	heat pipe
s	specific value of variable (variable per unit mass flow rate in lb/sec); also, denotes solid
t	heat pipe wall
u	optimum or maximum value for uniform pore, horizontal heat pipe with $L_e/L_c >> 1$ and arbitrary wick thickness
v	heat pipe vapor
w	heat pipe wick

INTRODUCTION

The heat pipe is a hollow closed tube which, by virtue of its internal construction, has the capability of transferring heat isothermally at significant rates over a significant distance. Since development of the heat pipe concept at Los Alamos Scientific Laboratory in 1964, industrial and government organizations have been exploring applications for this unique device.[1-12]

The gas turbine regenerator appears to be one application where the isothermal property of heat pipes may play a useful role. In the usual primary surface or extended surface regenerator, the compressed air and exhaust gas streams flow through a large number of very small flow passages in intimate proximity to each other. Since the air and gas streams are completely separated before entering and after leaving the regenerator, the necessity to bring them into close proximity in the regenerator introduces relatively complex header and ducting problems and/or may prevent use of the optimum counterflow arrangement.

With the advent of heat pipes, the need for large numbers of small air and gas flow passages is eliminated. Only a few relatively large flow ducts may be needed (in some instances a single duct may be sufficient for each flow stream). The small flow passages necessary for compactness and low weight are provided by adding large numbers of closely spaced, small-diameter heat pipes to the flow ducts. These heat pipes are oriented normal to the air and gas flow directions and completely span the width of the ducts. Heat then flows from the hot gas to the heat pipes, axially along the heat pipes which penetrate the wall separating the gas and air flow ducts, and finally from the heat pipes into the cooler, compressed air.

A preliminary investigation of gas turbine heat pipe regenerators has been carried out for operating conditions characteristic of U.S. Army advanced gas turbine powerplants for aircraft application. The study consisted of three phases:

1. Review of Heat Pipe Technology
2. Regenerator Design Study
3. Feasibility Evaluation

Results of the investigation follow. Calculational methods used are presented in detail in the appendixes.

REVIEW OF HEAT PIPE TECHNOLOGY

The relatively new technology of heat pipes has been reviewed in order to obtain a current picture of those aspects which are relevant to the use of heat pipes in gas turbine regenerators. The review was accomplished through examination of existing literature on the subject and contact with organizations known to have active heat pipe development programs.

PRINCIPLE OF OPERATION

A typical heat pipe cross section is shown in Figure 1. The inner surface of the heat pipe wall is lined with an annular layer of a porous material, which will be referred to as a capillary wick. The capillary wick is saturated with an appropriate heat transport liquid, whose vapor completely fills the remaining internal volume.

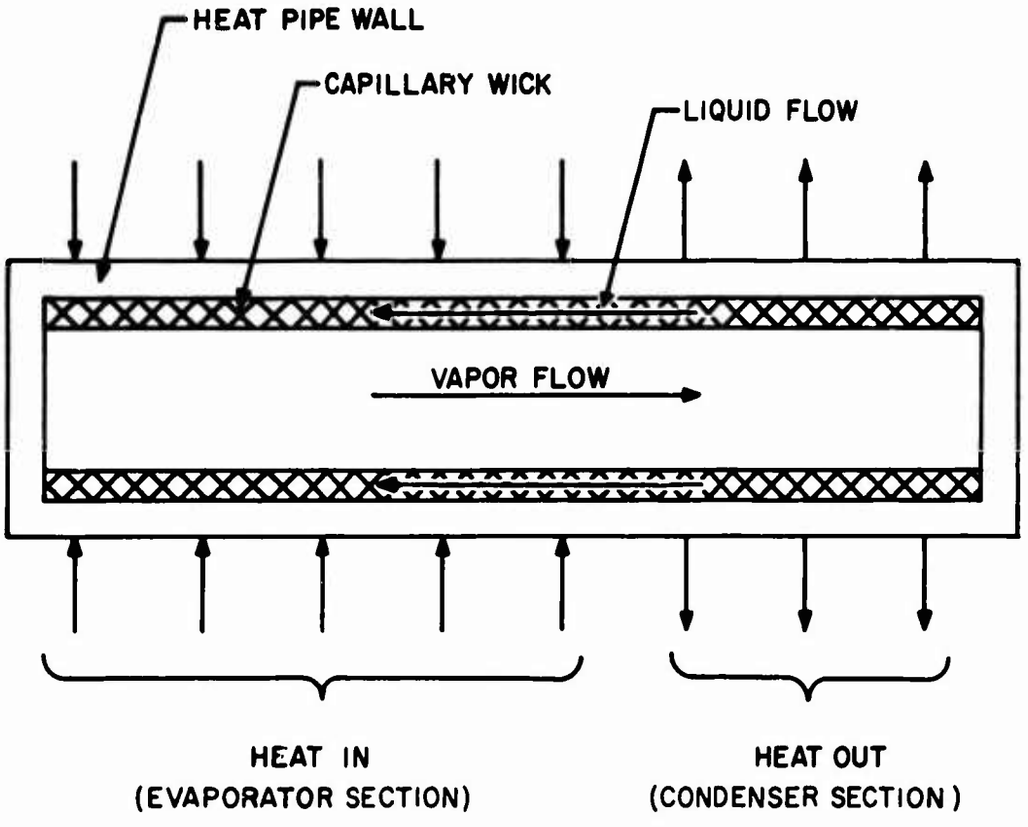

Figure 1. Heat Pipe Cross Section.

During operation, heat added through the outer surface of one section of the heat pipe evaporates liquid in the adjacent capillary wick. The vapor produced then flows down the pipe to the section where heat is being removed from the outer surface, and condenses on the capillary wick. The condensate flows through the capillary wick to the evaporator section, where the liquid once again evaporates.

Thus, heat is transported from one section of the heat pipe to another via a self-actuated process of internal convection. The convective cycle is maintained by liquid and vapor pressure heads which arise in a manner to be explained shortly. If the vapor pressure drop is small compared to the vapor pressure, then the temperature difference between the evaporator and condenser sections will be very small and for practical purposes the heat pipe may be considered isothermal.

HEAT TRANSPORT CAPACITY

The major question of interest concerning heat pipes is the heat transport capacity for isothermal operation. A theory has been developed from which the heat transport capacity may be predicted.[2] The physical basis for this theory is presented below.

In Figure 2, one-half of a horizontal heat pipe cross section is shown, along with the vapor and liquid pressure distribution along the pipe. The inner surface of the capillary wick is shown schematically as a perforated sheet with holes of radius r_{pn}. Initially, the heat pipe is assumed to be at its intended operating temperature and perfectly insulated. In this condition the contained liquid is assumed to fill the capillary wick completely, its inner surface parallel to and coinciding with the inner surface of the wick. The pressure of the liquid is then equal to the pressure P_v of its vapor, which fills the remainder of the heat pipe interior.

Now the insulation around the lateral surface is removed, and heat is added uniformly over the evaporator section and is removed uniformly at the same rate over the condenser section, the nominal temperature remaining unchanged. The addition of heat produces evaporation of some liquid into the vapor space, raising the pressure of the vapor in the evaporator section and causing the unevaporated liquid to withdraw into the pores of the capillary wick. The removal of heat produces condensation of some vapor, lowering the pressure of the vapor in the condenser section and causing an accumulation of liquid in the capillary pores.

A pressure difference now exists in the vapor, tending to drive it from the evaporator to the condenser section. At the same time, the curvature introduced to the liquid vapor interface at the pore openings, as the result of liquid loss in the evaporator and accumulation in the condenser, produces a pressure difference in the liquid, tending to drive it from the condenser section to the evaporator section. The pressure difference arises because the pressure on the convex side of a curved

liquid-vapor interface with radius of curvature r and surface tension σ must exceed the pressure on the concave side by $2\sigma/r$ (Reference 2).

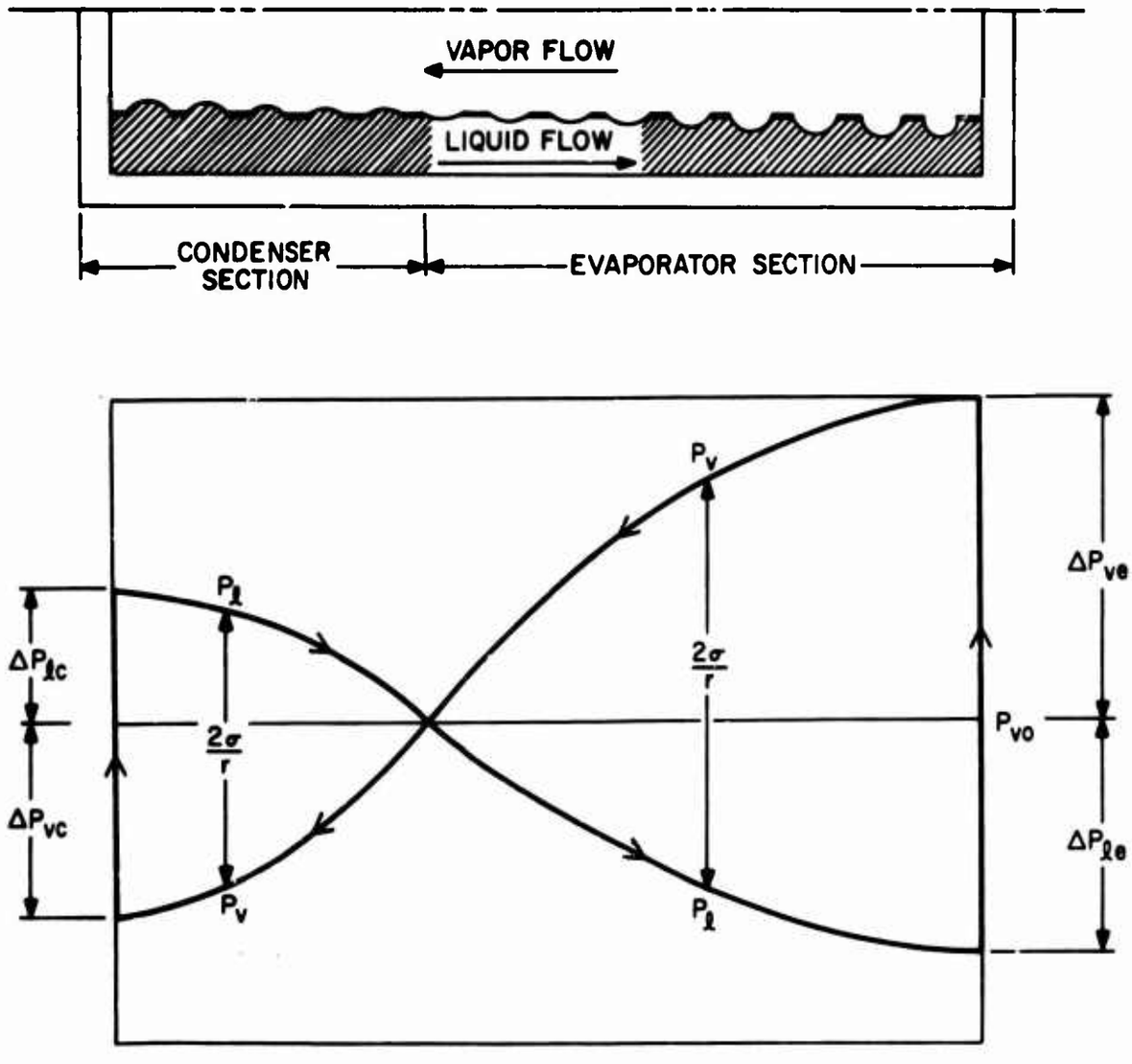

Figure 2. Vapor and Liquid Pressure Distribution in Heat Pipe.

Thus, in the evaporator section the pressure P_ℓ of the liquid (concave side) is less than the vapor pressure P_V by $2\sigma/r$. Similarly, in the condenser section the pressure P_ℓ of the liquid (now the convex side of the liquid-vapor interface) exceeds the vapor pressure P_V by $2\sigma/r$. (In most heat pipe analyses, the radius of curvature in the condenser section is always assumed to be infinite.)

The pressure distribution in the heat pipe is then as shown in Figure 2. The arrows on the curves denote the pressure changes seen by an observer traveling down the heat pipe with the vapor and then in the opposite direction with the liquid. From Figure 2 it can be seen that

$$\frac{2\sigma}{r_e} = \Delta P_{ve} + \Delta P_{\ell e}$$

and

$$\frac{2\sigma}{r_c} = \Delta P_{vc} + \Delta P_{\ell c}$$

where the subscripts e and c denote conditions at the evaporator and condenser ends. The above pressure drops can be expressed in terms of the heat transport rate. The heat transport rate is a maximum when either r_e or r_c takes on its minimum possible value. For a liquid which fully wets the wick material, the minimum value of the radius of curvature is just the radius r_{pn} of the wick pores at the liquid-vapor interface. Explicit equations for the heat transport capacity are presented in Appendix I.

In the above treatment there is no indication whether the heat pipe will be isothermal when the heat transport capacity is reached. Since the vapor inside the heat pipe is a saturated vapor, its temperature is determined by the vapor pressure. The drop in vapor pressure must then be restricted to a value which will insure a negligible temperature variation along the heat pipe length. If the vapor pressure drop when heat is being transported at the capacity rate is too large for isothermal operation, the heat transport rate will have to be reduced.

Other possible limitations on the heat transfer rate may arise from sonic velocity and boiling considerations. The maximum vapor velocity should always be less than sonic velocity in the vapor to avoid flow choking. The temperature of the liquid at the outer wick surface should not exceed the temperature at the inner wick surface by more than the minimum superheat needed to initiate boiling, in order to avoid possible buildup of vapor within the wick to the point where the flow of heat and liquid across the wick to the liquid-vapor interface would be inhibited.

The heat transport capacity is affected by orientation of the heat pipe and external acceleration. The capacity will increase over that for the horizontal position if the evaporator section is lower than the condenser section, or if external acceleration is applied opposite to the direction of liquid flow. A decrease in capacity will occur if the condenser section is lower than the evaporator section, or if external acceleration is applied in the direction of liquid flow. The influence of orientation and external acceleration can be minimized by the use of very small pores at the inner wick surface.

In the event that the heat transport capacity is exceeded, the heat pipe will undergo burnout, floodout, or both. Burnout occurs at the beginning of the evaporator section, when the heat input is such that liquid leaves the wick pores faster than it can be replenished. The result is complete loss of fluid from a portion of the wick, effectively shortening the heat pipe length. Very little heat will then be removed from the dried-out section, and its temperature will tend to approach that of the heat source.

Floodout occurs at the end of the condenser section, when the heat input is such that condensed liquid accumulates in the wick pores faster than it can flow away. The result is flooding at the condenser end of the heat pipe, effectively shortening its length. The temperature of the flooded section will drop, tending to approach that of the heat sink.

Neither burnout nor floodout is necessarily catastrophic, as the heat pipe may continue to function with its shorter effective length, although it would probably function at a higher temperature. However, failure of the heat pipe could result if the temperature of the burned-out section becomes excessive.

MATERIALS

Heat pipes have been fabricated with a wide variety of heat transport fluids and wick and container materials. The prime determining factor in the selection of the heat pipe fluid is the desired operating temperature. Selection of the wick and container material follows from considerations of compatibility with the heat pipe fluid and the external heat pipe environment.

In the temperature range of interest for the gas turbine regenerator (650° to 1350°F), the liquid metals sodium, potassium, cesium, and mercury appear to be the most appropriate heat pipe fluids. Sodium, potassium, and cesium are known to be compatible with stainless steel, Hastelloy X, and other nickel alloys, and they are also believed to be compatible with titanium. Mercury appears to be most compatible with ferritic-type stainless steels. The alloy CROLOY 9M may possibly be suitable at temperatures of 1000°F or less.*

Wettability of the heat pipe fluid is also an important consideration, since adequate functioning of heat pipes is dependent on the ability of the fluid to wet the wick. Wettability does not appear to be a problem with the alkali metals, but it can be a problem with mercury. It appears that almost all metals are partially wetted by

---

* Personal communication with J. DeVan, Oak Ridge National Laboratory, Oak Ridge, Tennessee.

mercury in the 750° to 1000°F range, extreme cleanliness being a requirement. Wetting is promoted by the use of small quantities of materials such as sodium, potassium, rubidium, manganese, and titanium hydride.*

The demonstrated life of a number of heat pipe fluid-container combinations is shown in Table I. (These heat pipes were presumably tested in air.)

TABLE I. DEMONSTRATED LIFE OF HEAT PIPES

Fluid	Container and Wick	Demonstrated Life
Cesium	Titanium	2000 hr @ 750°F*
Potassium	Stainless	6500 hr @ 930°F*
Potassium	Nickel	8000 hr**
Sodium	Stainless	1500 hr @ 1380°F*
Sodium	Stainless	6600 hr**
Mercury	Stainless (container)	2000 hr**

* Personal communication with Dr. J.E. Deverall, Los Alamos Scientific Laboratory, Los Alamos, New Mexico.

** Personal communication with G.Y. Eastman, Radio Corporation of America, Lancaster, Pennsylvania.

Table I suggests that, from the standpoint of internal corrosion, liquid-metal heat pipes can readily meet the regenerator design goal of 1000 hours between overhaul, and most probably can meet the design goal of 5000 hours total life (see Table II). The container materials would, of course, have to withstand the exhaust gas environment in a regenerator.

CAPILLARY WICKS

The capillary wick has a strong influence on heat transport capacity. Pores should be large in the direction parallel to the heat pipe axis to reduce the pressure drop

---

* Personal communication with A.E. Miller, Liquid Metal Engineering Center, Canoga Park, California.

in the returning liquid condensate. At the same time, the pores in the radial direction should be small in order to produce a large pressure difference across the liquid-vapor interface at the inner wick surface. Such a nonisotropic pore distribution can result in increased heat transport capacity compared to that obtainable with a wick whose pore size is independent of direction. Small pore size in the radial direction also reduces the sensitivity of heat transport capacity to changes in heat pipe orientation and acceleration.

For maximum heat transport capacity in a horizontal heat pipe with a uniform wick (pore size independent of direction), the wick should occupy one-third of the internal cross-sectional area.[2] Appreciable weight savings can be realized, at the expense of heat transport capacity, by the use of thinner wicks.

Wicks have been fabricated from woven-mesh screen, sintered metal powder, and sintered metal fibers, and from slotted grooves cut into the inner heat pipe surface. Slotted metal sheet wicks have also been considered. These wick types are illustrated in Figure 3. The slotted metal sheet wick readily provides the desired nonisotropic pore distribution. For the other wick types, the nonisotropic pore distribution can be approximated by the use of two wick layers, one of which has relatively fine pores while the other has relatively coarse pores.

An extensive investigation of woven-mesh, sintered powder, and sintered fiber wicks has been carried out.[8-10] The wicks were fabricated of nickel and stainless steel. It was concluded that the sintered fiber wicks were preferable because of low resistance to flow, high porosity, and easy fabricability. The mean pore radius in the sintered fiber wicks lay in the 13- to 22-micron range.

A porous stainless filter material with pore radii in the 0.25- to 2.5-micron range is expected to be available in early 1968.* This material, which should be available in thicknesses of 15 mils or less, may prove to be useful for the slotted sheet configuration of Figure 3 or as a thin layer over the inner surface of a thicker wick with coarser pores.

FABRICATION

Fabrication of a heat pipe involves insertion of an annular wick into a tube, bonding or mechanically securing the wick to the inner tube surface, evacuation and heating of the tube and wick, introduction of the heat pipe fluid, and sealing of the tube ends. This process, as currently practiced in developmental laboratories, is

---

* Personal communication with W.A. Preston, Advanced Structures Division, Fansteel Metallurgical Corporation, Harbor City, California.

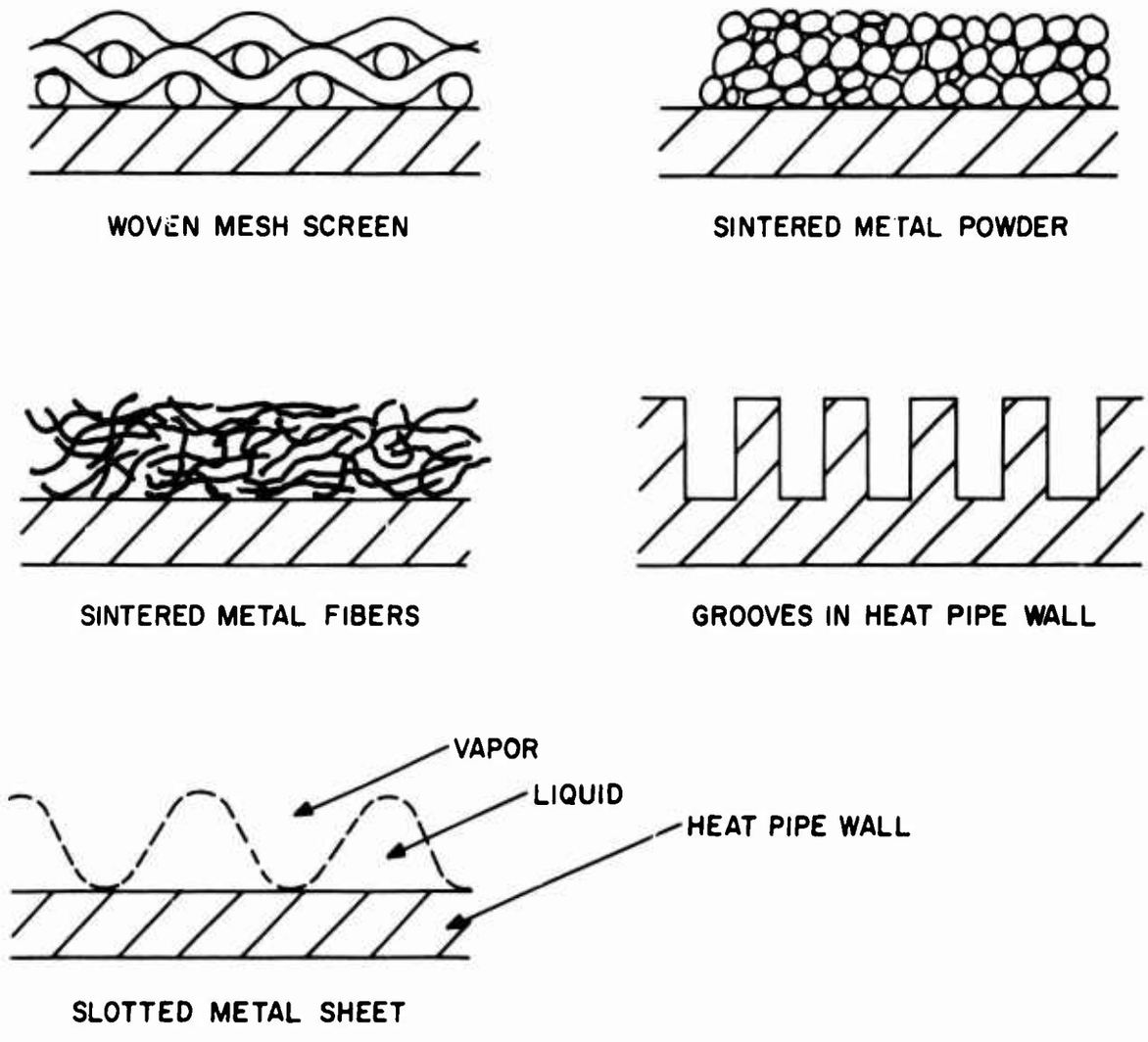

Figure 3. Heat Pipe Capillary Wick Configurations.

time-consuming and costly. [5] However, the fabrication process bears many similarities to that utilized in the manufacture of electron tubes, in which a tube is evacuated and heated, the internal structure is inserted, an inert gas is added, and the tube is sealed. Should the need arise, mass production of heat pipes can

probably be accomplished with the aid of manufacturing techniques employed by the electron tube industry.*

Heat pipes have been fabricated with diameters in the range of 0.25 to 1 inch and with lengths ranging from 3-1/2 inches to 10 feet.

TRANSIENT RESPONSE

Transient response of heat pipes has apparently not been studied either analytically or experimentally as yet. Response is expected to be largely a function of thermal capacity (weight times specific heat). Semiquantitative observations suggest fairly rapid response to thermal transients. For example, a tantalum heat pipe (with lead as the heat transport fluid) about 3/4 inch in diameter and 2 feet long can be inductively heated to a uniform temperature of 2370° F from room temperature in less than a minute.**

OPERATIONAL PROBLEMS

A number of operational problems have occurred or may be anticipated during heat pipe operation.

Startup

Occasionally, isothermal operation of a heat pipe at its design temperature has been difficult or impossible to achieve following startup from room temperature at high heat input rates.[5] The problem has been attributed to interference with the return flow of liquid from the condenser section by high-velocity vapor traveling to the condenser section. The liquid cannot then return to the evaporator section at the rate at which liquid is being evaporated, and burnout occurs. The vapor velocity is very high during a startup for which the heat input rate is comparable to that of steady-state operation. This occurs because the vapor density is quite small at startup temperatures, while the mass flow rate is comparable to the steady-state value.

Two techniques for overcoming this problem have been suggested.*** One involves the use of fine screening at the inner surface of the wick to minimize the drag of

---

* Personal communication with G.Y. Eastman, Radio Corporation of America, Lancaster, Pennsylvania.

** Personal observation at Los Alamos Scientific Laboratory, Los Alamos, New Mexico.

*** Personal communication with J.E. Kemme, Los Alamos Scientific Laboratory, Los Alamos, New Mexico.

high-velocity vapor on the exposed surface of the returning liquid. (The startup problem has been particularly noticeable for the grooved wick of Figure 3.) The other introduces a noncondensible gas such as helium to the heat pipe vapor space. The gas density is high enough at startup temperatures to inhibit excessive flow velocity in the vapor space, but low enough that at the design temperature the gas will occupy a very small fraction of the vapor space.

Noncondensibles

The presence of noncondensible vapors or gases in a heat pipe has a deleterious effect on performance. The gases are swept to the condenser section, where they form a separate zone which the vapor of the heat pipe fluid does not penetrate. The heat pipe length is then effectively reduced by the length of the noncondensible zone.[2]

The presence of noncondensibles can be minimized by effective outgassing of the heat pipe interior during fabrication. However, noncondensibles can be produced by chemical reaction of the heat pipe fluid with the heat pipe material. For example, it has been found that hydrogen accumulates in the condensing end of water-aluminum heat pipes.*

A possible problem with stainless steel heat pipes operating in a combustion gas environment, as would be the case in a regenerator, could be the permeation of hydrogen into the heat pipes and subsequent formation of a noncondensible zone. Hydrogen readily penetrates metals such as stainless steel. If the length of the noncondensible zone were to become appreciable during the regenerator lifetime, regenerator performance would be degraded. Heat pipes have been successfully operated in natural gas and propane flames at a flame temperature of 2000° F, but in these instances the heat pipe outer surface was protected with a coating of aluminum oxide to prevent corrosion and possible diffusion of free hydrogen into the heat pipe interior.

Vibration and Acceleration

A heat pipe has been operated under vibration and acceleration conditions characteristic of a missile launch. Operation was unaffected by vibration, but it was limited by acceleration in a direction which opposed the return flow of condensate to the evaporator section of the heat pipe.** While the vibration and acceleration environment during the launching of a missile differs from that of an operating aircraft gas turbine, these results provide some indication of heat pipe response to vibration and acceleration. Since sensitivity to acceleration is a function of heat pipe length and wick pore radius at the liquid-vapor interface, it is controllable through design.

---

* Personal communication with G.Y. Eastman, Radio Corporation of America, Lancaster, Pennsylvania.

** Personal communication with G. Whiting, Sandia Corporation, Albuquerque, New Mexico.

DESIGN STUDY

A design study of gas turbine regenerator cores using heat pipes as the active heat transfer elements has been carried out. The design criteria are listed in Table II.

TABLE II. DESIGN CRITERIA FOR HEAT PIPE REGENERATOR STUDY

Regenerator effectiveness	50-70%
Air-plus-gas side core pressure drop	6%
Flow rate	5-15 lb/sec
Turbine exhaust gas temperature	1350 °F
Turbine exhaust gas pressure	15.5 psia
Compressor discharge air temperature	650 °F
Compressor discharge air pressure	147 psia
Gas temperature transients	to 1800 °F
Regenerator life	5000 hr
Time before overhaul	1000 hr

Results of the study are presented below. The basic heat pipe regenerator concept is described first. Then considerations involved in the design of heat pipes for regenerator cores are discussed. Finally, the characteristics of heat pipe regenerator cores are presented.

HEAT PIPE REGENERATOR CONCEPT

The basic heat pipe regenerator core consists of an array of heat pipes which completely spans adjacent flow ducts through which air and gas move past each other in a counterflow arrangement. The heat pipe array, stacked in either a staggered or an in-line arrangement, is oriented with the heat pipe axes normal to the air and gas flow directions. All the heat pipes at a given point along the core length are isothermal, the heat pipe temperature being intermediate between the air and gas temperatures at that point. The temperature of individual heat pipes varies from a minimum at the air inlet end of the core to a maximum at the air outlet end.

Because the air and gas flow over banks of closely spaced heat pipes, the effective hydraulic diameter can be quite small even though the flow duct dimensions are relatively large. Large core flow duct dimensions simplify and minimize regenerator header and external ducting requirements.

The basic core module is shown in Figure 4. The module width is equal to the heat pipe length L_p; the flow length is L and the height is H. The module is separated by a wall into an air passage of width L_a and a gas passage of width L_g. The heat pipes, of diameter d, are shown arranged in a staggered pattern with transverse spacing $X_t d$ and longitudinal spacing $X_\ell d$. (The heat pipes can also be stacked in an in-line arrangement.)

Core modules can be stacked end-on, side-on, or in combination to build up a core of any desired size and shape. A four-module core is shown in Figure 5. In the stacking process, the flow length L, having been established from pressure-drop considerations, remains constant. The frontal area increases in proportion to total flow rate requirements.

The heat pipe regenerator core is also adaptable to arrangement in a cylindrical configuration. Four possibilities are shown in Figure 6. On the left, the heat pipes are oriented radially while the flow is in the axial direction. On the right, the heat pipes are oriented axially while the flow is in the radial direction. In the central figure, the heat pipes are arranged circumferentially. In the upper half of the figure, flow is in the radial direction; in the lower half, flow is in the axial direction. Selection of a particular configuration will depend largely on the size and shape of the gas turbine to which the regenerator is to be mated.

The characteristics of cores with rectangular geometries have been investigated analytically. Results should be roughly applicable to the cylindrical configurations of Figure 6.

HEAT PIPE DESIGN CONSIDERATIONS

The heat pipes which comprise a gas turbine regenerator core should be designed in accordance with the following objectives:

- Long length
- Low weight per unit surface area
- Low sensitivity to orientation and acceleration

Long length is desirable to minimize the number of flow ducts, thus simplifying the headers and external ducting and reducing their weight. In addition, the number of heat pipes to be fabricated is reduced. Low weight per unit surface area reduces total core weight. Low sensitivity to orientation and acceleration is important, since these parameters may vary substantially during flight. Also, it may be impractical to orient all heat pipes in the same direction (see Figure 6).

Heat pipe design variables include: the heat pipe fluid, wick characteristics, heat pipe diameter, wall thickness, and heat pipe and wick material. The influence of these variables on design objectives will now be examined. The influence of orientation and acceleration on heat pipe design is also considered.

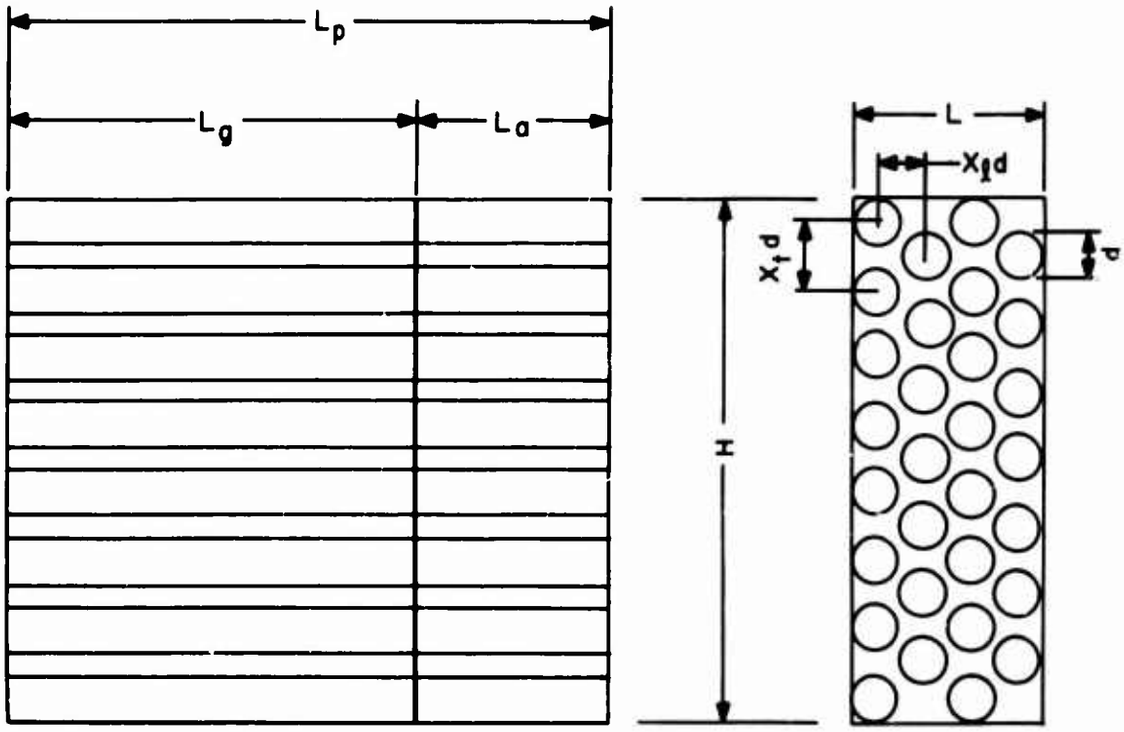

Figure 4. Basic Module for Heat Pipe Regenerator Core.

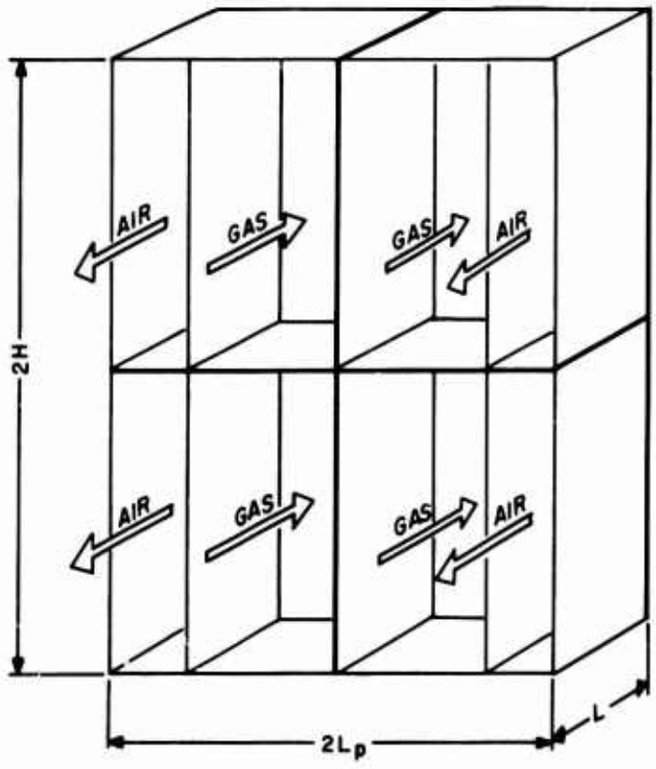

Figure 5. Four-Module Heat Pipe Core.

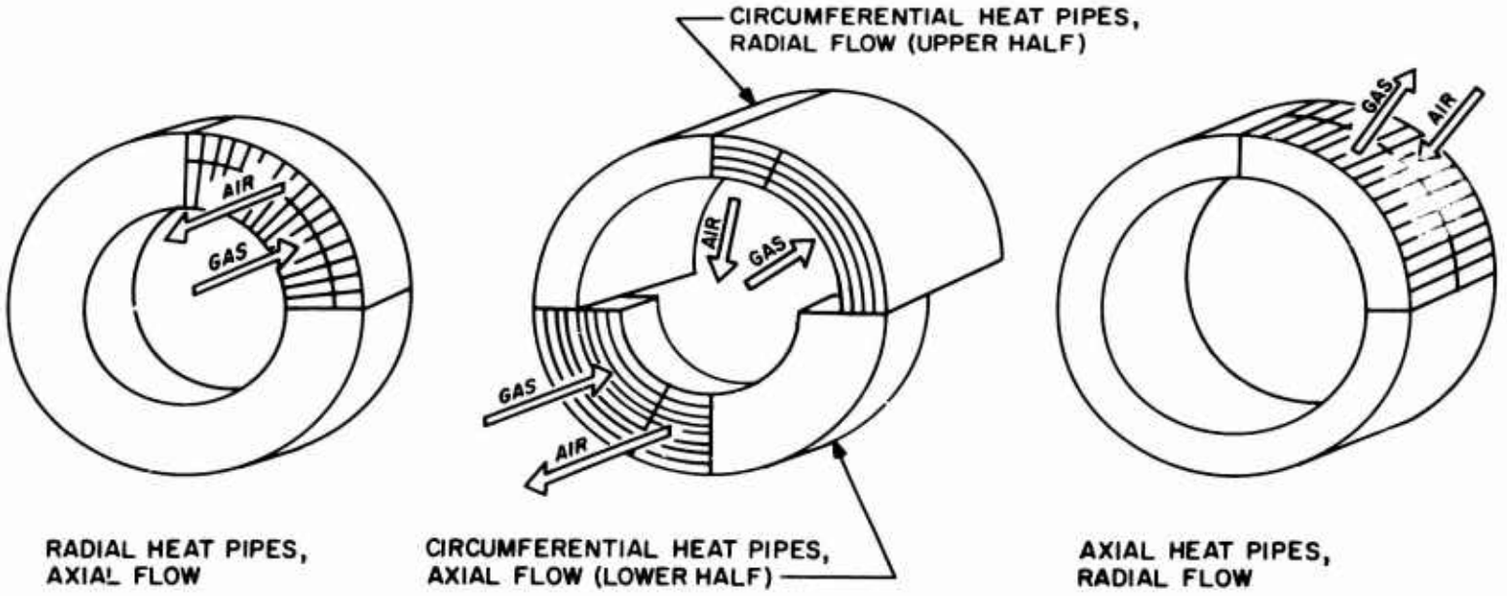

Figure 6. Heat Pipe Regenerator Cores - Cylindrical Configuration.

Heat Pipe Fluid

In Appendix II, an expression for the maximum heat pipe length L_p for isothermal operation is developed. For any given geometry, L_p is shown to be proportional to a parameter β which depends on fluid properties only. The fluid parameter β is equal to 12 $(\kappa P_v/\nu_v)^{1/2}$, where P_v is the vapor pressure (psi), κ is the heat of vaporization (Btu/lb), and ν_v is the kinematic viscosity of the vapor (ft^2/hr). The units of β are $(Btu\text{-}hr)^{1/2}/ft^2$.

In Figure 7, β is shown as a function of temperature for several potential heat pipe fluids (solid lines). Fluid property data on which these curves are based are given in Appendix III. These fluids were selected for consideration because they have vapor pressures of 0.1 psi or greater at the minimum heat pipe temperatures in the regenerator core (750° to 800°F). For vapor pressures below 0.1 psi, β is too small to yield heat pipe lengths of interest for heat pipe regenerators.

From Figure 7, we see that the length of a cesium heat pipe is about twice as great as that of a potassium heat pipe and about an order of magnitude greater than the length of a sodium heat pipe. A sulphur heat pipe can be 6 times longer than a cesium heat pipe, while a mercury heat pipe may be 40 times longer. On the basis of the fluid parameter β, the list of potential heat pipe fluids was reduced to three: cesium, sulphur, and mercury.

If the heat pipe length is to equal the maximum length for isothermal operation, the heat transport capacity should be equal to the maximum isothermal heat transfer rate. The desired heat transport capacity is achieved, for a given axial pore radius r_p, by selection of a radial pore radius r_{pn} for which the pressure difference across the liquid-vapor interface is sufficiently large. The radial pore radius should not be smaller than the lower limit for wick fabricability (estimated to be about 0.5 micron).

Unfortunately, the required r_{pn} is not a simple function of fluid properties. However, it is shown in Appendix I that r_{pn} is proportional to fluid properties for the following special cases:

$$r_{pn} \propto \frac{\sigma}{P_v} \quad , \quad \frac{r_p}{r_{pu}} = 1$$

$$r_{pn} \propto \frac{\nu_v}{\nu_\ell}\left(\frac{\sigma}{P_v}\right) , \quad \frac{r_p}{r_{pu}} \ll 1$$

Here r_{pu} is an optimum pore radius for uniform wick heat pipes which maximizes the heat transport capacity in a horizontal heat pipe for which $L_e/L_c \gg 1$, σ is the surface tension at the heat pipe liquid-vapor interface, and P_v is the vapor pressure.

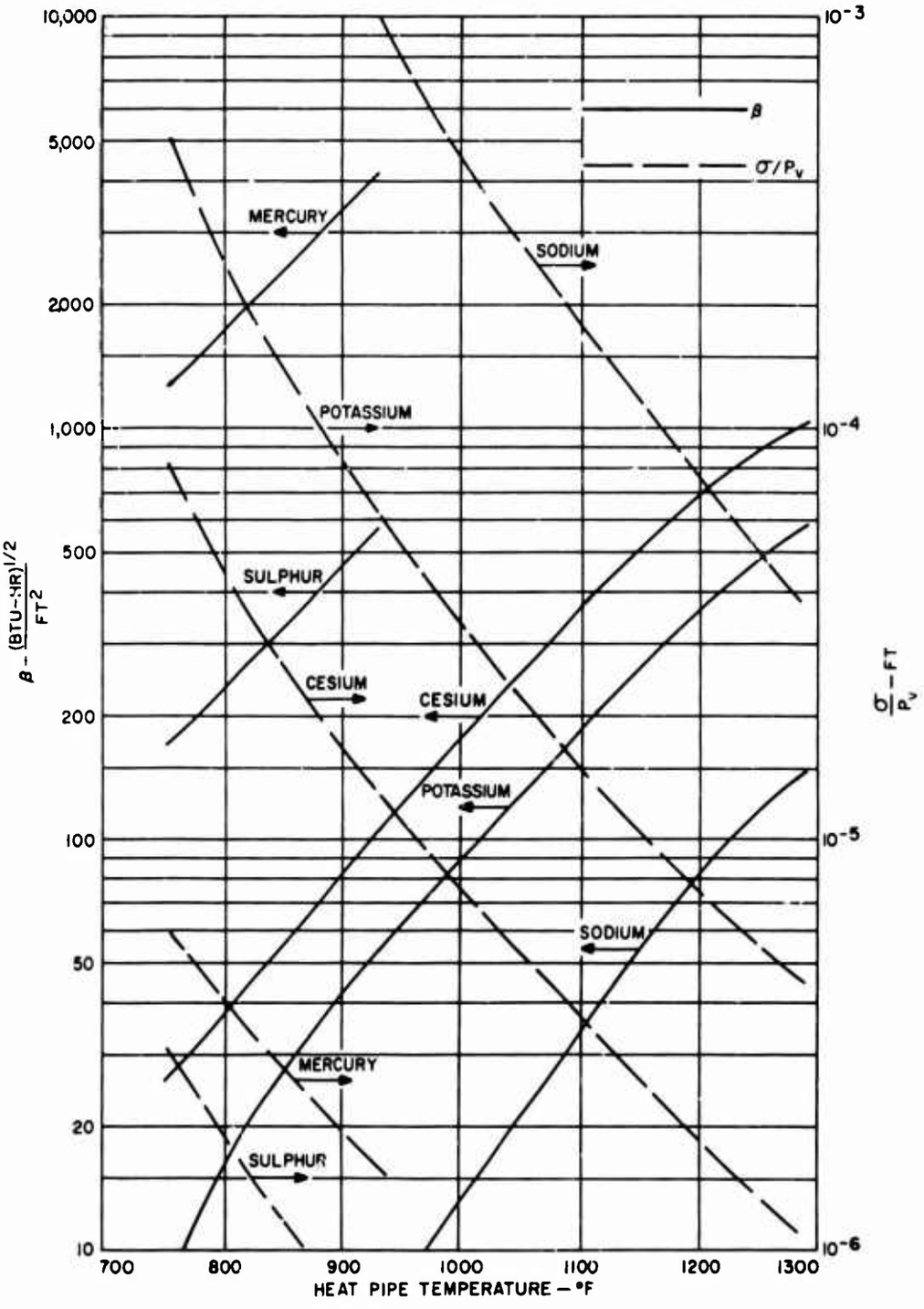

Figure 7. Variation of Fluid Parameters β and σ/P_V With Temperature.

In Figure 7, the ratio σ/P_v is shown as a function of temperature for the heat pipe fluids under consideration (dashed lines). For the heat pipe dimensions considered in this report, r_p/r_{pu} is roughly close to 1 for cesium, potassium, and sodium. Therefore, r_{pn} for these fluids is roughly proportional to σ/P_v. For mercury and sulphur, however, r_p/r_{pu} is much smaller than 1, and r_{pn} for these fluids is proportional to $(\nu_v/\nu_\ell)(\sigma/P_v)$. Using approximate values of ν_v/ν_ℓ for mercury and sulphur, we find that

$$r_{pn} \propto 100\ \sigma/P_v \text{ (mercury)}$$

$$r_{pn} \propto 0.1\ \sigma/P_v \text{ (sulphur)}$$

From these relations and the dashed curves of Figure 7,

$$r_{pn} \text{ (mercury)} \approx 12\ r_{pn} \text{ (cesium)}$$

$$r_{pn} \text{ (sulphur)} \approx 0.005\ r_{pn} \text{ (cesium)}$$

Since calculations show that r_{pn} for cesium may be as small as 1.5 microns (see Table X), it is evident that r_{pn} for sulphur is well below the lower limit of feasibility. The longer isothermal length of sulphur heat pipes is thus not achievable, and no further consideration was given to sulphur as a possible heat pipe fluid.

On the other hand, r_{pn} for mercury is well within the limit of feasibility. Although mercury heat pipes which have been tested thus far have not performed too well (most probably because of poor wetting), the superior theoretical performance of mercury warrants its further consideration. Both cesium and mercury heat pipes were therefore used in the regenerator design study.

Wick Characteristics

Important wick characteristics include: thickness t_w and material, porosity ϕ and tortuosity b, and the mean pore radii r_p in the axial direction and r_{pn} in the radial direction.

Thickness and Material

The wick should generally be as thin as can be fabricated in order to minimize heat pipe weight. The wick should preferably be fabricated from the same material as the heat pipe wall to prevent or minimize internal corrosion problems. In this study, the wall and wick material are assumed to be identical.

Porosity and Tortuosity

The porosity ϕ is the fraction of the total wick volume which is occupied by the

heat pipe liquid. The tortuosity b is an empirically determined factor in the expression for the pressure drop through a porous medium. For laminar flow, the pressure drop per unit length is expressible as $b\mu V/r_p^2$, where μ is the fluid viscosity, V is the mean flow velocity in the pores, and r_p is the mean pore radius.[2] The tortuosity b has a value of 8 for a wick composed of simple axial capillary tubes.[2] Since the flow path through a porous material is more devious than through a simple tube, the pressure drop and hence b for a porous wick should exceed that for a tube with the same mean pore radius and mean pore flow velocity. The factor 8, therefore, should represent a lower limit for the tortuosity.

The factor $(b/\phi)^{1/2}$ is of significance in establishing the size of wick pores which will insure fluid flow at the required rate for isothermal operation in a heat pipe of maximum length. A wick with a relatively small $(b/\phi)^{1/2}$ will have larger pores than one with a larger value of $(b/\phi)^{1/2}$. The value of $(b/\phi)^{1/2}$ corresponding to $b = 8$ and $\phi = 1$ is 2.83, and should represent a lower limit.

In a recent study, the properties of sintered fiber, sintered powder, and woven-mesh screen wicks were measured.[10] All of the wicks had a thickness of 0.1 inch, were fabricated from nickel, and had relatively uniform pores. Properties measured included: mean diameter d_s of solid elements comprising the wick (fibers, particles, and wires), porosity ϕ, mean pore radius r_p, and the reciprocal of permeability K.

The measured data are shown in Table III, along with the tortuosity b and $(b/\phi)^{1/2}$. The tortuosity was calculated from the relation $b = \phi K r_p^2$. Surprisingly, for three of the wicks in Table III, the calculated tortuosity is less than the predicted minimum value of 8. The reason for these results is not known, but they may be attributable in part to experimental error (which could approach 10 percent for the K measurement), in part to lack of complete wick isotropy, and in part to uncertainity in selection of a pore radius which is truly representative of the pore size distribution within the wick.

For purposes of analysis, a wick of the sintered fiber type was selected. In addition to a reasonably small $(b/\phi)^{1/2}$, this type is readily fabricated into a high-porosity structure. High porosity results in lower heat pipe weight when the density of the heat pipe liquid is less than that of the wick material (as is the case, for example, with cesium and stainless steel).

Values of $b = 11.2$ and $\phi = 0.85$ were selected as representative of those attainable with sintered fiber wicks. The corresponding value for $(b/\phi)^{1/2}$ is 3.64. These values were used in all heat pipe calculations presented in this report.

TABLE III. PROPERTIES OF CAPILLARY WICKS (from Ref. 10)

Wick Type	Sample	d_s (mils)	ϕ	r_p (mils)	K ($ft^{-2} \times 10^{-8}$)	b	$(b/\phi)^{1/2}$
Sintered fiber	H1	0.4	0.84	0.86	21.9	9.45	3.36
Sintered fiber	H2	0.4	0.81	0.69	27.6	7.35	3.01
Sintered fiber	H3	0.4	0.69	0.52	61.3	7.98	3.40
Sintered powder	M4	11.7-33.1	0.54	1.58	11.5	10.70	4.45
Woven mesh	M10	2.2	0.65	0.99	12.0	5.24	2.84

Pore Radii

A heat pipe wick can have uniform pores ($r_p = r_{pn}$) or nonuniform pores ($r_{pn} < r_p$). A nonuniform-pore wick can be approximated by a two-layer wick, one layer having relatively large uniform pores and the other having relatively small uniform pores. The layer with the larger pores would be relatively thick and located next to the inner surface of the heat pipe wall. The layer with the smaller pores would be relatively thin and in contact with the heat pipe vapor space.

Whether or not the wick has uniform pores, the axial pore radius r_p is limited in maximum size to some fraction of the wick thickness t_w. It has been assumed here that $r_p \leq 1/4\ t_w$.

For a heat pipe with a uniform-pore wick of thickness t_w, there is an optimum pore radius for which the heat transport capacity takes on a maximum value. The magnitude of the optimum r_p and maximum Q depends on the length ratio L_e/L_c, the heat pipe orientation, and the external acceleration experienced by the heat pipe. A convenient reference heat pipe will be specified which is horizontal, is not subject to external acceleration, and has an L_e/L_c which approaches infinity. The optimum pore radius for this reference heat pipe will be designated r_{pu}. The corresponding heat transport capacity will be called Q_u.

The wick thickness t_w of the reference heat pipe also has an optimum value $t_{wo} = 0.185\ r_w$, where r_w is the outer wick radius. When $t_w = t_{wo}$, r_{pu} takes on the value r_{po}, and Q_u assumes its maximum possible value, Q_o. In Figure 8, the variation of Q/Q_o with r_p/r_{po} and t_w/t_{wo} is shown. For a given t_w/t_{wo}, the peak value of Q/Q_o is Q_u/Q_o, and the corresponding value of r_p/r_{po} is r_{pu}/r_{po}.

In Figure 9, the optimum pore radius r_{po} is shown as a function of outer wick radius r_w and temperature for cesium and mercury heat pipes. Corresponding values of the maximum heat transport capacity Q_o are given in Figure 10 for a heat pipe length L_p of 12 inches. Q_o varies inversely as L_p.

The heat transport capacity Q will be taken equal to the heat transport rate Q_i in an isentropic heat pipe of maximum length L_p, since maximum heat pipe length is an important design objective. For a given wick thickness t_w, if $Q_i \leq Q_u$, a uniform-pore wick may be used. If $Q_i > Q_u$, the desired heat transport rate exceeds that obtainable with a uniform wick, and a wick with nonuniform pores must be used.

Q_i/Q_u is equal to $(Q_i/Q_o)/(Q_u/Q_o)$. Q_u/Q_o is obtained from Figure 8. Q_i/Q_o is given in Figure 11 as a function of temperature and diameter d for cesium and

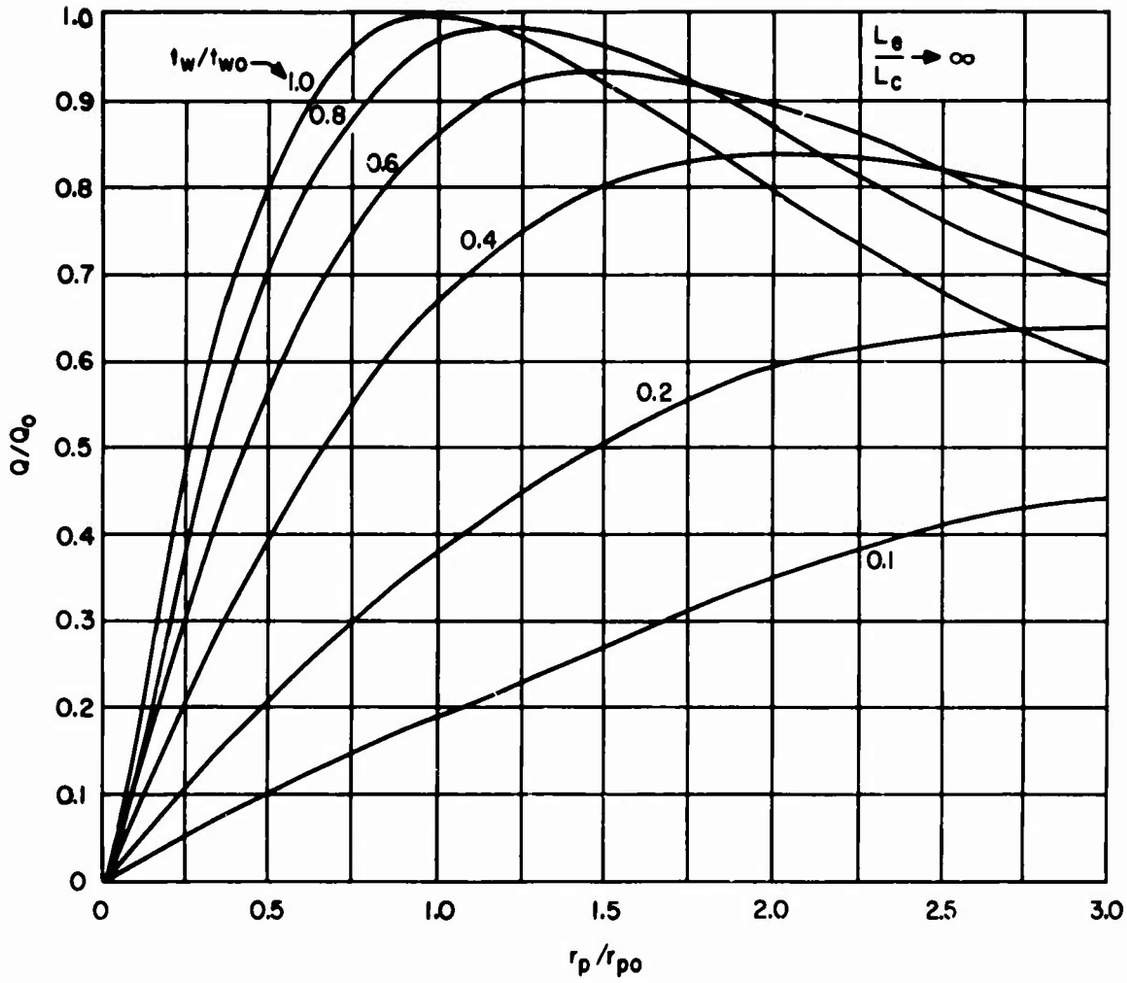

Figure 8. Effect of Wick Thickness and Pore Radius on Heat Transport Capacity of Horizontal Heat Pipe.

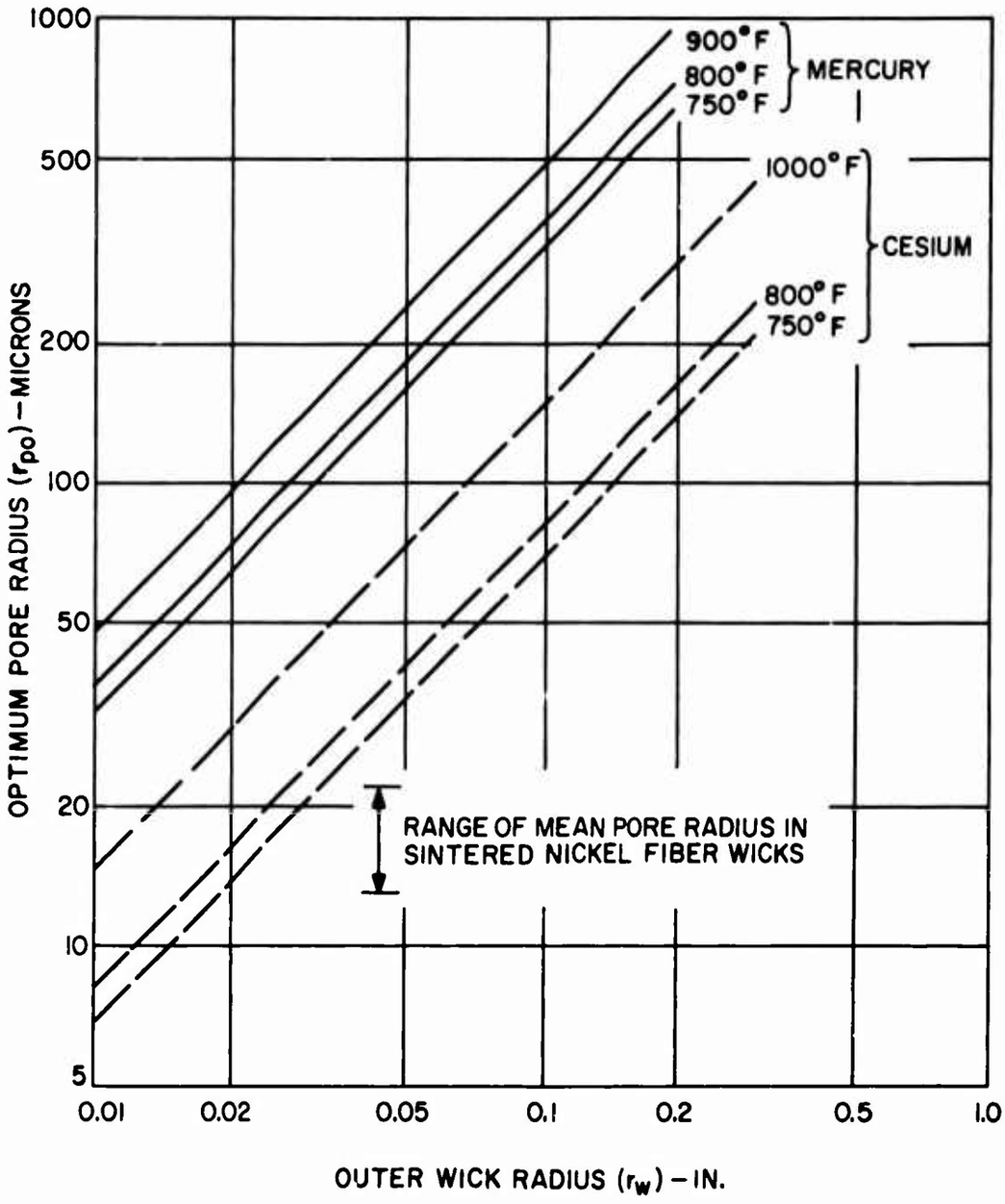

Figure 9. Optimum Pore Radius for Cesium and Mercury Heat Pipes.

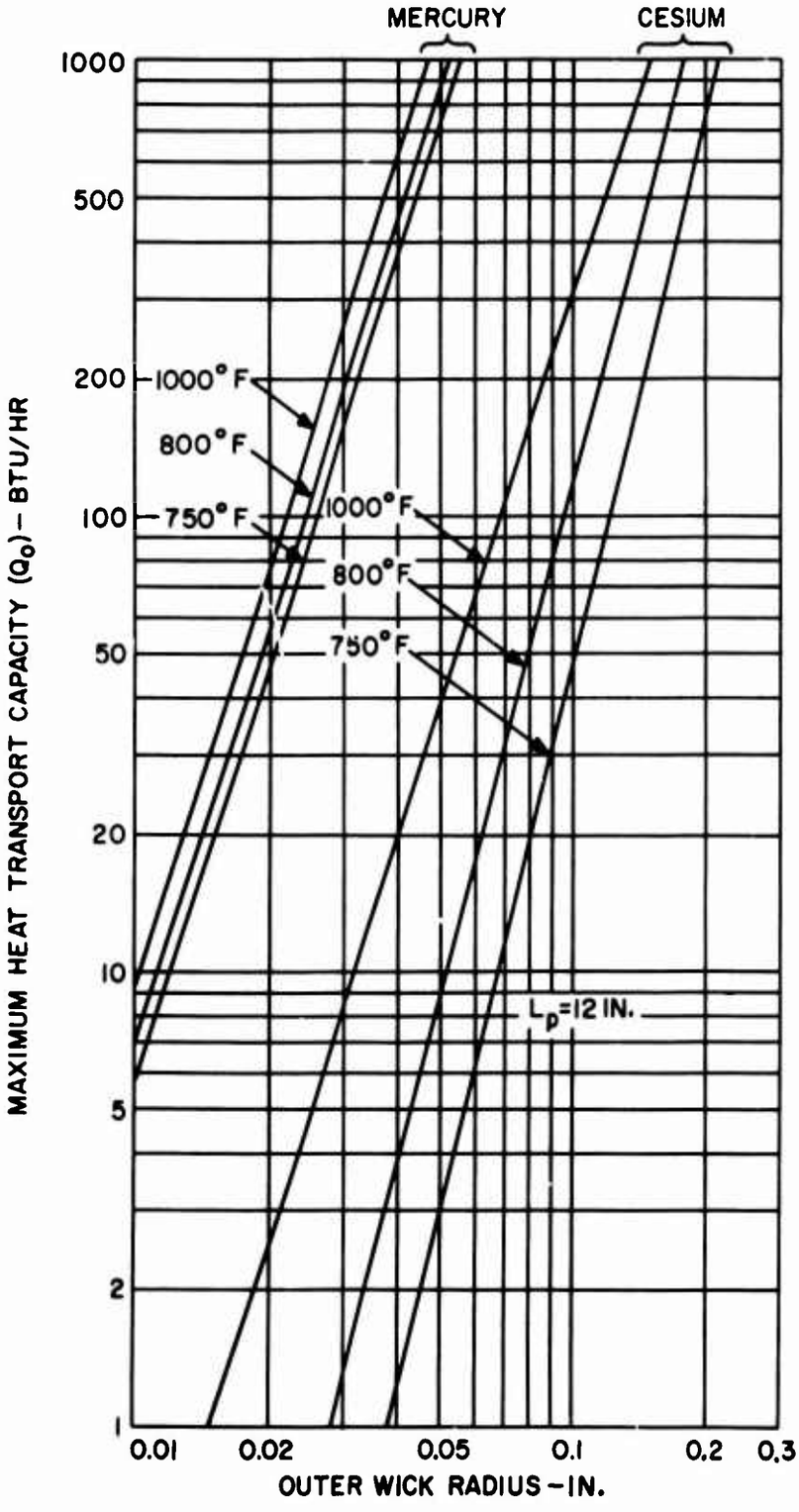

Figure 10. Maximum Heat Transport Capacity for 12-inch Horizontal Heat Pipe With Uniform Wick.

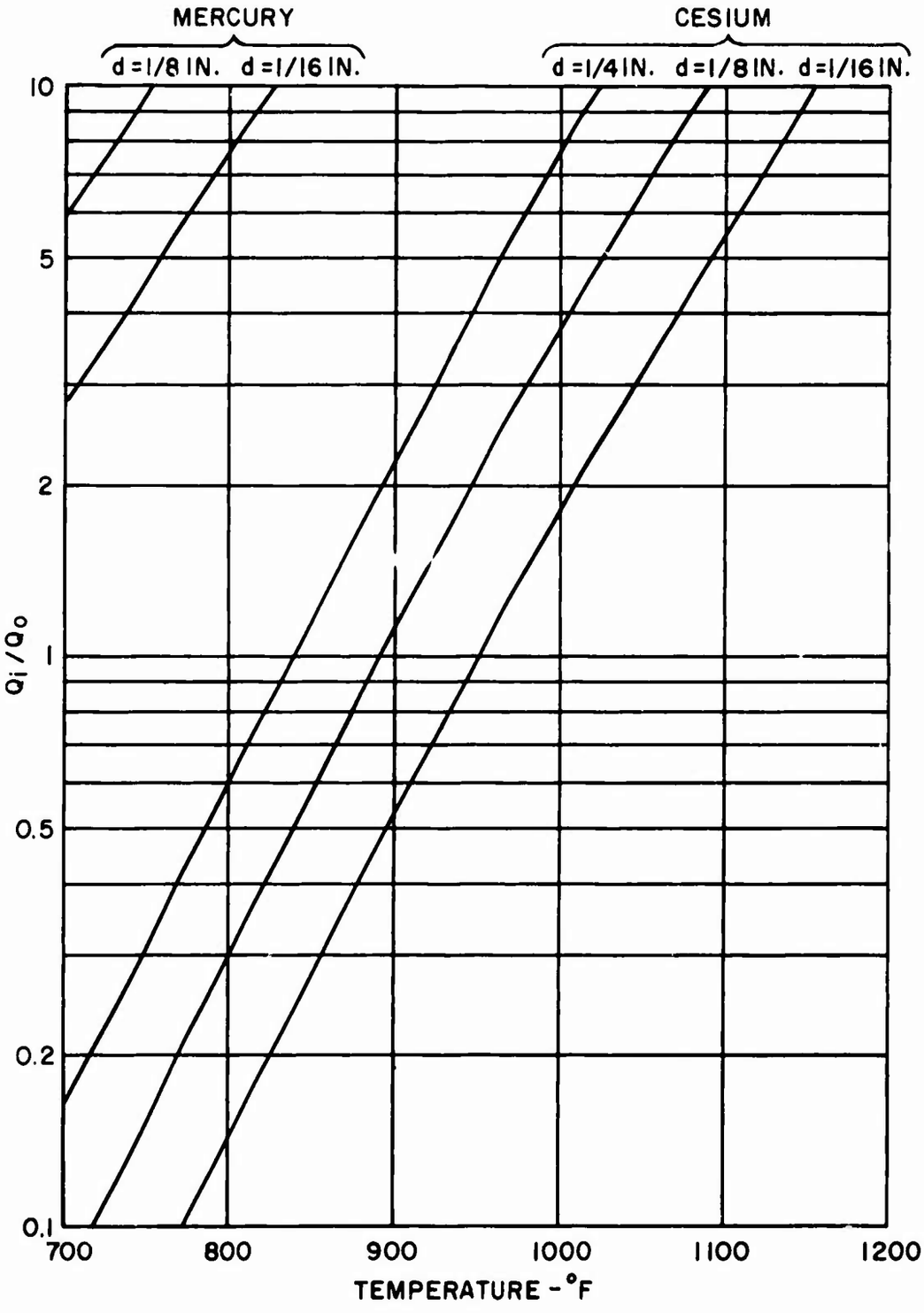

Figure 11. Variation of Q_i/Q_o With Temperature.

mercury heat pipes. The wall thickness t of the heat pipes is

d - in.	t - mils
1/16	3
1/8	4
1/4	6

The basis for selection of these wall thicknesses is discussed below.

In Figure 12, the variation of Q_i/Q_u with r_p/r_{pu} and r_{pn}/r_{pu} is shown. For a specified Q_i/Q_u, the pore radii of wicks with both uniform and nonuniform pores can be found from Figure 12.

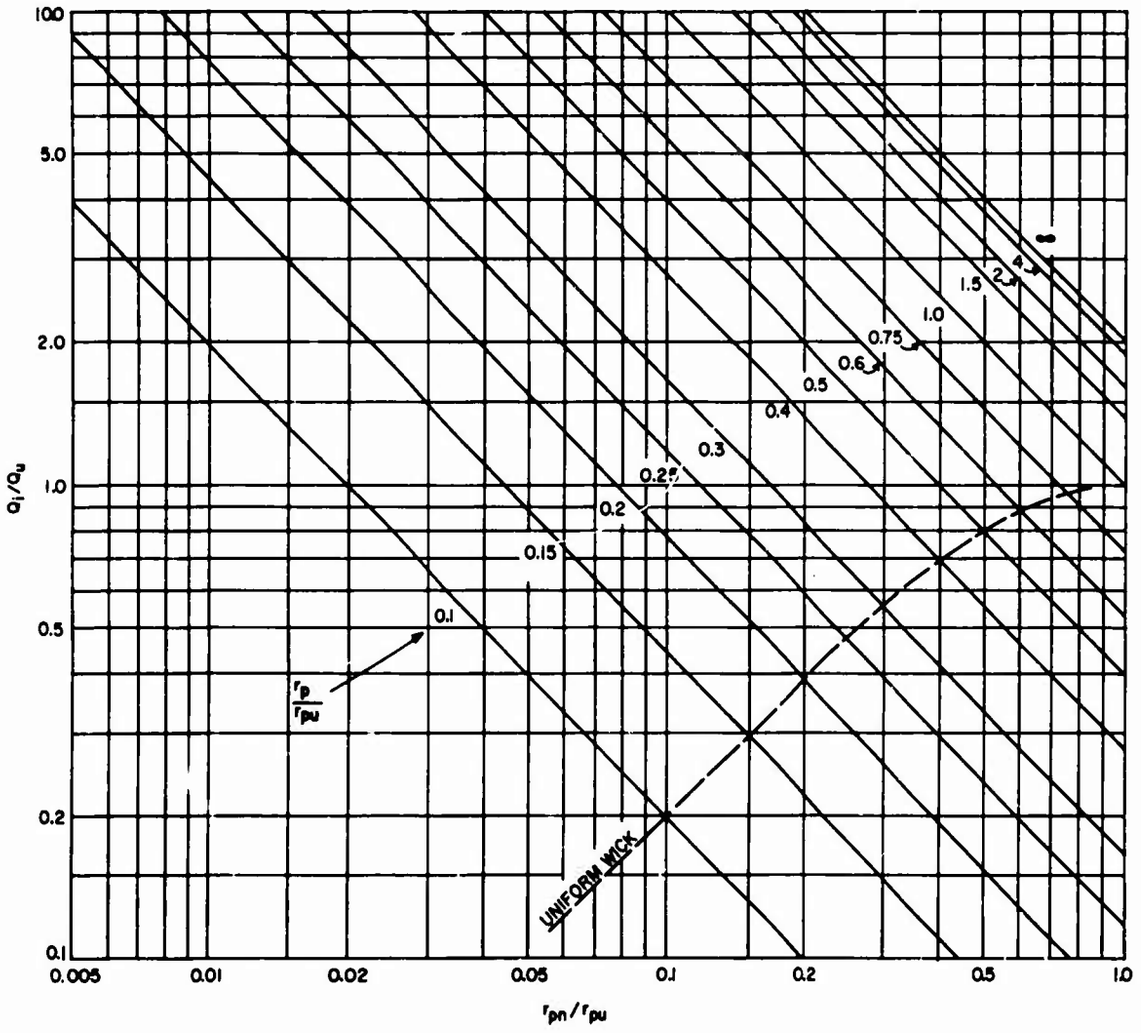

Figure 12. Variation of Q_i/Q_u With Axial and Radial Pore Radii.

The following example illustrates the procedure for using Figures 8, 9, 11, and 12 to determine the wick pore radii.

A 1/8-inch-diameter cesium heat pipe has a wick thickness t_w which is equal to the wall thickness t of 4 mils. The maximum permissible pore radius is 1/4 t_w or 1 mil. What are the required pore radii r_p and r_{pn} for isothermal operation over a maximum heat pipe length for heat pipe temperatures T_p of (a) 800° F and (b) 1000° F?

First, note that the optimum wick thickness t_{wo} is

$$t_{wo} = 0.185\, r_w = 0.185\, (r - t) = 0.185\, (62.5 - 4) = 10.8 \text{ mils}$$

Then

$$\frac{t_w}{t_{wo}} = \frac{4}{10.8} = 0.370$$

From Figure 8, when $t_w/t_{wo} = 0.370$, Q_u/Q_o (the maximum of the $t_w/t_{wo} = 0.370$ curve) is 0.81 and r_{pu}/r_{po} is 2.

(a) $T_p = 800°F$

From Figure 11, Q_i/Q_o is 0.3. From Figure 9, r_{po} is 46 microns. Also,

$$\frac{Q_i}{Q_u} = \frac{Q_i/Q_o}{Q_u/Q_o} = \frac{0.3}{0.81} = 0.37$$

From Figure 12, a uniform wick can be used with

$$\frac{r_p}{r_{pu}} = \frac{r_{pn}}{r_{pu}} = 0.19$$

Then

$$r_p = 0.19\, r_{pu} = 0.19\, (2\, r_{po}) = 0.19\, (2)\, (46) = 17.5 \text{ microns} = 0.69 \text{ mil}$$

The calculated uniform pore radius is well under the maximum permissible value of 1 mil.

(b) $T_p = 1000°F$

From Figure 11, Q_i/Q_o is 3.7. From Figure 9, r_{po} is 86 microns. Also,

$$\frac{Q_i}{Q_u} = \frac{Q_i/Q_o}{Q_u/Q_o} = \frac{3.7}{0.81} = 4.56$$

Now let r_p = 1 mil = 24.5 microns (its maximum permissible value). Then

$$\frac{r_p}{r_{pu}} = \frac{r_p/r_{po}}{r_{pu}/r_{po}} = \frac{24.5/86}{2} = 0.142$$

From Figure 12, $r_{pn}/r_{pu} = 0.009$, and

$$r_{pn} = 0.009\, r_{pu} = 0.009\,(2\, r_{po}) = 0.009\,(2)(86) = 1.55 \text{ microns}$$

Results such as those obtained for the pore radii r_p and r_{pn} are applicable to horizontal heat pipes with no external acceleration and with an evaporator section which is much longer than the condenser section ($L_e/L_c >> 1$). When the heat pipe is not horizontal and/or is subject to external acceleration, a reduction in r_{pn} may be necessary. This situation is discussed shortly.

When L_e exceeds L_c by only a moderate factor, the required pore radii are larger than when $L_e/L_c >> 1$. As will be shown, the desired L_e/L_c for regenerator heat pipes is in the range 3-5. Hence, the above procedure for determining the wick pore radii yields conservative results.

Heat Pipe Diameter

The heat pipe diameter d is largely determined by regenerator heat transfer surface requirements. To meet regenerator design goals of compactness and low weight, d should be small, preferably not exceeding 1/4 inch. In this study, diameters of 1/16, 1/8, and 1/4 inch have been considered. Since the maximum heat pipe length L_p for isothermal operation varies as $d^{3/2}$ [see Equation (59), Appendix II], the heat pipe diameter selected will represent a compromise between the conflicting design goals of long heat pipe length on the one hand and regenerator compactness and low weight on the other.

Wall Thickness and Material

The heat pipe wall should be as thin as possible to minimize regenerator weight. Wall thickness and material are determined by considerations of fabricability, corrosion, strength, and mechanical stability.

Fabricability

Stainless steel tubes 1/16 inch in diameter have been fabricated with 3-mil walls, and 1/4-inch-diameter tubes have been fabricated with 4-mil walls.[13,14] Tubes of 1/8-inch diameter with 3-mil walls also appear to be feasible.

Corrosion

The heat pipe wall must successfully withstand corrosion from both the heat pipe fluid inside the heat pipe and the hot air and turbine exhaust gas which flows over the heat pipe exterior. Limited corrosion studies indicate that cesium should be compatible with austenitic and ferritic stainless steels and Haynes 25 alloy at temperatures up to 1600°F.[15] There does not appear to be any corrosion data for the cesium-Hastelloy X combination, but the corrosion behavior in this case is probably similar to that experienced with stainless steels.

Although little surface damage was observed after cesium-stainless steel compatibility tests, at temperatures above 1200°F there was some decarburization and leaching of carbide precipitates. Should such decarburization extend to the outer heat pipe surface, corrosion resistance to the external heat pipe environment could be adversely affected.

Titanium has successfully withstood exposure to cesium vapor for 10,000 hours at 1052°F, although surface tarnishing has been observed.[15] A cesium-titanium heat pipe has been successfully operated for 2000 hours at 750°F (see Table I).

Mercury appears to be most compatible with ferritic stainless steels. The alloy CROLOY 9M may be suitable at temperatures below 1000°F, although problems have been encountered at 1100°F.*

Tests of 0.060-inch-diameter, 3-mil-thick, 347 stainless tubes in a typical gas turbine regenerator environment with a gas inlet temperature of $\sim$1350°F resulted in excessive intergranular oxidation due to precipitation of chromium carbides at the grain boundaries. Further tests with Hastelloy X 3-mil sheet in a similar environment produced no significant oxidation.[13]

The above information indicates that cesium heat pipes at temperatures below 1000°F can be successfully fabricated from stainless steel and possibly titanium. Above 1000°F, Hastelloy X may be necessary to provide sufficient oxidation

---

* Personal communication with J. DeVan, Oak Ridge National Laboratory, Oak Ridge, Tennessee.

resistance to the exhaust gas environment. For mercury heat pipes at temperatures below 1000°F, ferritic stainless or CROLOY 9M may be considered.

Strength and Mechanical Stability

Wall stresses and the mechanical stability of cesium and mercury heat pipes have been evaluated. Since the external air-side pressure is 147 psia and the external gas-side pressure is 15.5 psia, the net radial pressure acting on the heat pipes, and its direction, will depend on the magnitude of the internal vapor pressure as well as on the position along the heat pipe. The net radial pressure for cesium and mercury heat pipes is shown in Table IV. Radially inward net pressure is indicated by (+), and radially outward pressure is indicated by (-).

TABLE IV. NET RADIAL PRESSURE ON HEAT PIPE WALLS

Heat Pipe Fluid	Cesium		Mercury	
Temperature (°F)	785	1296	785	1000
Vapor Pressure (psi)	0.45	18	40	175
Net Radial Pressure				
Gas Side (psi)	+15.0	-3	-24.5	-159.5
Air Side (psi)	+146.5	+129	+107	-28

The compressive or tensile circumferential wall stress and required pressure for radial buckling are shown in Table V for heat pipes of the indicated diameters and wall thicknesses. The compressive stress was calculated for a net radial pressure of +146.5 psi, and the tensile stress was calculated for a net radial pressure of -159.5 psi.

TABLE V. HEAT PIPE STRESSES AND BUCKLING PRESSURE

Diameter (in.)	Thickness (mils)	Compressive Stress (psi)	Tensile Stress (psi)	Buckling Pressure (psi)
1/16	3	1452	1580	8500
1/8	4	2220	2480	2400
1/4	6	3000	3270	965

At temperatures of 1300°F or less, the stress for 1 percent creep in 10,000 hours is greater than 4500 psi for stainless and Hastelloy X; therefore, cesium or mercury heat pipes of these materials with the indicated diameters and thicknesses should be structurally adequate.[16] They should also be stable against buckling, since the required buckling pressures are in excess of the net radially-inward pressure of 146.5 psi.

For cesium-titanium heat pipes at 1000°F or less, the required buckling pressure is one-half that indicated above, but it is still in excess of the net external pressure. However, the stress for rupture in 1000 hours in titanium is 3000 to 5000 psi.[17] The stress for 1 percent creep in 10,000 hours may be roughly 50 percent of the stress for rupture. The indicated heat pipe thicknesses may therefore be too small for a cesium-titanium heat pipe at 1000°F, but they are probably satisfactory at somewhat lower temperatures.

The above heat pipe thicknesses will be used for regenerator core weight calculations. While a 3-mil wall is probably adequate for 1/8-inch heat pipes from the strength and stability viewpoint, a 4-mil wall will be used for added protection against corrosion.

Stresses due to vibration, acceleration, or restraints introduced by fabrication of heat pipes into a regenerator core have not been considered here, as these will be a function of specific mission requirements, regenerator configuration, and fabrication procedures. Consideration of these stresses could require modification of the wall thicknesses which have been selected for analysis.

Effect of Orientation and Acceleration

In the preceding discussion, it has been assumed that the heat pipes are oriented in a horizontal position and are not subject to accelerative forces. Since the heat pipe regenerator is to be mounted in an aircraft, variations in orientation and external acceleration are to be expected. Aside from operational considerations, the core configuration itself may include large numbers of heat pipes which are oriented at an angle to the horizontal (see Figure 6).

When a horizontal heat pipe is inclined and/or subjected to external acceleration along its axis, the heat transport capacity will be affected. The geometry of an inclined heat pipe subjected to vertical acceleration is shown in Figure 13. When the condenser section C is lower than the evaporator section E, the angle θ to the horizontal is taken to be positive. When the condenser section C is higher than the evaporator section E, θ is negative. The vertical external acceleration on the heat pipe is taken to be positive when directed upward and negative when directed downward. The acceleration n is expressed as the number of "g's", where g is the acceleration due to gravity. The component of acceleration along the heat pipe axis is $n\sin\theta$.

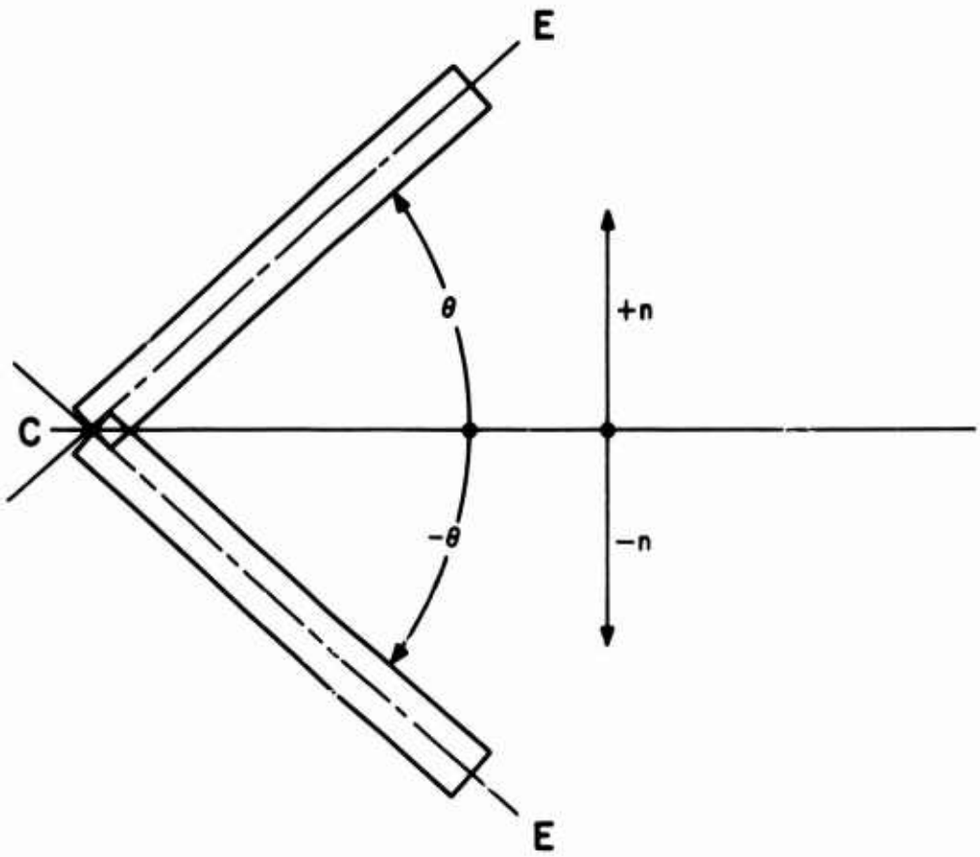

Figure 13. Geometry of Nonhorizontal Heat Pipe Subjected to Vertical Acceleration.

When the angle θ is negative, the return of condensate to the evaporator section is aided by gravity, and the heat transport capacity is increased. The addition of n g's of upward external acceleration would increase the effective weight of condensate, facilitating the condensate's return to the evaporator section and further increasing the heat transport capacity. One g of acceleration in the downward direction would effectively neutralize the weight of condensate, and the heat transport capacity would then remain the same as it was in the horizontal position. More than one g in the downward direction would retard the flow of condensate to the evaporator section, reducing the heat transport capacity below its horizontal value. A sufficiently large downward acceleration would reduce the heat transport capacity to zero.

When the angle θ is positive, the situations described for the negative angle are reversed. Gravity now retards the return of condensate to the evaporator. A

sufficiently long heat pipe and/or large upward acceleration will reduce the heat transport capacity to zero. In this case, a downward acceleration of one g will completely neutralize the effect of gravity. A downward acceleration in excess of one g will facilitate the return flow of condensate, resulting in an increase in the heat transport capacity over its horizontal value.

Acceleration Parameter

The effects of orientation and acceleration on heat pipe performance are quantitatively described by the dimensionless acceleration parameter α, where

$$\alpha = \frac{(1 + n)\rho_\ell r_{pn} L_p \sin\theta}{2\sigma}$$

[See Equation (11), Appendix I] α is equal to the fractional change in heat transport capacity which occurs when a heat pipe is inclined and/or subjected to vertical acceleration. The heat transport capacity decreases when α is positive and increases when α is negative. In Figure 14, α is shown as a function of the effective vertical heat pipe height $L_p \sin\theta$ and the vertical acceleration n. The data apply to a temperature of 785°F, cesium or mercury heat pipe fluids, and a radial pore radius r_{pn} of 24 microns. The horizontal line at $\alpha = 1$ identifies conditions for which the heat transport capacity is zero. (The horizontal line at $\alpha = -2$ identifies another limiting condition which will be discussed shortly.)

The variation of α, and hence the fractional change in heat transport capacity, with radial pore radius r_{pn} is shown in Figure 15 for a heat pipe with $L_p \sin\theta = 10$ inches. Again, the data are applicable to cesium and mercury at 785°F. Figure 15 indicates that the sensitivity of heat transport capacity to orientation and acceleration is greatly reduced for radial pore radii on the order of 2.5 microns or less.

Heat pipes for regenerators should be designed to function at full effectiveness under the most adverse combination of orientation and acceleration which persists over an appreciable fraction of total flight time. Accelerations of short duration may occur during takeoff, landing, and momentarily during flight. A loss of regenerator effectiveness during these periods will have little effect on overall fuel economy. For purposes of analysis, therefore, the most adverse condition was considered to be that for which the heat pipes are oriented vertically with the condensor end down, with no external acceleration. This condition would exist, for example, during horizontal, constant-velocity flight in an aircraft utilizing a regenerator with radial heat pipes oriented normal to the aircraft axis (see Figure 6). The acceleration parameter α would then be that corresponding to $\theta = 90°$ and n = 0.

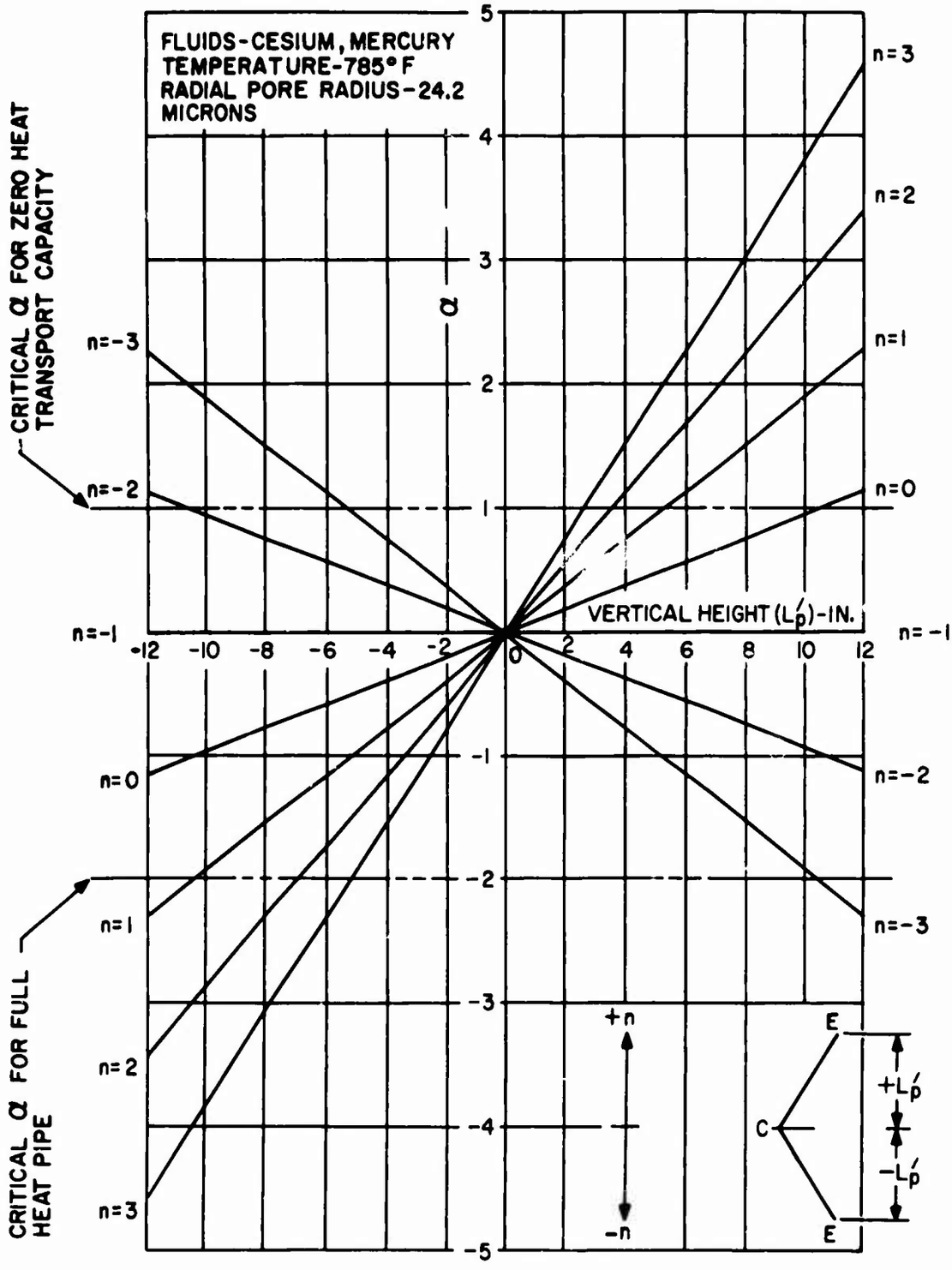

Figure 14. Effect of Heat Pipe Orientation, Vertical Height, and Vertical Acceleration on Acceleration Parameter α.

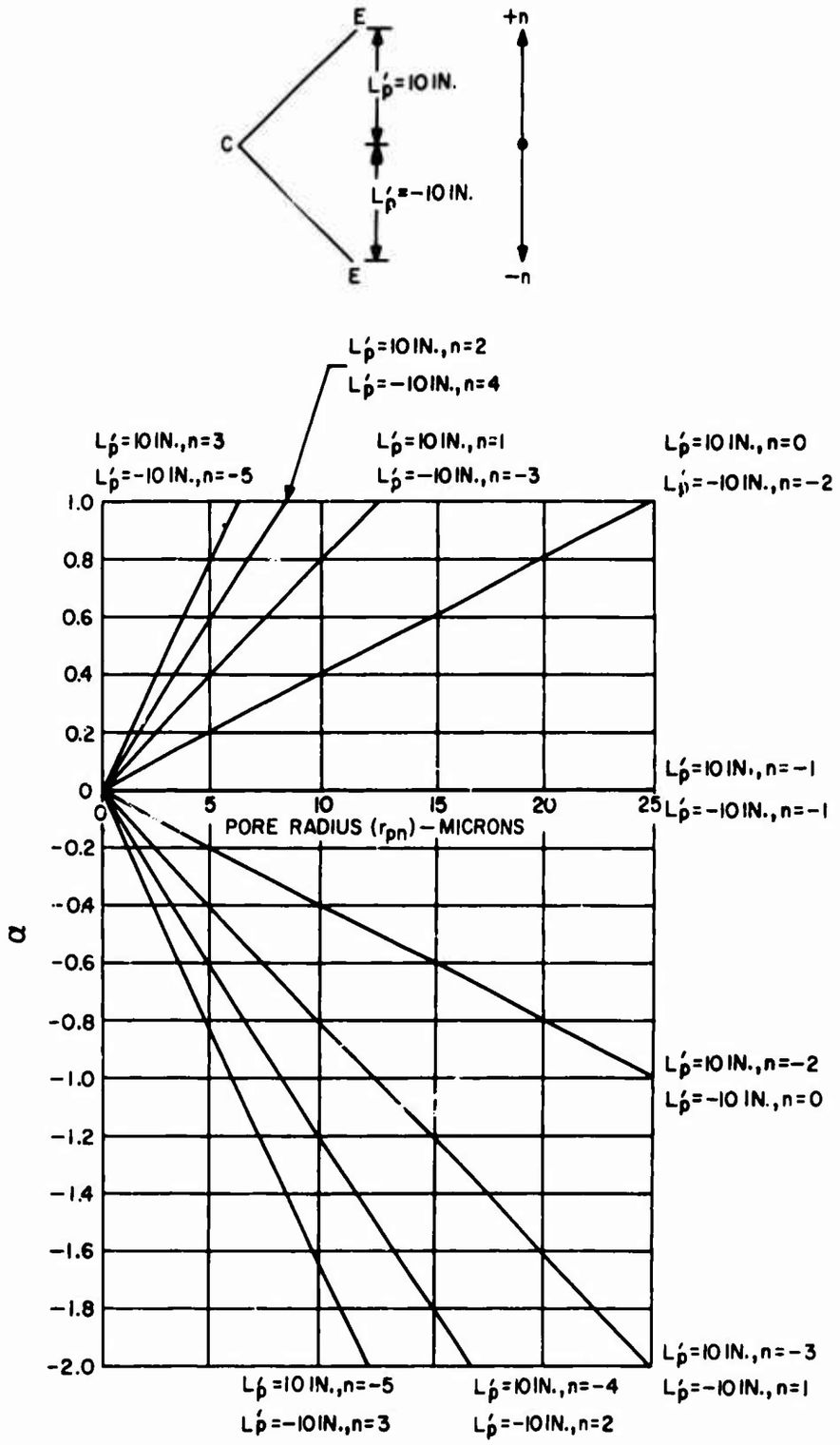

Figure 15. Effect of Pore Radius r_{pn} on Acceleration Parameter α.

In order to assure that the heat transport capacity will be equal to the heat input rate when α is positive, suitable corrections must be made to either the pore radius r_{pn} or the heat pipe length L_p which has been determined for horizontal heat pipes (i.e., for heat pipes with $\alpha = 0$). These corrections can be established from Equations (11), (15), (19), and (21) in Appendix I and Equation (57) in Appendix II. They take the form

$$\frac{r_{pn}(\alpha)}{r_{pn}(\alpha = 0)} = \frac{1}{1 + \alpha} \quad , \quad \alpha > 0$$

$$\frac{L_p(\alpha)}{L_p(\alpha = 0)} = \sqrt{1 + \frac{\alpha^2}{4}} - \frac{\alpha}{2} \quad , \quad \alpha > 0$$

and are plotted in Figure 16.

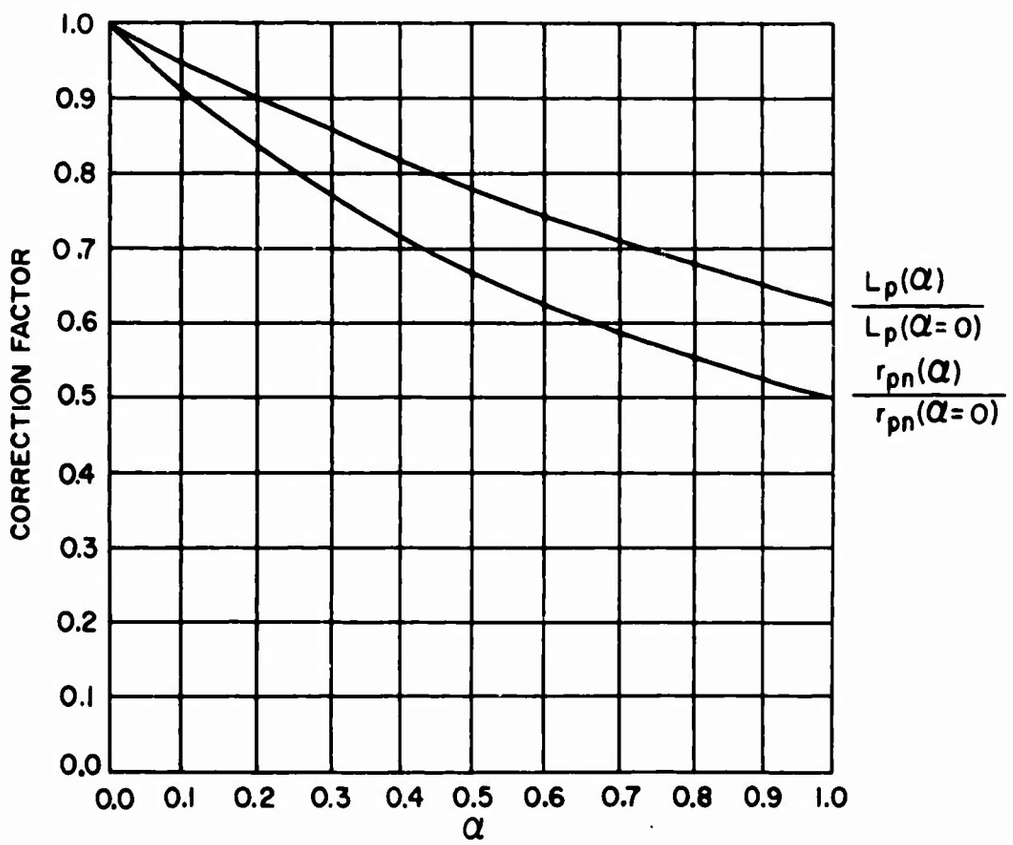

Figure 16. Correction Factors for r_{pn} and L_p When $\alpha > 0$.

Since maximum heat pipe length L_p is an important design objective, the correction to assure proper operation when $\alpha > 0$ should be made to the pore radius r_{pn}. If the corrected r_{pn} is impractically small, then a reduction in L_p will be necessary, to the extent indicated in Figure 16.

Still another method for maintaining the heat transport capacity of a heat pipe when the acceleration parameter α becomes positive involves adjusting the ratio L_e/L_c, where L_e is the evaporator (gas-side) length and L_c is the condenser (air-side) length. As shown in Figure 17, the heat transport capacity varies significantly with L_e/L_c. For a given α, there is an optimum L_e/L_c at which the heat transport capacity assumes a maximum value. For a horizontal heat pipe ($\alpha = 0$), the optimum L_e/L_c is 1, and the maximum heat transport capacity is twice the value for $L_e/L_c = \infty$.

The use of a variable L_e/L_c to control the heat transport capacity complicates the analysis of heat pipe regenerators, since the heat transfer and friction parameters which determine the frontal area, length, and heat transfer surface of the regenerator core also depend on L_e/L_c. In this report, only adjustments in r_{pn} and L_p were considered in order to maintain proper heat pipe performance when $\alpha > 0$.

Since the actual L_e/L_c will probably lie in the range from 3 to 5, Figure 17 indicates that actual heat transport capacities may be 20 to 30 percent larger than values which have been predicted on the assumption that $L_e/L_c = \infty$. Thus, a margin of safety is implied in all previous calculations involving the heat transport capacity.

Design Criterion for Negative α

The heat transport capacity increases when the acceleration parameter α is negative, as has already been mentioned. If the heat pipe has been designed to operate at the design heat transfer rate in the horizontal ($\alpha = 0$) or condenser-down ($\alpha > 0$) position, one might assume that operation at the design rate in the condenser-up ($\alpha < 0$) position does not represent a problem.

However, for negative α when $|\alpha| > 1$, a minimum heat rate Q_{min} is required to maintain a fully saturated wick over the entire heat pipe length. If the design heat input is less than Q_{min}, a portion of the condenser section will dry out, the liquid accumulating at the bottom of the evaporator section. The heat pipe would then have undergone "burnout" at the condenser end and "floodout" at the evaporator end.

A minimum heat input is not required when $|\alpha| \leq 1$, because then the interface pressure difference $2\sigma/r_e$ at the evaporator end is large enough to support a

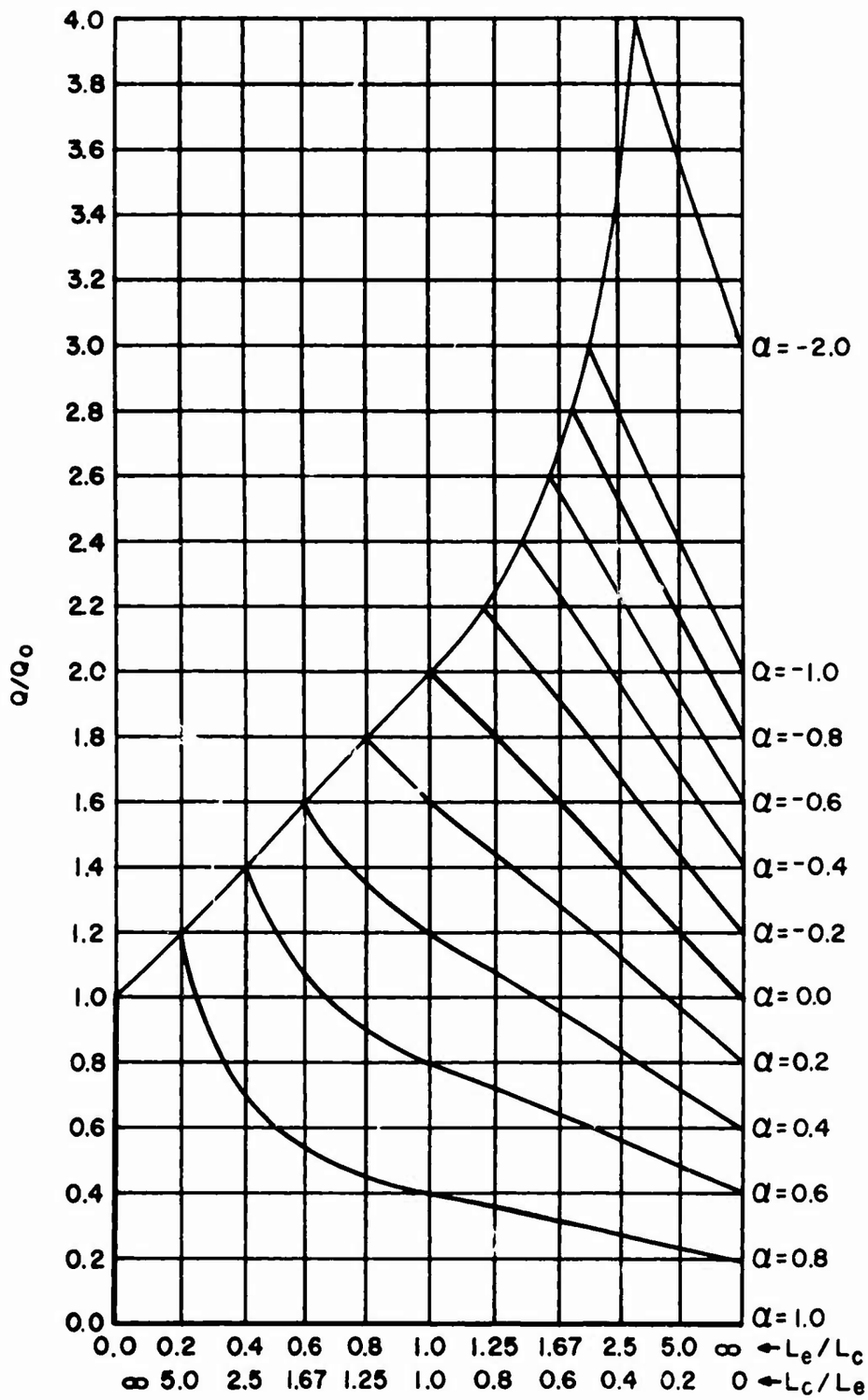

Figure 17. Variation of Heat Transport Capacity With L_e/L_c and α for Uniform Wick Heat Pipe.

column of liquid equal in height to the vertical heat pipe height $L_p \sin\theta$ with an effective density of $(n + 1)\rho_\ell$, even when no heat is being transported. (In this case, liquid bulges out of the pores in the evaporator section.)

When $|\alpha| > 1$, the liquid pressure at the base of the column would exceed that available at the interface, unless the column of liquid were moving through the wick toward the evaporator section. The frictional pressure drop (at a sufficiently high flow rate) would then reduce the pressure at the column base to the available interface pressure, thus permitting the entire length of the heat pipe wick to remain saturated with liquid. The minimum heat rate Q_{min} is then that value at which the liquid pressure drop is just sufficient to maintain the pressure of liquid arriving at the evaporator section just equal to the maximum available interface pressure.

Analysis of this problem (see Appendix I) indicates that the design heat input rate will always be equal to or greater than Q_{min}, guaranteeing proper operation for negative values of α, whenever the following criterion is met:

$$|\alpha| \leq 2$$

If this criterion is not met, the effective heat pipe length will be shortened, and the design heat input rate or temperature cannot be maintained.

With reference to Figure 15, consider a 10-inch cesium or mercury heat pipe oriented vertically with the condenser end up, and having an r_{pn} of 25 microns. The effective heat pipe length would drop below 10 inches upon application of an upward acceleration in excess of 1g, since then $|\alpha| > 2$. The same pipe, if fitted with a wick for which $r_{pn} = 12.5$ microns, would function properly under upward accelerations as high as 3g's. In the absence of external acceleration, the heat pipe easily meets the $|\alpha| \leq 2$ criterion with an r_{pn} of 25 microns.

If a heat pipe operates at the design heat transport rate when in the condenser-down position in the absence of external acceleration, then of necessity α must be less than one. It then follows that there is no minimum heat input requirement when the heat pipe is operated in the condenser-up position. Thus, if the heat pipes in the radial configuration of Figure 6 are designed to transport heat at the required rate when in the condenser-down position in the absence of external acceleration, they will operate properly in any orientation.

REGENERATOR CORE CHARACTERISTICS

Heat pipe regenerator cores have been analyzed on the basis of the rectangular geometry shown in Figures 4 and 5. The core characteristics of primary interest include: core or flow length L, specific frontal area A_{fs}, specific heat transfer surface area A_s, specific weight W_{cs}, and air-plus-gas duct width L_p (same as heat pipe length). Also of interest are the pore radii r_p and r_{pn} of the heat pipe capillary wick. (The term "specific" denotes the indicated quantity per unit mass flow rate of air or gas.)

The flow length, specific frontal area, and specific heat transfer surface area can be determined independently of internal heat pipe properties. The other characteristics of interest require consideration of internal heat pipe properties as well as external flow conditions.

The analysis was carried out under the following assumptions:

1. The exhaust gas mass flow rate is equal to the air mass flow rate.

2. The exhaust gas has the same pressure-independent physical properties as the compressed air at a given temperature.

3. The momentum contribution to pressure drop in the gas and air flow ducts is negligible. (For all cases of interest, the momentum contribution was less than 2 percent of the friction contribution.)

4. The surface area of the wall separating the air and gas flow ducts is small compared to the total heat pipe surface area; thus, it can be neglected in the calculation of specific heat transfer surface area.

5. Only the weight of the heat pipes was included in the calculation of specific core weight. The weight of internal structure such as flow duct walls, brazing compound, etc., was not considered because it is dependent on specific regenerator design configurations and fabrication techniques. Because of the simple core geometry, structural weight should constitute only a small fraction of total core weight, most probably less than 20 percent.

6. A maximum temperature variation of 10°F over the heat pipe length is allowed when calculating heat pipe length. This temperature variation corresponds to a 10-percent drop in vapor pressure.

7. The heat pipe temperature is considered to be constant when calculating gas-to-air heat transfer rates.

8. The heat pipe wick is fully wetted by the heat pipe fluid.

The basic core configuration studied employed the same heat pipes throughout the entire core (single-zone core) in a staggered arrangement. Modifications to the basic configuration were also considered, including:

1. Single-zone, staggered cores in which externally finned rather than smooth heat pipes are used.

2. Single-zone cores in which the heat pipes are arranged in an in-line rather than a staggered arrangement.

3. Two-zone, staggered cores in which the heat pipes above 1000°F differ from those below 1000°F in diameter, heat pipe fluid, and/or material.

Core characteristics for the basic configuration are presented first, followed by a discussion of the design alternatives. Calculational methods used to determine regenerator core characteristics are described in Appendix II.

Single-Zone Cores With Smooth, Staggered Heat Pipes

Core Length, Specific Frontal Area, and Specific Heat Transfer Surface Area

The variation of core length, specific frontal area, and specific heat transfer surface area with the ratio of gas-to-air duct width $L_g/L_a = L_e/L_c$ and heat pipe spacings $X_t d$ and $X_\ell d$ is shown in Figures 18, 19, and 20. A regenerator effectiveness of 0.7 and a heat pipe diameter of 1/8 inch were used to calculate the data for these figures. (For $X_t = 1.2$, the heat pipes are in contact when $X_\ell = 0.8$. Therefore, for this case the smallest value of X_ℓ used was 1.0.)

From Figure 18, core length is seen to be an increasing function of L_g/L_a. From Figure 19, the specific frontal area is a minimum at $L_g/L_a = 5$. From Figure 20, the specific heat transfer surface area, to which core weight is proportional, reaches a minimum at $L_g/L_a = 3$. A value of $L_g/L_a = 4$ was selected as best meeting the design objectives of low core weight and small frontal area. (Small frontal area reduces header weight and may be required for regenerator compatibility with gas turbine frontal area limitations.) With $L_g/L_a = 4$, the specific frontal area and the specific heat transfer surface are only slightly larger than the minimum values.

Since the core characteristics L, A_{fs}, and A_s all increase with the longitudinal spacing parameter X_ℓ, the smallest value of X_ℓ which is feasible from fabrication considerations should be used. While L and A_s both increase with the transverse spacing parameter X_t, A_{fs} decreases with increasing X_t. The

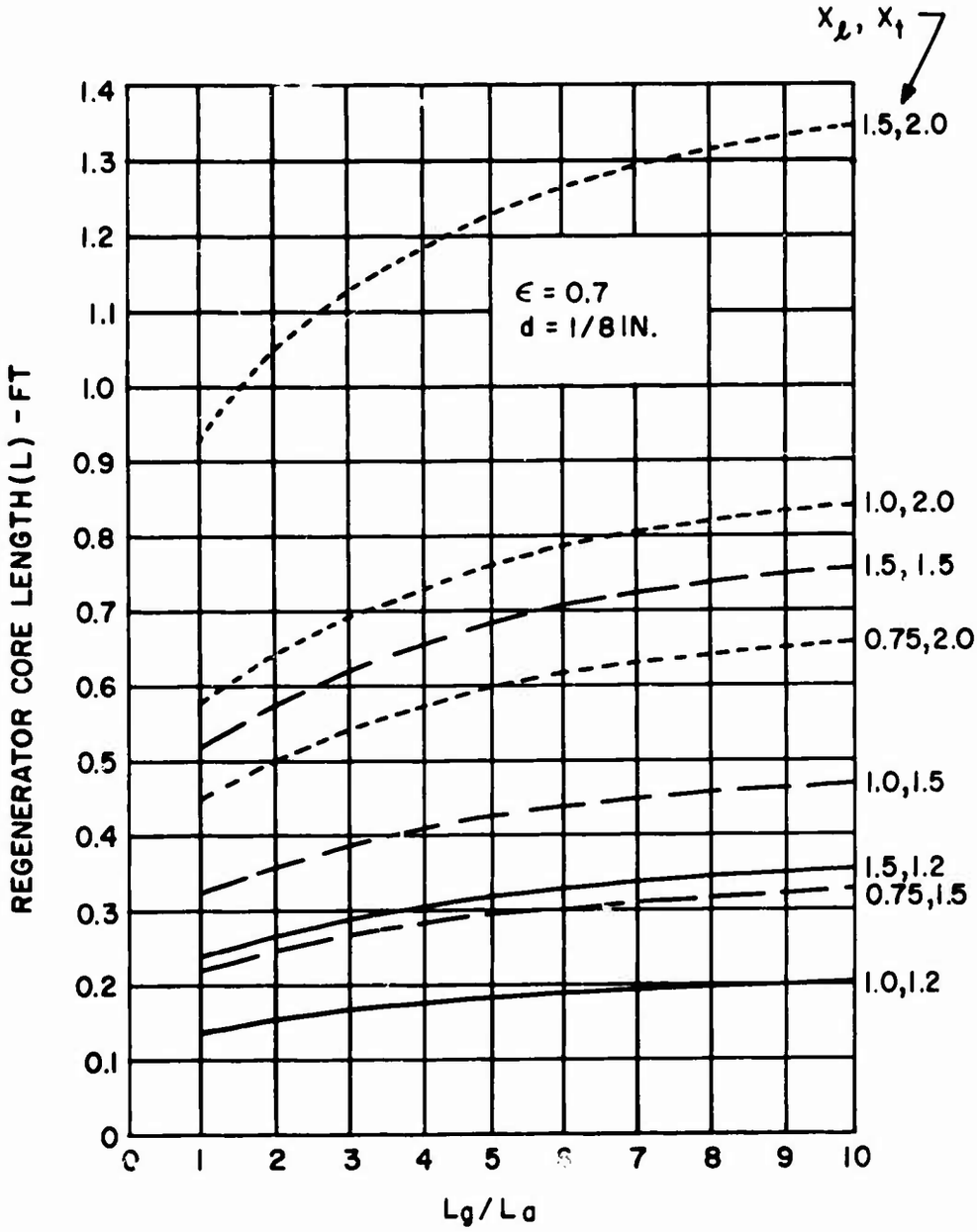

Figure 18. Variation of Core Length With Gas-Air Duct Width Ratio and Heat Pipe Spacing.

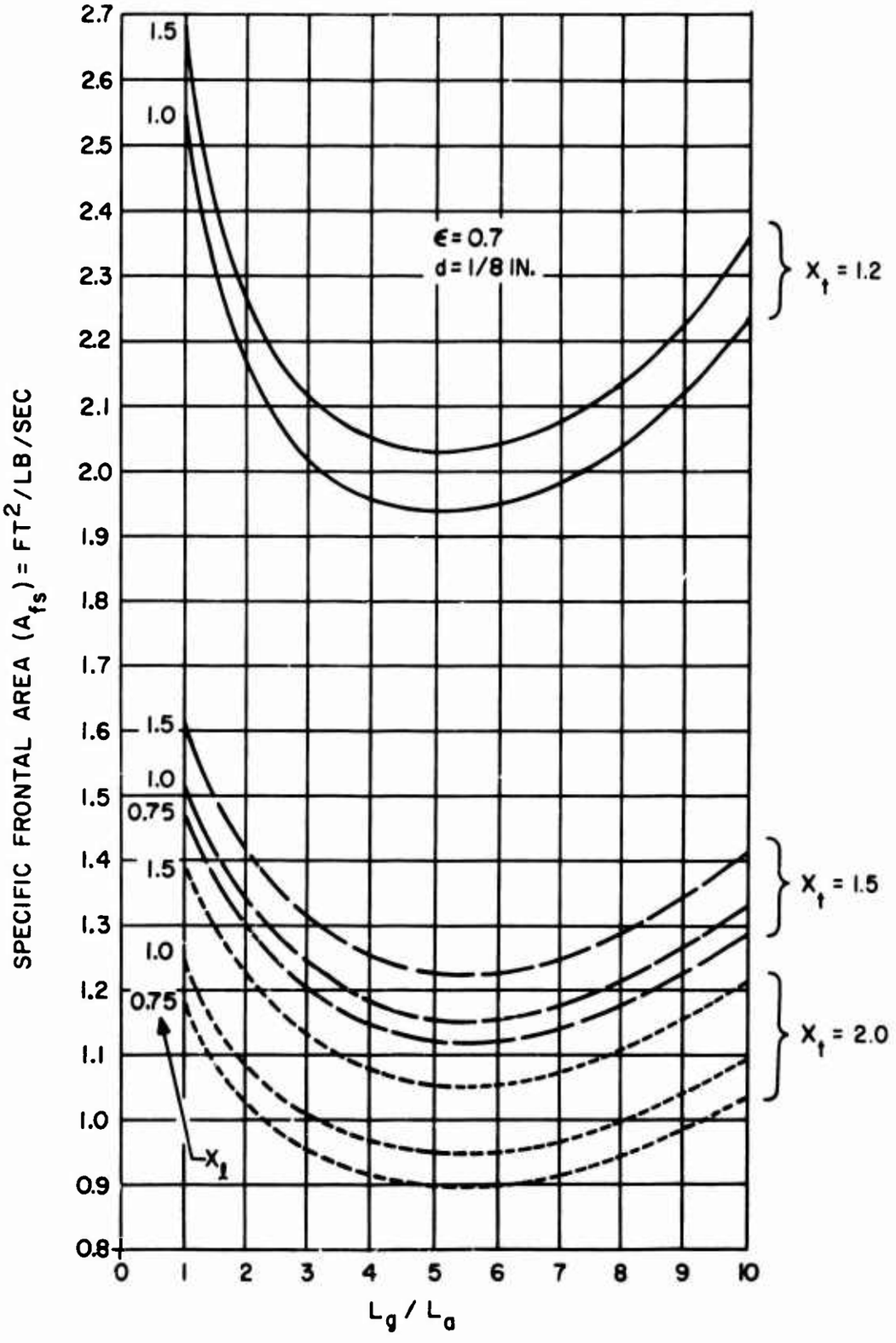

Figure 19. Variation of Specific Frontal Area With Gas-Air Duct Width Ratio and Heat Pipe Spacing.

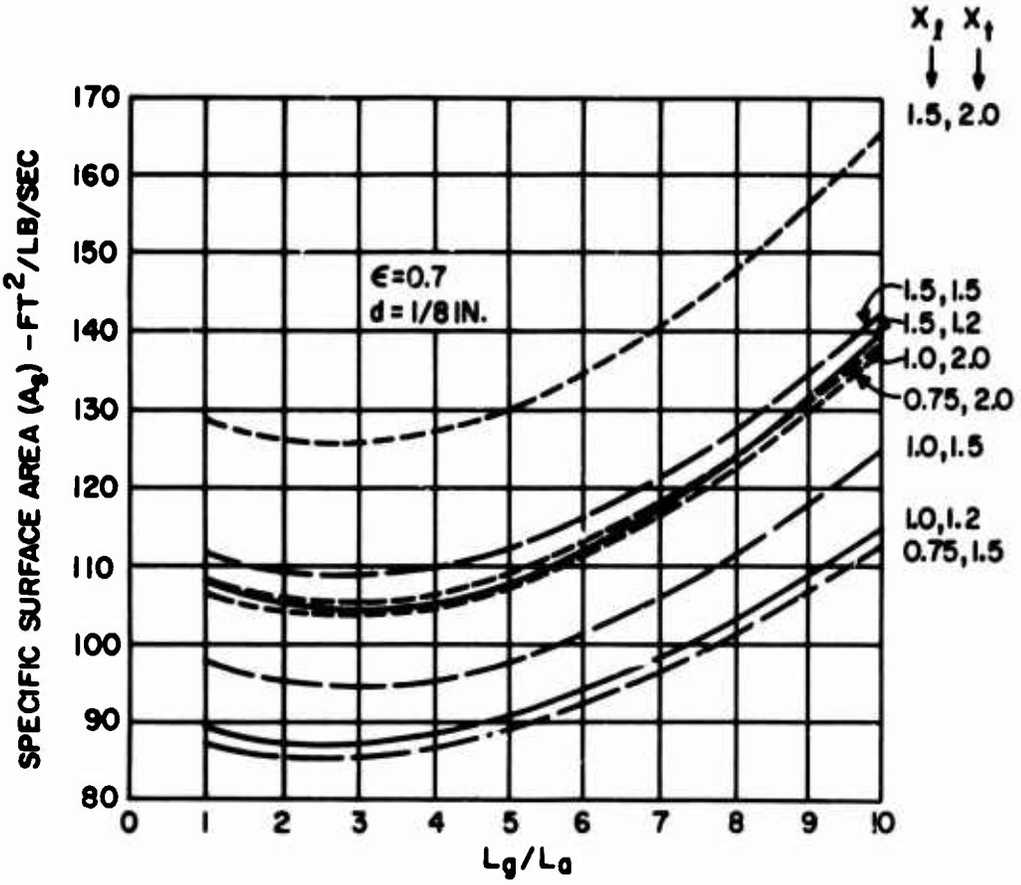

Figure 20. Variation of Specific Heat Transfer Surface Area With Gas-Air Duct Width Ratio and Heat Pipe Spacing.

choice of X_t is then dependent on the relative importance of small heat transfer surface area and short length versus small frontal area for a specific design application.

The effect of heat pipe diameter d and spacing on core characteristics is shown in Figures 21, 22, and 23 for $\epsilon = 0.7$ and $L_g/L_a = 4$. The effect of spacing is the same as that pointed out in the previous set of figures. As expected, the smallest feasible heat pipe diameter should be used to minimize core length, frontal area, and heat transfer area.

Specific Core Weight

The variation of specific core weight with heat pipe diameter d, wall thickness t, and the ratio of wick thickness to optimum wick thickness t_w/t_{wo} is shown

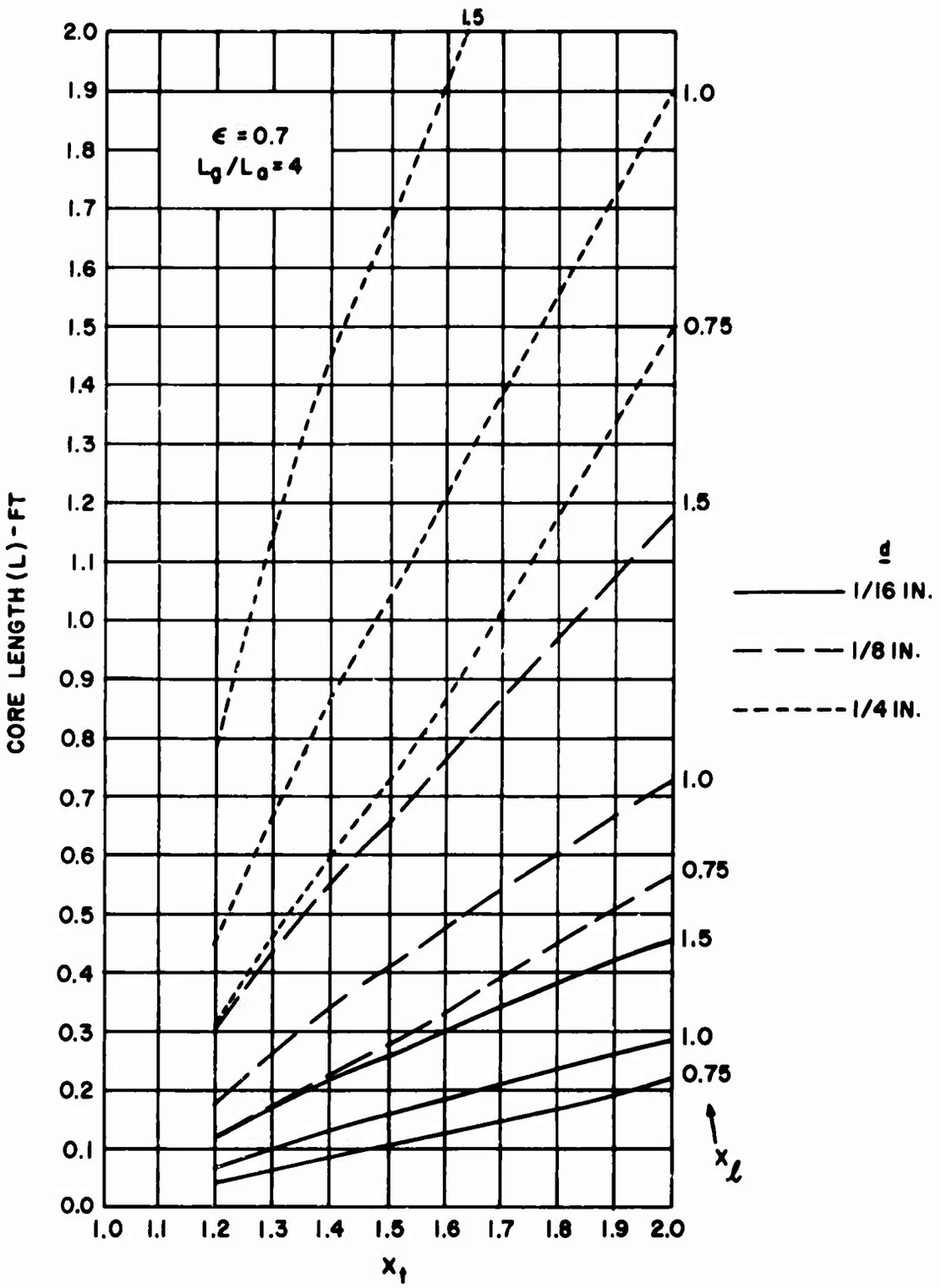

Figure 21. Effect of Heat Pipe Diameter and Spacing on Core Length.

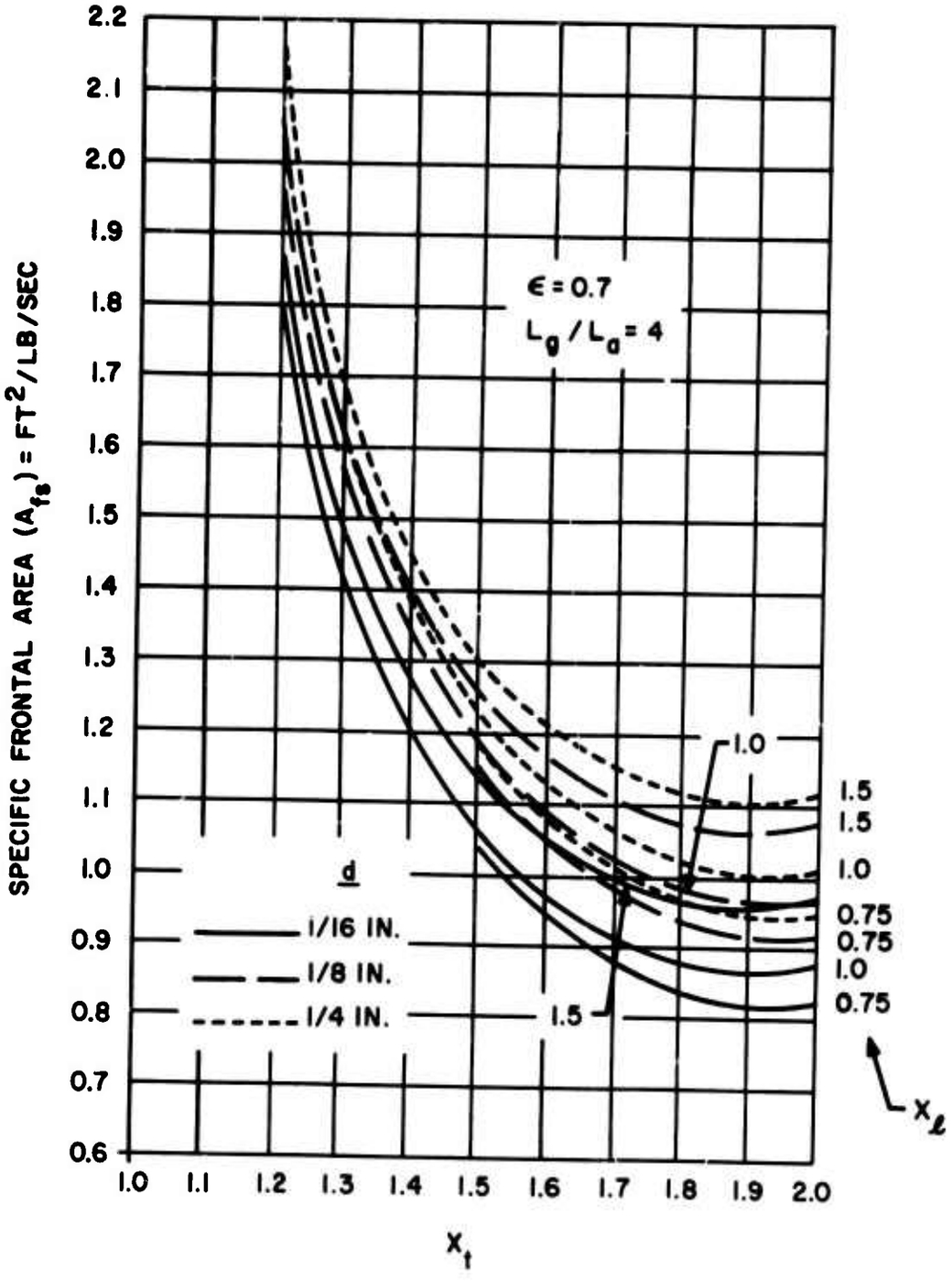

Figure 22. Effect of Heat Pipe Diameter and Spacing on Specific Frontal Area.

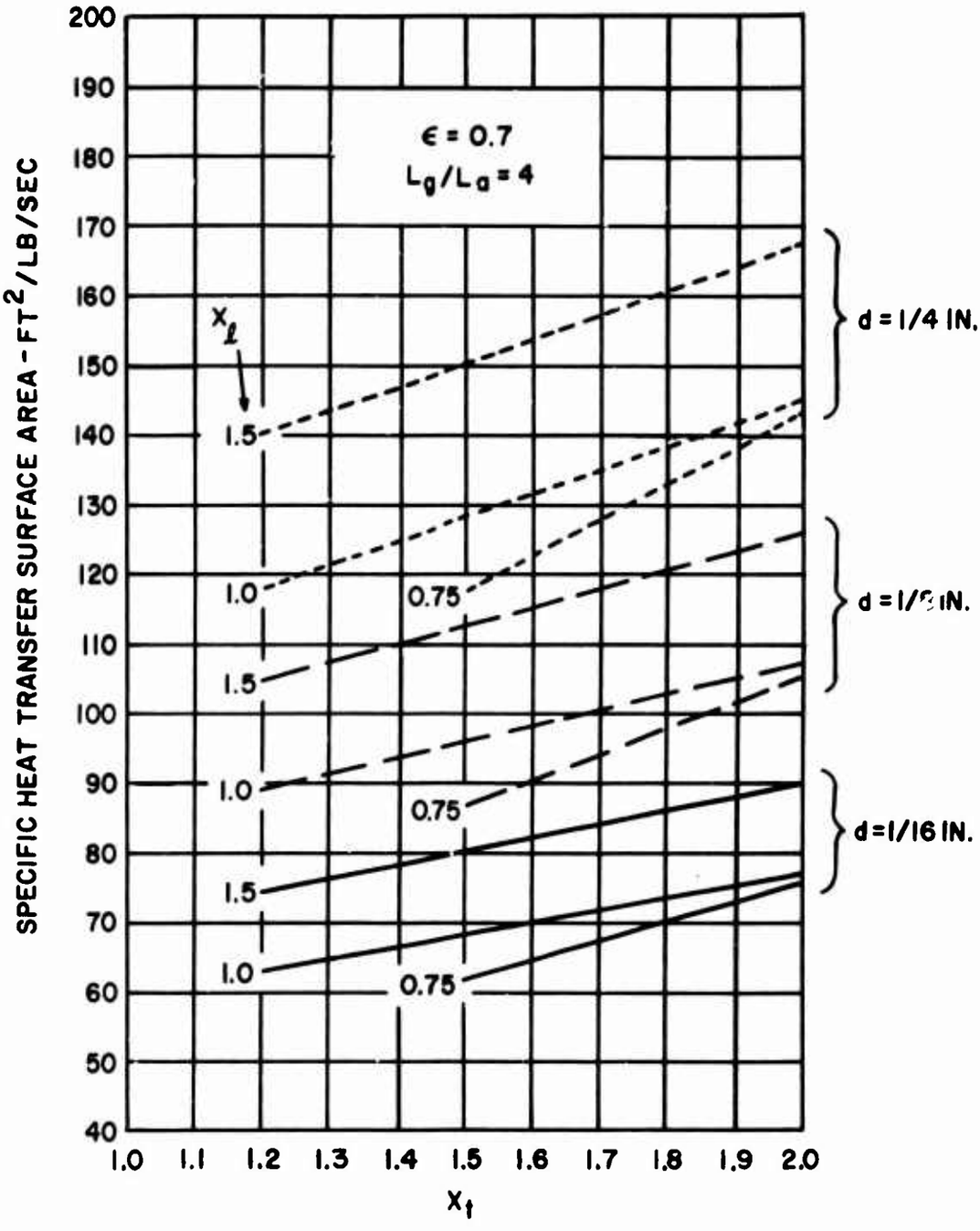

Figure 23. Effect of Heat Pipe Diameter and Spacing on Specific Heat Transfer Surface Area.

in Figure 24 for cesium heat pipes and in Figure 25 for mercury heat pipes. In both figures, $\epsilon = 0.7$, $L_g/L_a = 4$, $\phi = 0.85$, the heat pipe wall and wick are stainless steel, and the mean heat pipe liquid temperature is 932°F.

The heat pipe spacing parameters have the values $X_\ell = 1.0$ and $X_t = 1.5$. These values were selected as representative of spacings which could be fabricated without undue difficulty. A reduction of about 10 percent in A_s and W_{cs} and a slight reduction in A_{fs} would result from letting $X_\ell = 0.75$. If X_t were equal to 1.2, A_s and W_{cs} would be reduced by about 8 percent, but at the expense of roughly a 75-percent increase in A_{fs}. (See Figures 22 and 23.)

Figures 24 and 25 indicate, as expected, that for minimum core weight the minimum feasible wall and wick thicknesses should be used. When a 3-mil heat pipe wall is considered, the total heat pipe weight using the optimum wick thickness ($t_w/t_{wo} = 1$) is twice that of the heat pipe wall alone ($t_w/t_{wo} = 0$) for cesium heat pipes. For mercury heat pipes, the total weight is five times that of the wall. Thus, it is desirable to use a wick of less than optimum thickness. The penalty which must be paid for exercising this option is smaller wick pore radii.

In Figure 26, the specific core weight is shown as a function of diameter for cesium and mercury heat pipes, in which the wick thickness t_w is equal to the wall thickness t, using wall thicknesses which are believed to be feasible from the fabrication and corrosion viewpoint. The wall thicknesses used are shown as a function of heat pipe diameter. The data of Figure 26 were taken from Figures 24 and 25.

The minimum value of specific core weight, 10.7 lb/lb/sec, is attained with a 1/16-inch-diameter cesium heat pipe with 3-mil wall and wick thicknesses. The specific core weight is 20.2 lb/lb/sec for a 1/8-inch-diameter cesium heat pipe with 4-mil wall and wick thicknesses. If the wall and wick thicknesses of the 1/8-inch cesium heat pipe were less conservatively chosen to be 3 mils, the specific core weight would drop to 15.9 lb/lb/sec.

Heat Pipe Length

Since the maximum heat pipe length for isothermal operation is an increasing function of temperature, the length should be established at the minimum heat pipe temperature. The minimum heat pipe temperature T_{pmin} occurs at the compressed air inlet of the regenerator and is a function of the gas-side/air-side length ratio L_g/L_a and the regenerator effectiveness ϵ. Table VI shows T_{pmin} as a function of ϵ for $L_g/L_a = 4$.

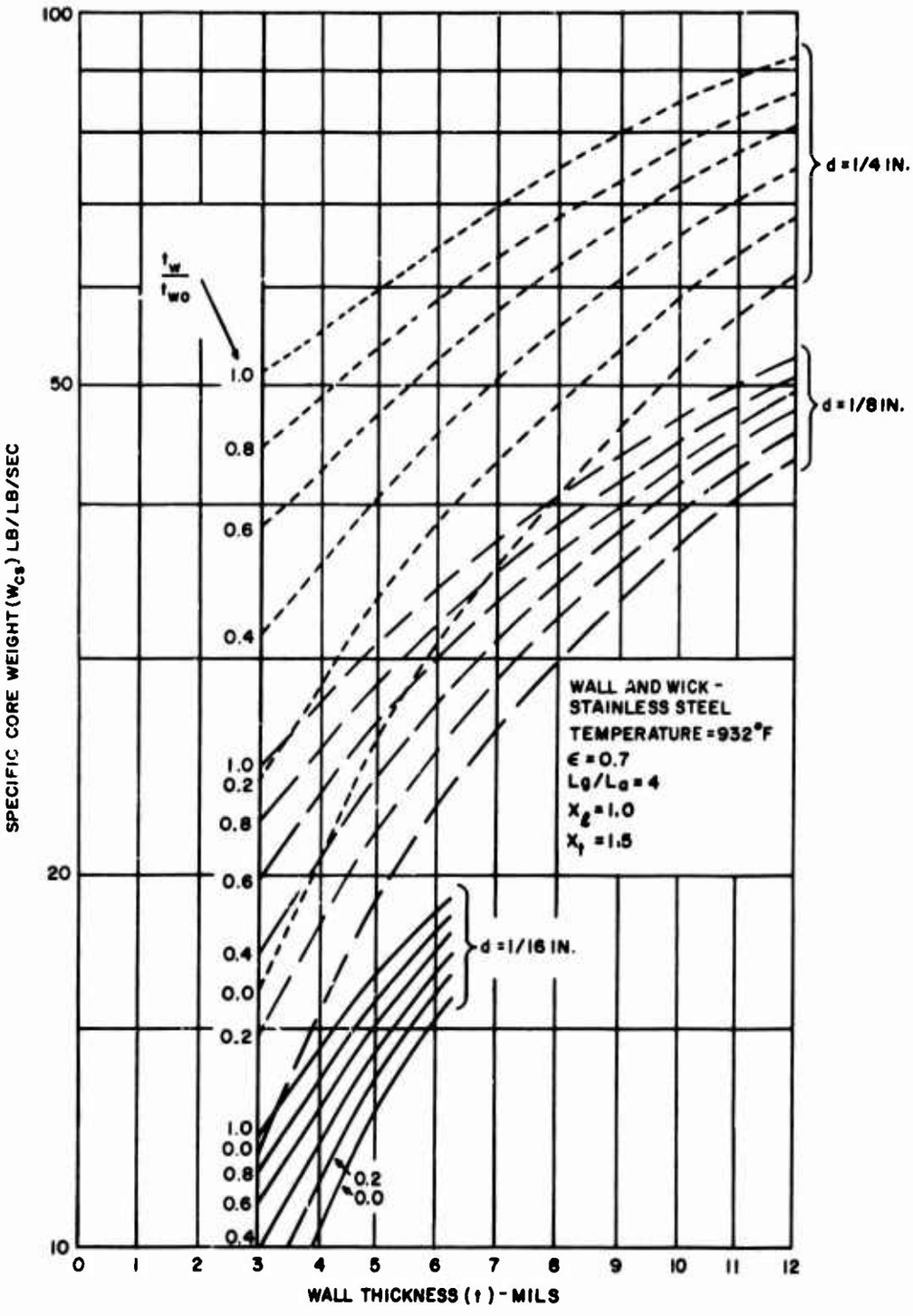

Figure 24. Effect of Wall and Wick Thickness on Specific Core Weight - Cesium Heat Pipes.

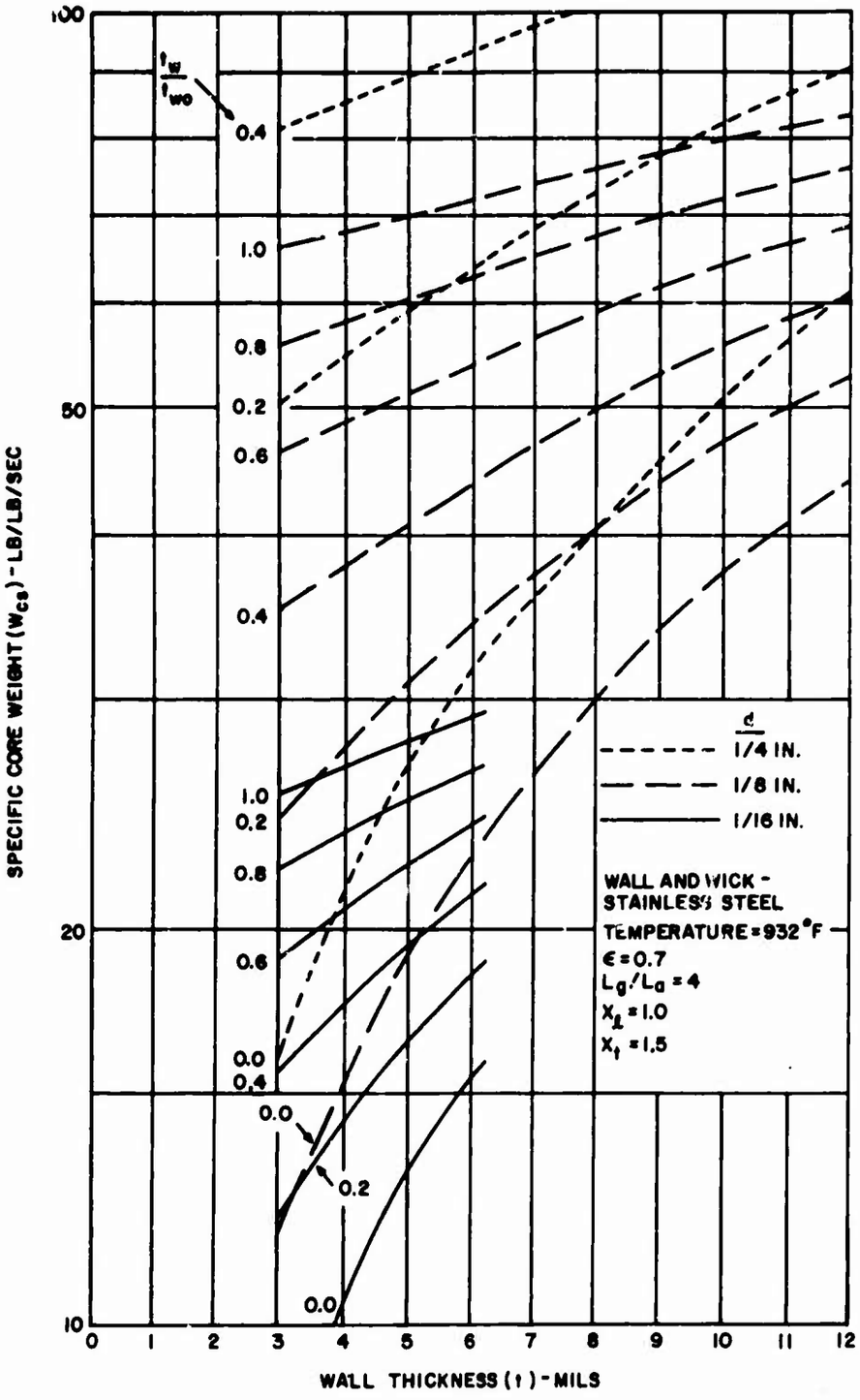

Figure 25. Effect of Wall and Wick Thickness on Specific Core Weight - Mercury Heat Pipes.

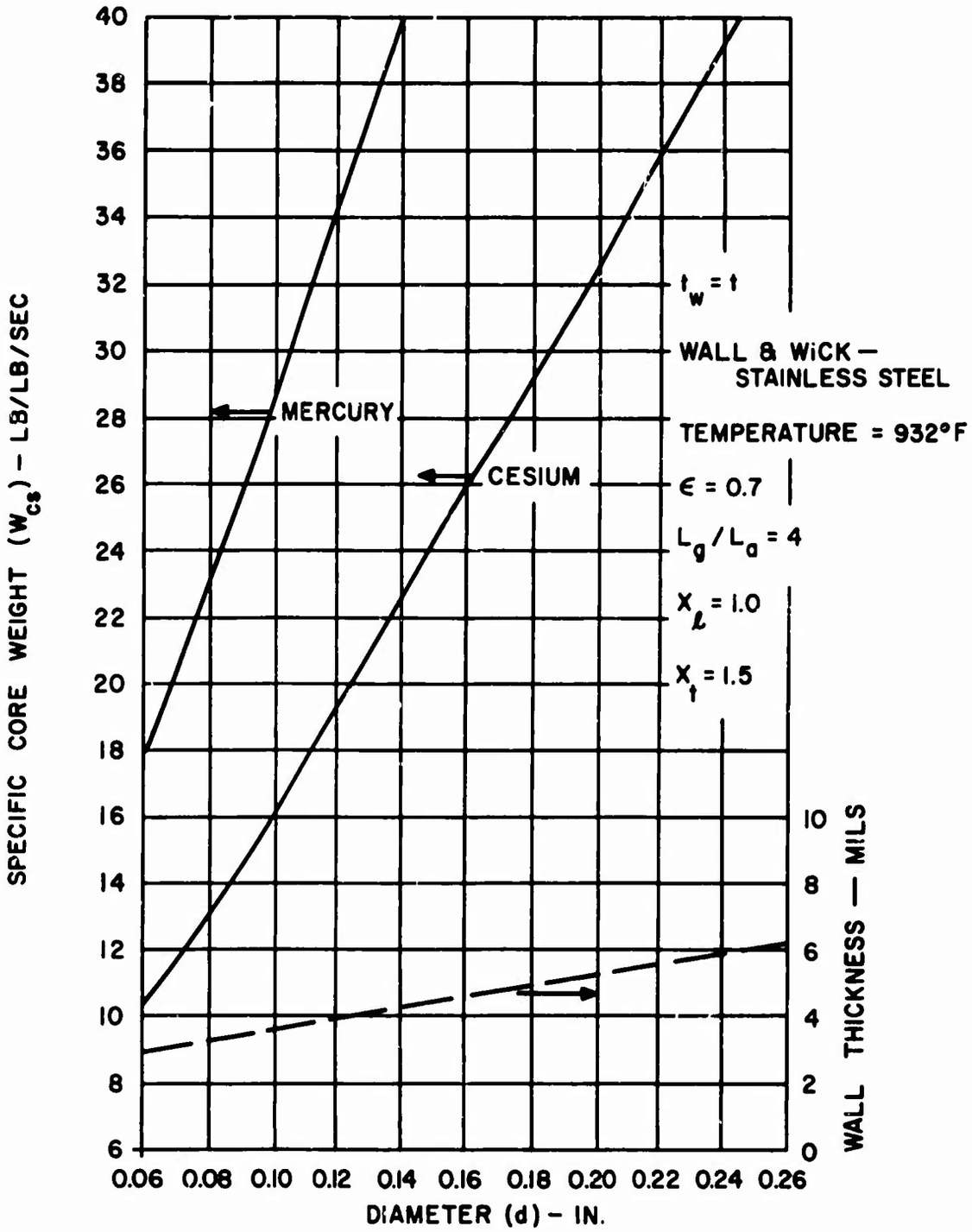

Figure 26. Regenerator Core weight vs. Heat Pipe Diameter.

TABLE VI. MINIMUM HEAT PIPE TEMPERATURE	
ϵ	T_{pmin} (°F)
0.5	874
0.6	830
0.7	785

In Figure 27, the maximum heat pipe length for isothermal operation L_p is shown as a function of heat pipe temperature and diameter for the indicated wall and wick thicknesses. The data apply for a regenerator effectiveness $\epsilon = 0.7$. From Equation (59) of Appendix II, L_p varies as $(T_g - T_{pmin})^{-1/2}$, where T_g is the outlet gas temperature. Since both T_g and T_{pmin} are functions of ϵ, the heat pipe lengths of Figure 27 must be multiplied by a correction factor for ϵ other than 0.7. The correction factors are:

Regenerator effectiveness	0.5	0.6	0.7
Correction factor	0.772	0.866	1.00

At a regenerator effectiveness of 0.7 and 785°F (the minimum heat pipe temperature), the length of the 1/16-inch-diameter heat pipe is 0.79 inch; for the 1/8-inch diameter, 2.85 inches; and for the 1/4-inch diameter, 9.80 inches. These lengths increase with temperature at a significant rate.

Where the required heat pipe length is larger than can be attained in a regenerator core with pipes of a single diameter, the required length may be achieved with the use of two different heat pipe diameters. For example, a length of 9.8 inches is unattainable in a core with 1/8-inch-diameter heat pipes. However, the 9.8-inch length is achievable if 1/4-inch-diameter pipes are used at heat pipe temperatures below 945°F and 1/8-inch-diameter pipes are used above 945°F.

Another possibility for increasing the allowable heat pipe length is to divide the heat pipe length into three ducts. Gas would flow through the central duct, and compressed air would flow through the two outside ducts. This arrangement would permit the heat pipe length to be doubled because the actual internal flow length would then be one-half the total pipe length.* While a doubling of the heat pipe length is achieved by the above scheme, a more complex ducting design results.

---

* Personal communication with J.E. Kemme, Los Alamos Scientific Laboratory, Los Alamos, New Mexico.

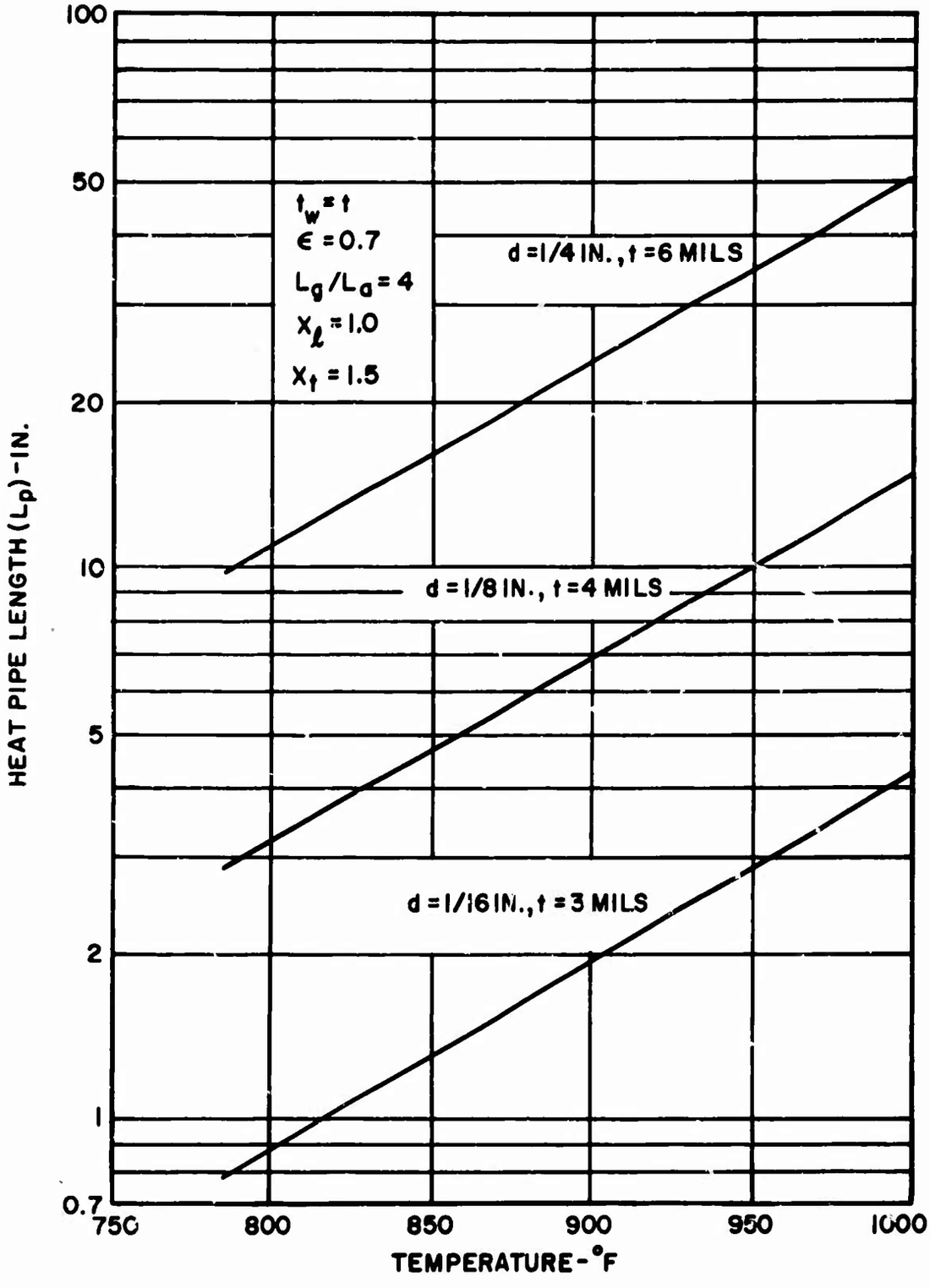

Figure 27. Maximum Length for Isothermal Operation of Cesium Heat Pipe.

For mercury at 785°F, the maximum isothermal length is 34 inches for a 1/16-inch-diameter pipe and in excess of 100 inches for 1/8- and 1/4-inch-diameter heat pipes. (The wall and wick thicknesses for which these data apply are the same as those indicated in Figure 27.) Since it is unlikely that such lengths will be required in a regenerator, mercury heat pipes of any reasonable length can be incorporated into a regenerator core with the assurance that they will function isothermally. (It must be stressed, however, that this conclusion is dependent on complete wetting of the heat pipe wick. Limited tests with mercury heat pipes indicate that wetting can be a problem.*)

Single-Zone Cores with Finned, Staggered Heat Pipes

The merits of using finned rather than smooth heat pipes in a regenerator core have been evaluated. The comparison was made on the basis of 1/4-inch-diameter, stainless steel heat pipes in a staggered arrangement.

The finned heat pipe geometry used is that of tube bank CF 8.72, which is described in Table 9.4 of Reference 18. The fin cross section is triangular. The absolute fin dimensions and heat pipe spacing are equal to 25/38 times the dimensions for tube bank CF 8.72, since the tube diameter of CF 8.72 is 0.38 instead of 0.25 inch. The height of fins on the 1/4-inch heat pipes is 0.178 inch, the mean fin width is 0.01183 inch, the pitch is 0.0755 inch, the transverse spacing is 0.642 inch, and the longitudinal spacing is 0.526 inch. The method of analysis for a finned heat pipe core is basically the same as that used for unfinned heat pipe cores. Both the analytical method and the heat transfer and friction data for tube bank CF 8.72 are given in Reference 18.

The unfinned 1/4-inch heat pipe core with which the finned heat pipe core was compared had a transverse spacing of 0.375 inch and a longitudinal spacing of 0.25 inch. In both cases an $L_g/L_a = 4$ was used, and the heat pipe wall thickness was 6 mils. The weight of the wick and heat pipe fluid, which is the same for the finned and unfinned pipes, was not included in the comparison of relative core weights. Results of the analysis are shown in Table VII.

The subscript "f" denotes the finned heat pipe core, and the subscript "u" denotes the unfinned heat pipe core. A_p denotes the primary surface area; i.e., the surface area of the pipe on which the fins are mounted. For the unfinned pipes, $A_p = A_s$. It can be seen from Table VII that the length of the finned core is about 60 percent longer than that of the unfinned core and that it has about 40 percent less frontal area. The finned core has more than twice the heat transfer surface of the

* Personal communication with G.Y. Eastman, Radio Corporation of America, Lancaster, Pennsylvania

unfinned core, but only about 20 percent of the primary surface. Since the total length of heat pipes in a core is proportional to the primary surface area, the total heat pipe length for the finned core is 20 percent of that for the unfinned core. Despite this fact, the finned core is almost twice as heavy as the unfinned core. The high weight of the finned core is due to the fins, whose weight is 8.13 times the weight of the heat pipe wall.

TABLE VII. COMPARISON OF FINNED AND UNFINNED HEAT PIPE REGENERATOR CORES

L_f/L_u	A_{fsf}/A_{fsu}	A_{sf}/A_{su}	A_{pf}/A_{pu}	W_{csf}/W_{csu}
1.61	0.59	2.33	0.2[illegible]	1.92

The high weight of the finned core offsets any advantages which might accrue from smaller frontal area and smaller total heat pipe length. Therefore, unfinned heat pipes are preferable to finned heat pipes for use in a regenerator core.

Single-Zone Cores with Smooth, In-line Heat Pipes

The merits of arranging the heat pipes in an in-line array instead of the staggered array which has been used have been evaluated. The comparative study was performed for 1/8-inch-diameter heat pipes with equal transverse and longitudinal spacings of 1.5 diameters, equal wall and wick thicknesses, a regenerator effectiveness of 0.7, and a gas-side/air-side length ratio of 5. Results of the study are presented in Table VIII.

TABLE VIII. COMPARISON OF IN-LINE AND STAGGERED HEAT PIPE REGENERATOR CORES

L_i/L_s	A_{fsi}/A_{fss}	$A_{si}/A_{ss} = W_{csi}/W_{css}$
1.24	0.775	0.972

The subscript "i" denotes in-line pipes, and the subscript "s" denotes staggered pipes.

It can be seen that the in-line core is about 3 percent lighter than the staggered core, has about 23 percent less frontal area, and is 24 percent longer. The increased length for the in-line core results from a lower pressure drop per unit flow length for in-line tube banks than for staggered tube banks. Since there is little change in the total heat transfer surface area, the increase in core length is accompanied by a comparable decrease in core frontal area.

A core with in-line heat pipes is thus somewhat preferable to one with staggered heat pipes, particularly when small frontal area is important. All the regenerator calculations in this report have been performed for the staggered arrangement, primarily because heat transfer and friction data were more readily available for flow normal to staggered tube banks. Application of the factors given in Table VIII to the characteristics of staggered heat pipe arrays with other diameters and spacings should yield a reasonable estimate of core characteristics for comparable in-line arrays.

Two-Zone Cores with Smooth, Staggered Heat Pipes

The basic heat pipe regenerator concept is quite flexible, permitting the use of different heat pipes in various sections of the core. In order to test this flexibility, five cores were investigated in which two distinct types of heat pipes were employed. In all the cores, the heat pipes above an arbitrarily selected temperature of 1000°F were 1/8-inch cesium-stainless heat pipes with a 4-mil wall and a 4-mil wick thickness. These are referred to as Zone A heat pipes. The Zone B heat pipes, defined as those with temperatures below 1000°F, are distinguished from those of Zone A by a different heat pipe fluid, wall and wick material, and/or pipe diameter.

The various Zone B heat pipes have the characteristics shown in Table IX.

TABLE IX. CHARACTERISTICS OF ZONE B HEAT PIPES

Zone	Fluid	Wall and Wick	Pipe Diameter (in.)	Wall Thickness (mils)	Wick Thickness (mils)
B1	Cesium	Titanium	1/8	4	4
B2	Cesium	Titanium	1/4	6	6
B3	Cesium	Stainless	1/4	6	6
B4	Mercury	Stainless	1/8	4	4
B5	Mercury	Stainless	1/16	3	3

For both Zones A and B, the longitudinal spacing is 1 diameter, the transverse spacing is 1.5 diameters, the gas-side/air-side length ratio is 4, and the heat pipes are the same length.

Complete cores consisting of a Zone B plus a Zone A are denoted by B1-A, B2-A, etc. A single-zone core composed entirely of Zone A heat pipes is denoted by A-A and is included for comparative purposes.

The core length, specific frontal area, specific weight, heat pipe length, and specific number of heat pipes N_s of the various core types are shown as a function of regenerator effectiveness in Figures 28 through 31. The core length, specific weight, and specific number of heat pipes were found by weighting L, W_{cs}, and N_s for single-zone cores by the fraction of the total heat transfer surface above 1000°F (for single-zone cores composed of Zone A heat pipes) and the fraction below 1000°F (for single-zone cores composed of Zone B heat pipes) and then by adding the weighted values. The frontal area was taken to be that for the single-zone core with the largest A_{fs}. The heat pipe length in the combined core was taken to be that for the single-zone core with the smallest heat pipe length.

The core length, specific frontal area, specific weight, and specific number of heat pipes increase with regenerator effectiveness for all core types. The heat pipe length increases with ϵ for the mercury cores (B4-A, B5-A), reaches a maximum at $\epsilon = 0.6$ for the 1/4-inch-diameter cesium cores (B2-A, B3-A), and decreases with ϵ for the 1/8-inch-diameter cesium cores (A-A, B1-A).

There is little variation in frontal area for the various core types. The core length increases by about 70 percent over that of a single-zone core when 1/4-inch-diameter pipes replace 1/8-inch-diameter pipes in Zone B (cores B2-A, B3-A), and decreases by about 25 percent when 1/16-inch-diameter pipes are used in Zone B (core B5-A).

The change in core weight from that of the single-zone core depends on the specific combination of diameter, fluid, and wall and wick material used in Zone B. The use of 1/8-inch, cesium-titanium heat pipes (core B1-A) reduces weight by 13 percent. Weight is reduced slightly with 1/16-inch, mercury-stainless heat pipes (core B5-A). Core weight goes up by 15 percent with 1/4-inch, cesium-titanium heat pipes (core B2-A), 50 percent with 1/4-inch, cesium-stainless heat pipes (core B3-A), and 35 percent with 1/8-inch-diameter, mercury-stainless heat pipes (core B4-A).

One objective of changing the heat pipe fluid and/or the heat pipe diameter in Zone B was to increase the maximum heat pipe length significantly. Figure 30 shows that this objective is achieved. The length of the 1/8-inch-diameter cesium heat pipes (cores A-A, B1-A) is in the range from 2.85 to 3.9 inches. For the 1/4-inch-diameter cesium heat pipes (cores B2-A, B3-A), L_p lies in the range from

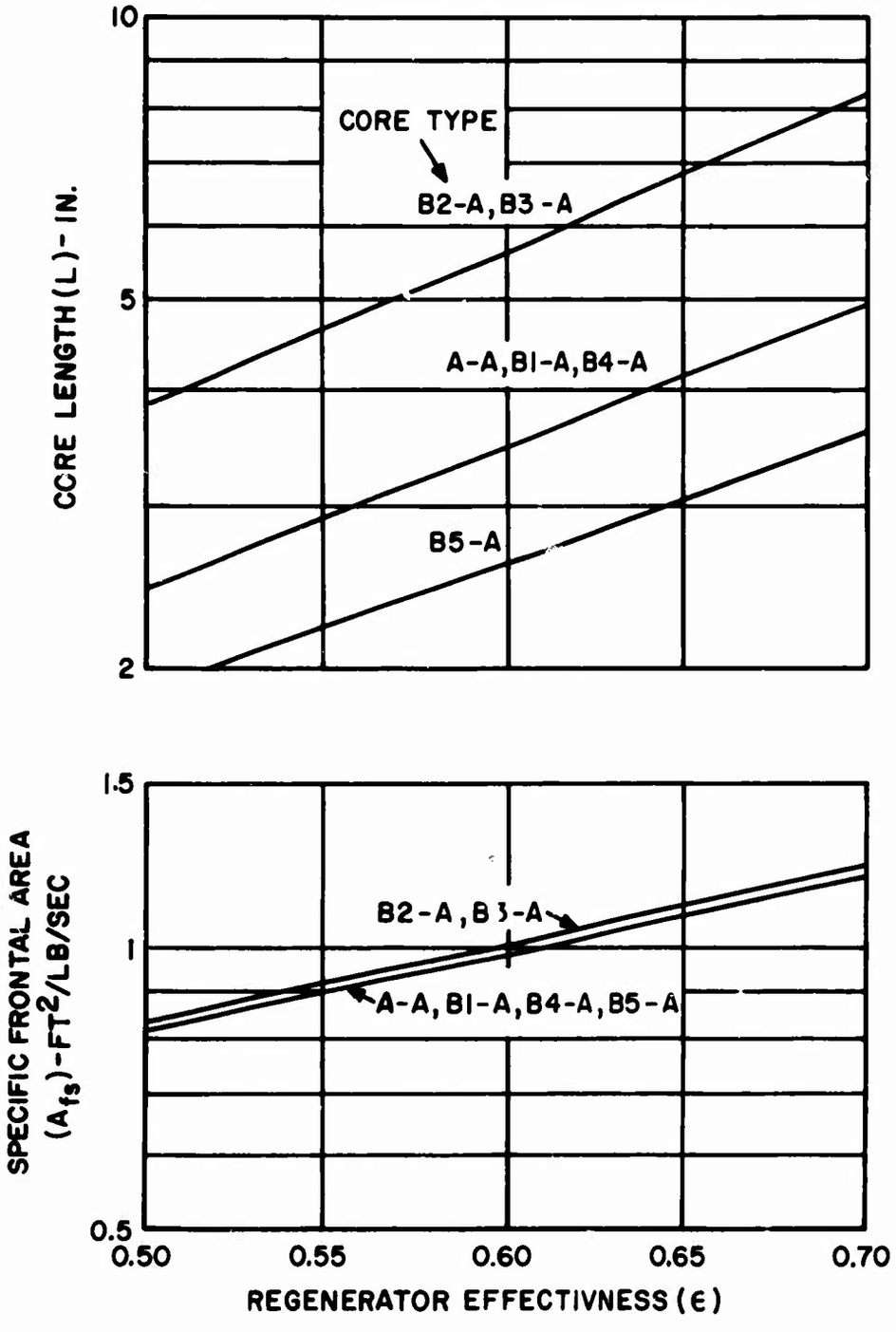

Figure 28. Core Length and Specific Frontal Area of Two-Zone Regenerator Cores.

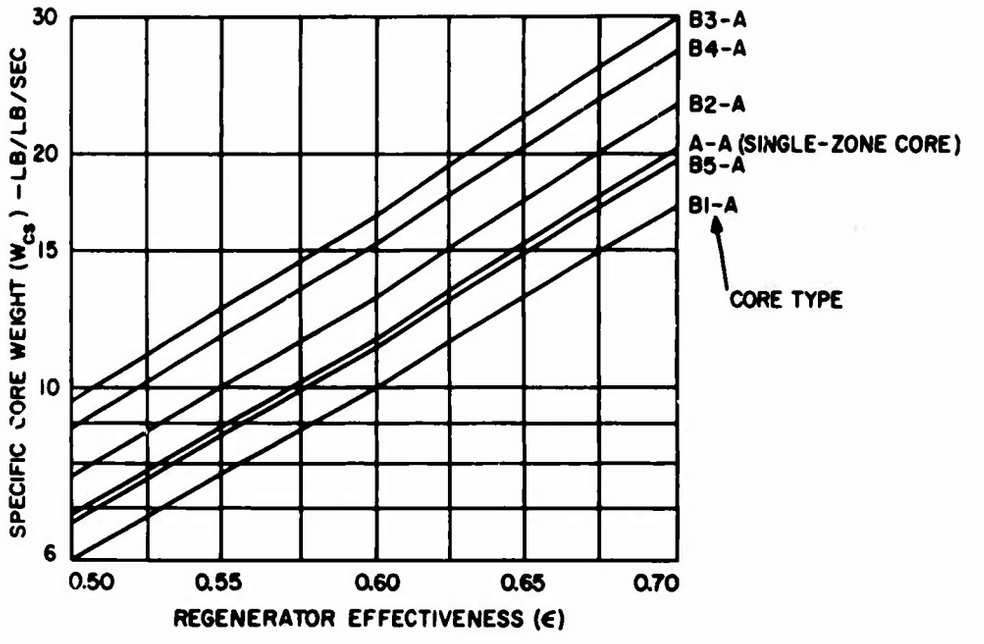

Figure 29. Specific Core Weight of Two-Zone Regenerator Cores.

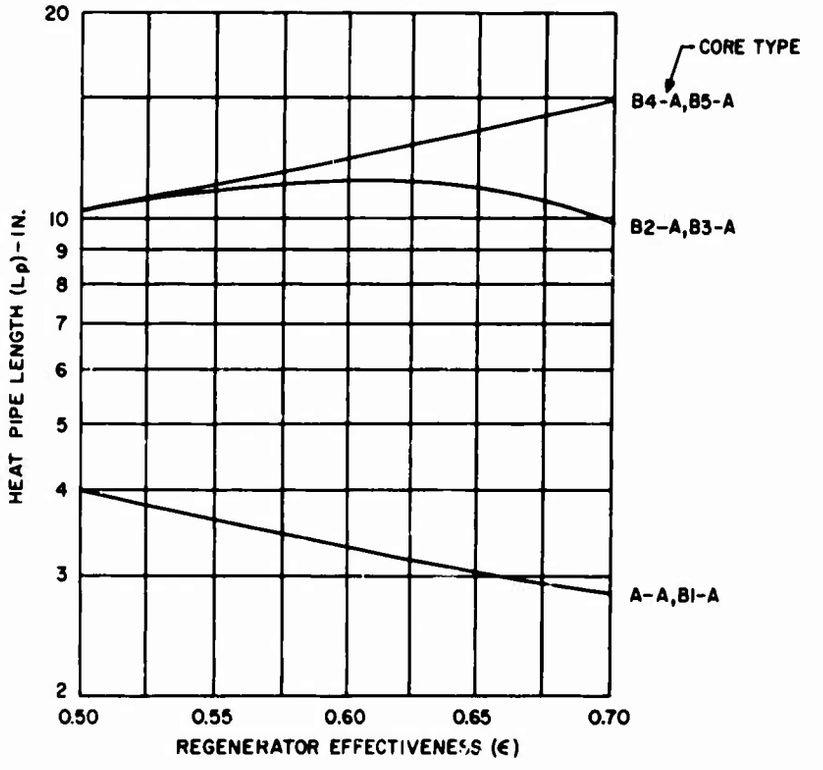

Figure 30. Heat Pipe Length of Two-Zone Regenerator Cores.

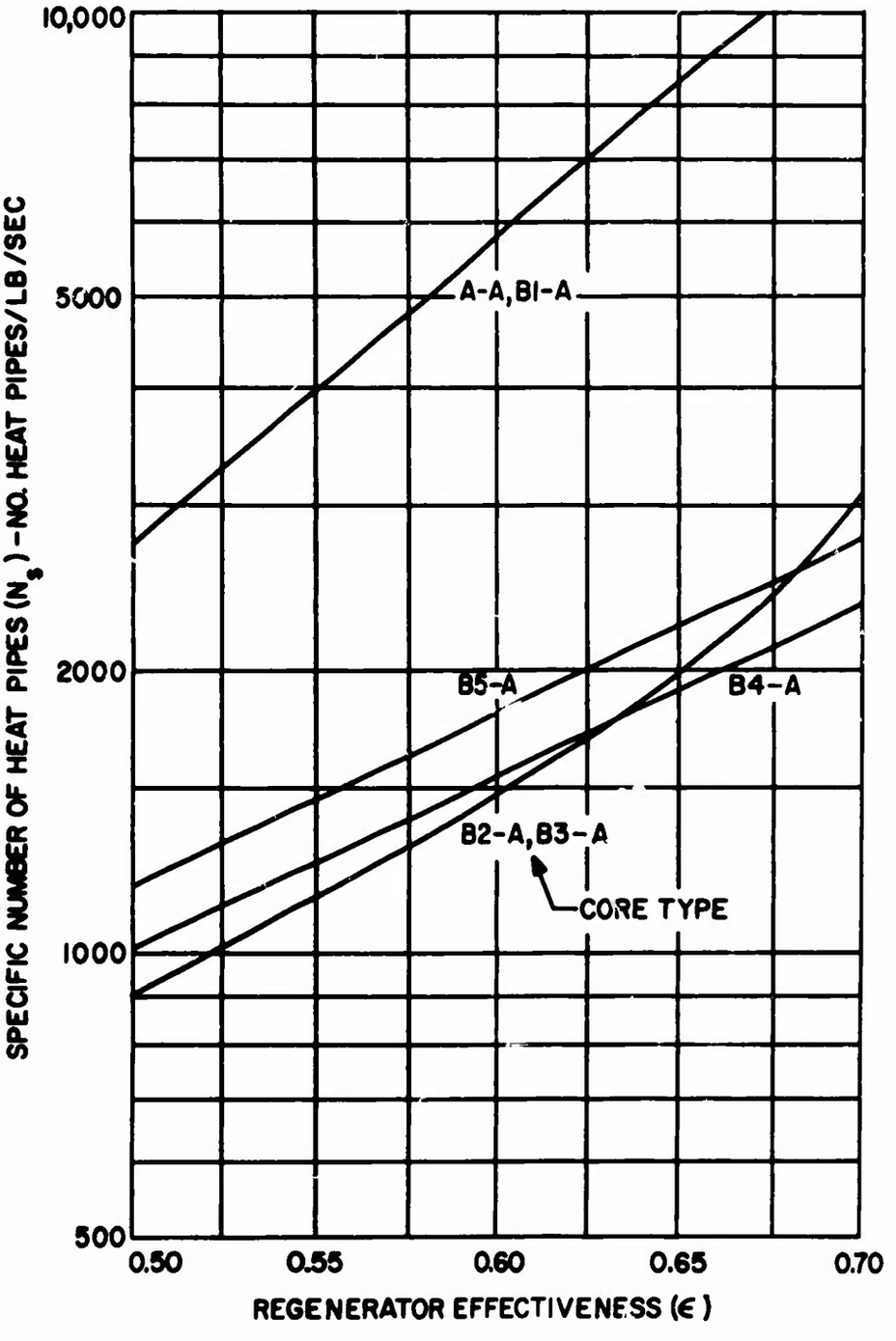

Figure 31. Specific Heat Pipe Number of Two-Zone Regenerator Cores.

9.6 to 11.3 inches. For the mercury heat pipes (cores B4-A, B5-A), L_p varies from 10.3 to 15 inches. An increase in heat pipe length is accompanied by a sharp reduction in the number of heat pipes to be fabricated, as is evident from Figure 31.

The wick pore radii r_p and r_{pn} for the heat pipes of each zone are given in Table X. All the cores require nonuniform wicks ($r_{pn} < r_p$) in order to utilize the heat pipe lengths shown in Figure 30. The pore radii vary in size from 1.5 to 38 microns. The radial pore radii r_{pn} have been corrected to insure proper functioning of the heat pipes when they are aligned in any orientation (in the absence of external acceleration).

From the above discussion, it may be concluded that the use of larger diameter and/or mercury heat pipes in the cooler zone of a cesium heat pipe core can substantially increase the allowable heat pipe length. The increased length requires the use of nonuniform wicks with radial pore radii as small as 1.5 microns. At the same time, the number of heat pipes required undergoes a sharp decrease. A weight penalty is generally incurred, which can be minimized by the use of titanium as the heat pipe wall and wick material in the cooler section of the core. The changes in core length and frontal area accompanying the cooler zone modifications can probably be accommodated with little difficulty.

TABLE X. WICK PORE RADII FOR TWO-ZONE REGENERATOR CORES

Core Type	Regenerator Effectiveness											
	0.5				0.6				0.7			
	Zone B		Zone A		Zone B		Zone A		Zone B		Zone A	
	$r_p(\mu)$	$r_{pn}(\mu)$	$r_p(\mu)$	$r_{pn}(\mu)$	$r_p(\mu)$	$r_{pn}(\mu)$	$r_p(\mu)$	$r_{pn}(\mu)$	$r_p(\mu)$	$r_{pn}(\mu)$	$r_p(\mu)$	$r_{pn}(\mu)$
A-A	25.5	9.3	25.5	9.3	25.5	16.8	25.5	16.8	25.5	19.9	25.5	19.9
B1-A	25.5	9.3	25.5	9.3	25.5	16.8	25.5	16.8	25.5	19.9	25.5	19.9
B2-A	38.0	3.1	25.5	1.5	38.0	6.1	25.5	1.7	38.0	10.4	25.5	3.3
B3-A	38.0	3.1	25.5	1.5	38.0	6.1	25.5	1.7	38.0	10.4	25.5	3.3
B4-A	25.5	11.6	25.5	1.5	25.5	8.2	25.5	1.5	25.5	7.5	25.5	1.5
B5-A	19.1	2.8	25.5	1.5	19.1	2.7	25.5	1.5	19.1	2.6	25.5	1.5

EVALUATION OF HEAT PIPE REGENERATORS

In previous sections of this report, the current status of heat pipe technology was reviewed, and the results of heat pipe regenerator design studies were presented. In this section, the characteristics of heat pipe regenerators are assessed with respect to anticipated Army aircraft propulsion system needs, and technical problems which have a bearing on feasibility are discussed.

The evaluation will take into account the following design considerations: weight, integration with gas turbine, structural integrity, lifetime and reliability, operational performance, cost, and fabrication. A nominal, single-zone core design will be used as a basis for reference. Modifications to the nominal design which result in improved characteristics will also be considered. The characteristics of the nominal core design are presented in Table XI for regenerator effectivenesses of 0.5 to 0.7.

TABLE XI. CHARACTERISTICS OF NOMINAL REGENERATOR CORE DESIGN

	Regenerator Effectiveness		
	0.5	0.6	0.7
Heat Pipe			
Fluid	Cesium	Cesium	Cesium
Wall and Wick	Stainless	Stainless	Stainless
Diameter (d) - in.	1/8	1/8	1/8
Gas-Side Length/Air-Side Length (L_g/L_a)	4	4	4
Wall Thickness (t) - mils	4	4	4
Wick Thickness (t_w) - mils	4	4	4
Wick Porosity (ϕ)	0.85	0.85	0.85
Wick Tortuosity (b)	11.2	11.2	11.2
Heat Pipe Length (L_p) - in.	3.92	3.28	2.85
Minimum Heat Pipe Temperature (T_p) - °F	874	830	785
Heat Transport Rate (Q) - Btu/hr*	112.0	66.7	38.6
Wick Mean Pore Radii			
Axial (r_p) - microns	25.5	25.5	25.5
Radial (r_{pn}) - microns	9.3	16.8	19.9
Acceleration Parameter (α)*	0.161	0.196	0.223

TABLE XI - Continued

	Regenerator Effectiveness		
	0.5	0.6	0.7
Core			
Heat Transfer Area/Unit Vol. (α) - ft^2/ft^3	202	202	202
Free-Flow Area/Unit Frontal Area	0.333	0.333	0.333
Heat Pipe Spacing (staggered)			
Transverse ($X_t d$) - in.	3/16	3/16	3/16
Longitudinal ($X_l d$) - in.	1/8	1/8	1/8
Length (L) - in.	2.46	3.44	4.92
Specific Frontal Area (A_{fs}) - ft^2/lb/sec	0.815	0.975	1.19
Specific Heat Transfer Surface (A_s) - ft^2/lb/sec	32.8	54.9	96.0
Specific Weight (W_{cs}) - lb/lb/sec	6.90	11.5	20.2
Specific Number of Heat Pipes (N_s) - No./lb/sec	2740	5800	12,400

*No external acceleration.

SPECIFIC CORE WEIGHT

In Table XII, the specific core weight of the nominal design is compared with the estimated total specific regenerator weights presented in Reference 19 and with the core and total specific regenerator weights for a tube-type regenerator with the same design criteria.[13]

TABLE XII. REGENERATOR SPECIFIC WEIGHT COMPARISON (lb/lb/sec)

	Regenerator Effectiveness					
	0.5		0.6		0.7	
	Core	Regenerator	Core	Regenerator	Core	Regenerator
Nominal Heat Pipe Design	6.9		11.5		20.2	
Ref. 19		7-8.5		11-13		19-22
Tube-type, Ref. 13					10.2-11.3	20.2-21.3

The nominal design core weight is seen to be about twice that of the tube-type core. In order to fall within the range of estimated total regenerator weights of Reference 19, the structural, header, and duct specific weight of the nominal design would have to be on the order of 1.5 lb/lb/sec or less. Although total regenerator weight studies have not been carried out in this report, it is estimated that a heat pipe regenerator arranged in a cylindrical configuration with radial heat pipes would have a specific total regenerator weight about 2 to 4 lb/lb/sec greater than the specific core weight.

The primary factor responsible for the specific core weight differential between the heat pipe and tube-type cores is tube diameter. From Figure 26, a cesium core with 0.060-inch-diameter heat pipes (the same as the tube diameter of the tube-type core) would have a specific weight of 10.5 lb/lb/sec. Heat pipes of 0.060-inch diameter were not specified for the nominal design because (1) it was felt that this represented too great an extension of the limits of current heat pipe technology (the smallest heat pipes thus far fabricated have 1/4-inch diameters), (2) the heat pipe length would then be less than 1 inch, and (3) the number of heat pipes required would be about 5 times that for 1/8-inch-diameter heat pipes.

Specific weights of the nominal heat pipe core design could be reduced by about 20 percent if the wall and wick thicknesses were taken to be 3 mils rather than 4 mils. The 3-mil thickness is adequate from static structural considerations. However, in view of the corrosion problems encountered in exhaust gas with the tube-type core (which had 3-mil-thick stainless tube walls) and the probable need for greater structural rigidity in a vibration environment, the 4-mil thickness was specified.

The core specific weight could be reduced by about 7 percent if a transverse spacing of 1.2 diameters rather than 1.5 diameters were used. While such a step is conceivably feasible from fabrication considerations, the frontal area would then increase by about 65 percent. This large increase in frontal area was considered to be undesirable, as it could lead to an excessive number of flow ducts for a core with relatively short heat pipes.

Another possibility for reduction of core weight involves the use of a two-zone core in which titanium is substituted for stainless steel in the heat pipes below 1000°F. From Figure 29, specific core weight can be reduced by about 15 percent in this manner. This design alternative would increase heat pipe costs by about 50 percent.

Should longer heat pipes than are available with single-zone cores be necessary to meet specific design requirements, then two-zone cores must be employed. While added heat pipe length can theoretically be achieved with a simultaneous weight reduction through the use of 1/13-inch-diameter mercury-stainless heat pipes in the cooler zone of the core (core B5-A), the uncertainty in both the heat transport capacity of actual mercury heat pipes and the fabricability of 1/16-inch-diameter heat pipes ruled out this possibility.

If core B4-A is also ruled out on the basis of uncertain performance of mercury heat pipes, the choice of two-zone core types would then reduce to B2-A or B3-A. These cores utilize 1/4-inch-diameter cesium-titanium or cesium-stainless heat pipes in Zone B and 1/8-inch-diameter cesium-stainless heat pipes in Zone A. (Hastelloy X is an alternate possibility for the heat pipe material in Zone A.) (Since the frontal area of Zone B of these cores is slightly larger than the frontal area of Zone A [see Figure 28], a small transition section will be required between the two core zones. The weight of this section should not significantly increase core weight.)

INTEGRATION WITH GAS TURBINE

The cylindrical core configuration of Figure 6, with radial heat pipes and axial flow paths, can be readily integrated with a gas turbine engine which utilizes an axial-flow turbine.* As shown in Figure 32, the core would be mounted directly in or behind the turbine exhaust duct. Ideally, single gas and air flow ducts would be used. Then the air duct would be located completely outside the exhaust gas duct. If multiple ducts are required, then some of the air ducts would have to be located inside the exhaust gas duct, compromising the simplicity of the concept.

Exhaust gas would flow axially over the gas-side length of the heat pipes and then be discharged without sharp directional changes. As a result, the total exhaust gas pressure loss should not be greatly in excess of that experienced by the exhaust gas in passing through the regenerator core. Also, it should be possible to accommodate the heat pipe regenerator core with a minimal increase in overall engine length. The engine may develop a "midriff bulge", however.

In contrast, other regenerator types may require the exhaust gas to undergo several changes of direction prior to discharge, which can result in exhaust duct losses of comparable magnitude to the pressure loss through the core. In addition, such regenerators can form a rather ungainly appendage to the rear of the engine, substantially increasing engine length.

Inlet air would be ducted from the compressor exit to an annular inlet plenum. After flowing over the air-side length of the heat pipes, the heated air would be collected in an annular exit plenum and then would be ducted to the combustor inlet.

---

*Although the rectangular configuration of Figure 4 has been used to evaluate regenerator core characteristics, the results should be applicable to the cylindrical configuration of Figure 6 if the mean spacings between heat pipes are comparable. Some differences are to be expected, however, because of the radially-varying transverse spacing in the latter case.

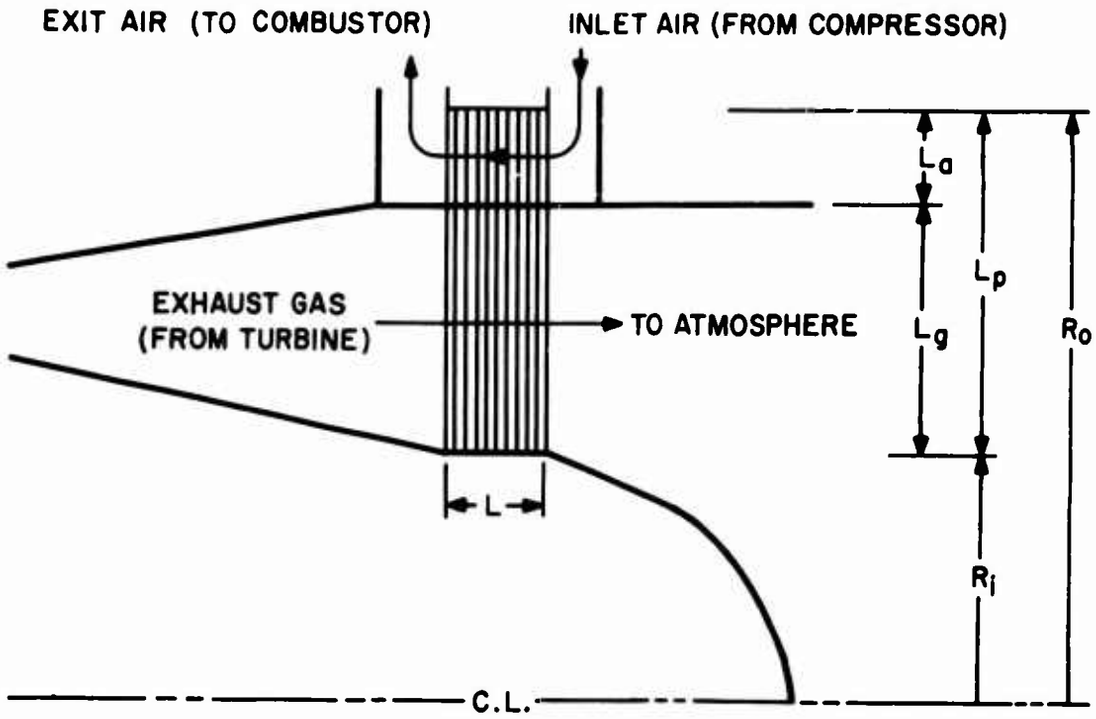

Figure 32. Schematic of Radial Heat Pipe Regenerator in Turbine Exhaust Gas Duct.

Because of lower probable duct pressure losses, the weight of heat pipe regenerators should compare more favorably to that of other regenerator types when the weight comparison is carried out on the basis of the same total pressure loss (rather than the same core pressure loss).

The feasibility of the configuration of Figure 32 will depend on the compatibility of regenerator core and engine dimensions. For a given frontal area and heat pipe length, the inner and outer regenerator radii are readily determined from geometrical considerations. In Figure 33, inner and outer regenerator radii are shown as a function of flow rate and regenerator effectiveness for the nominal design core and the two-zone cores B2-A and B3-A. The radii of the nominal design core, shown in tabular form in Figure 33, are too large to be of interest. For flow rates of 5 lb/sec and regenerator effectivenesses of 0.5 and 0.6, the regenerator radii for the two-zone cores do not appear to be unreasonable.

STRUCTURAL INTEGRITY

The wall thicknesses of 4 mils for 1/8-inch heat pipes and 6 mils for 1/4-inch heat pipes are adequate to withstand the stresses produced by radial pressure differences

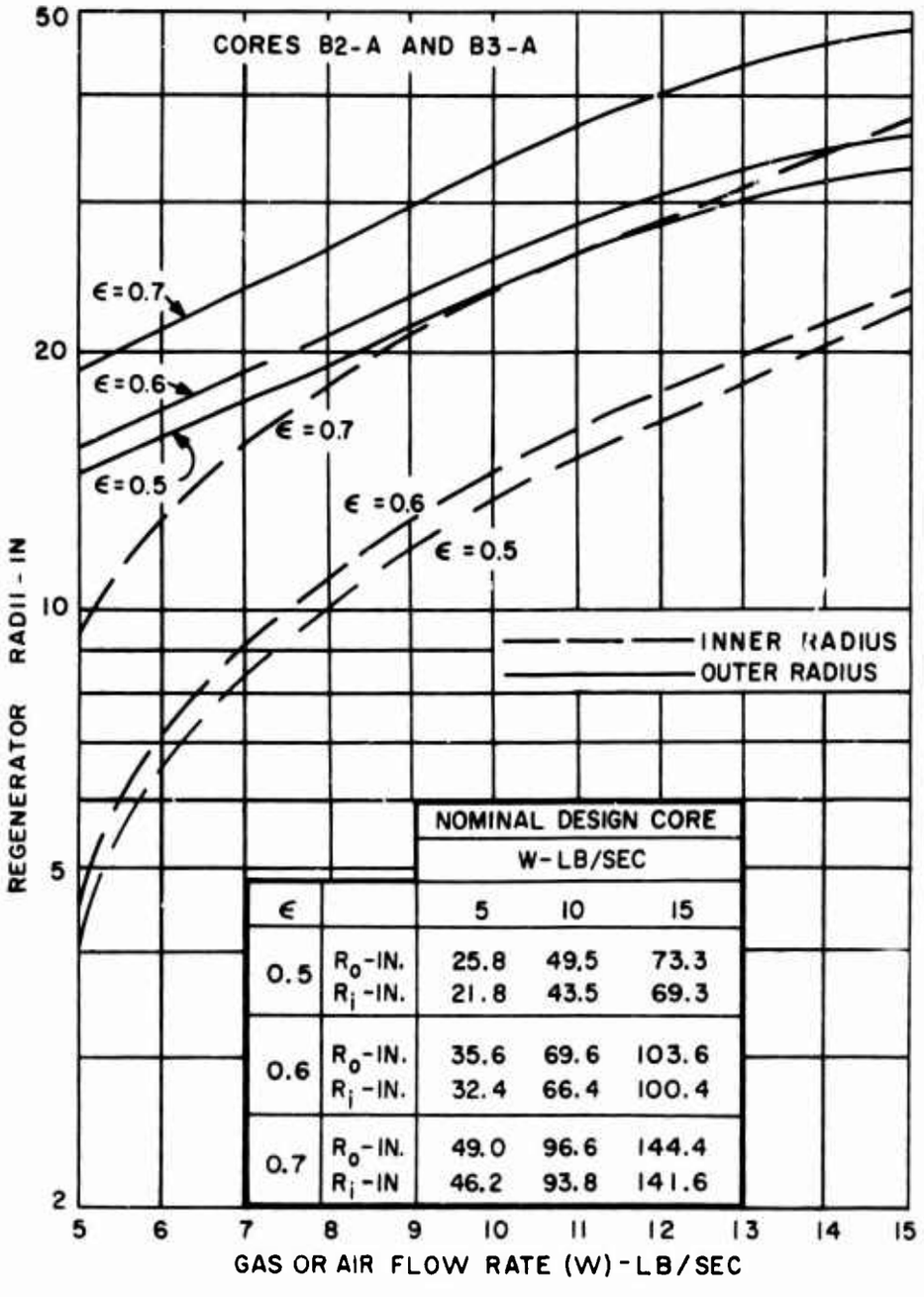

NOMINAL DESIGN CORE W-LB/SEC				
ϵ		5	10	15
0.5	R_o-IN.	25.8	49.5	73.3
	R_i-IN.	21.8	43.5	69.3
0.6	R_o-IN.	35.6	69.6	103.6
	R_i-IN.	32.4	66.4	100.4
0.7	R_o-IN.	49.0	96.6	144.4
	R_i-IN	46.2	93.8	141.6

Figure 33. Outer and Inner Regenerator Radii.

across the walls, although this situation could be altered by corrosion of a significant fraction of the wall thickness during operation. Additional stresses may arise as a result of the fabrication process. Also, vibration and acceleration loadings experienced during operation will produce stresses and deformations which could affect structural integrity. Evaluation of the regenerator structural adequacy subsequent to fabrication and under dynamic loading requires detailed design studies beyond the scope of this preliminary evaluation.

LIFETIME AND RELIABILITY

From the standpoint of internal corrosion, cesium heat pipes should function for thousands of hours at contemplated operating temperatures without significant degradation. Excessive corrosion of stainless steel by exhaust gases suggests that Zone A of cores B2-A or B3-A should be fabricated of Hastelloy X rather than stainless steel, as this alloy has been shown to resist exhaust gas corrosion effectively.

Failure of a small number of heat pipes during operation would in itself have little effect on regenerator performance. However, the heat released by the combustion of escaping cesium could conceivably cause overheating of surrounding heat pipes, which might increase the failure rate. Experimental studies are needed to evaluate the consequences of individual tube failure.

Experimental determinations are also needed to assess the possible occurrence of hydrogen gas permeation through heat pipe walls into the vapor space. The accumulation of hydrogen (which presumably would originate from reduction of water vapor in the exhaust gas) could eventually shorten the effective heat pipe length, reducing regenerator effectiveness.

PART-LOAD PERFORMANCE

The heat pipe cores considered in this report have been analyzed at a single engine operating point, corresponding to full engine power. When the engine is operating at part load, the temperature level of the cycle will drop. The heat transport capacity of those heat pipes whose temperatures drop below the minimum design temperature will be restricted, and these heat pipes may no longer function isothermally. The regenerator effectiveness at part load would then fall off. If a turbine with variable nozzle area is used, the turbine inlet temperature will remain relatively constant over a wide range of engine power, and adverse effects on regenerator effectiveness will be minimized.[19]

TEMPERATURE AND ACCELERATION TRANSIENTS

In the course of operation, a heat pipe regenerator mounted on an aircraft gas turbine will be subject to temperature and acceleration transients. Since these variations in operational environment are, by definition, of short duration, the actual change in heat pipe performance during a transient is in itself probably not of great consequence. What is important is the capability of the heat pipes to recover from transient-induced changes rapidly.

Perhaps the most critical transient is that associated with startup, when the temperature of the gas and air streams entering the regenerator is rising rapidly. If the temperature lag of the heat pipes is large enough, the velocity of the relatively cool, low-density heat pipe vapor may be so high as to impede the flow of returning condensate. Burnout would then occur. If such a situation were to persist after the heat pipes had come up to temperature, the regenerator effectiveness would be impaired. On the basis of present heat pipe technology, insufficient information exists for predicting whether this postulated startup problem is likely to be encountered.

COST

Since interest in heat pipes is but a few years old and since only a few hundred heat pipes have been fabricated (virtually all in connection with research and development programs), little basis exists for the prediction of firm heat pipe production costs.

Nevertheless, very rough heat pipe cost estimates have been made on the basis of experience with electronic devices of similar materials and complexity which require similar processing. On the assumption of an annual production rate of 10,000,000 alkali metal heat pipes, 12 inches long, 1/8 inch in diameter, and 10 mils thick, the following costs per heat pipe have been estimated:*

Material	Heat Pipe Cost
304 Stainless Steel	$0.70
Hastelloy X	1.05
A-40 Titanium	1.40

The B2-A and B3-A cores utilize heat pipes ranging in length from 9.6 to 11.3 inches. The 1/8-inch heat pipes in Zone A (>1000°F) have 4-mil walls, and the 1/4-inch heat pipes in Zone B (<1000°F) have 6-mil walls. Assuming that the above cost figures are applicable to both the 1/8- and 1/4-inch heat pipes of these

*Personal communication with G.Y. Eastman, Radio Corporation of America, Lancaster, Pennsylvania.

cores, the specific heat pipe costs (cost/unit air or gas flow rate) are arrived at in Table XIII.

TABLE XIII. SPECIFIC HEAT PIPE COST ESTIMATE ($/lb/sec)

Core Type	Material		Regenerator Effectiveness		
	Zone B	Zone A	0.5	0.6	0.7
B2-A	Titanium	Stainless	800	1350	2890
B2-A	Titanium	Hastelloy X	1030	1700	3600
B3-A	Stainless	Stainless	630	1030	2160
B3-A	Stainless	Hastelloy X	860	1380	2860

A target regenerator cost of $700/lb/sec has been suggested for a tubular regenerator of $\epsilon = 0.6$ and weighing 44 pounds. This cost is believed to be representative of today's production technology.* From Table X, the cost of the heat pipes alone equals or exceeds this figure. Thus, on the basis of the rough cost estimates available at this time, the cost of heat pipe regenerators will be considerably in excess of the target cost.

A large cost jump is evident between $\epsilon = 0.6$ and 0.7, indicating that economics as well as regenerator size considerations favor a regenerator effectiveness of 0.6 or less.

Since Hastelloy X is expected to be a requirement for adequate corrosion resistance against turbine exhaust gas in Zone A, the final choice of core type reduces to whether titanium or stainless should be used in Zone B. The use of titanium increases the heat pipe cost by about 25 percent, but it reduces core weight by the same percentage. On the assumption that the weight reduction is worth the extra cost, core B2-A, with 1/4-inch cesium-titanium heat pipes in Zone B and 1/8-inch cesium-Hastelloy X heat pipes in Zone A, is considered to be the preferred core type.

FABRICATION

A 5-lb/sec heat pipe regenerator with a regenerator effectiveness of 0.6 will require the fabrication of 2290 cesium-titanium heat pipes 1/4-inch in diameter and

*Personal communication with L. Bell, U.S. Army Aviation Materiel Laboratories, Fort Eustis, Virginia.

11.3 inches long (for Zone B), and 5050 cesium-Hastelloy X heat pipes 1/8 inch in diameter and 11.3 inches long (for Zone A). The 1/8-inch pipes will have 4-mil-thick walls and wicks, and the 1/4-inch pipes will have 6-mil-thick walls and wicks. The wicks will be composed of two layers. The layer in contact with the wall (with probably 75 percent of the total thickness) will have a mean pore radius of 38 microns in the 1/4-inch pipes and 25.5 microns in the 1/8-inch pipes. The thinner layer in contact with the vapor space will have a mean pore radius of 6.1 microns in the 1/4-inch pipes and 1.7 microns in the 1/8-inch pipes.

It is believed that the fabrication of heat pipes with such thin walls and thin, two-layer wicks has not yet been attempted. Therefore, considerable development effort can be anticipated before successful fabrication techniques are devised. The techniques must then be adapted to permit production of heat pipes at a reasonable rate.

Methods must also be devised for fabrication of individual tubes into modules which can then be assembled into a complete regenerator core. The experience of others in attempting to fabricate modules of small-hydraulic-diameter heat transfer elements indicates that successful accomplishment of this task will require a major effort. The fact that two different materials, such as titanium and Hastelloy X, may be involved will present additional problems in core fabrication, although the situation is eased by the isolation of each material in a specific core zone.

From these remarks, it is evident that the heat pipe regenerator, as is the case with other advanced regenerator types, will require extensive development to achieve a successful prototype.

CONCLUSIONS

The concept of a gas turbine regenerator which utilizes heat pipes as the active heat transfer elements is technically feasible. The core of a heat pipe regenerator can be fabricated as an annular ring with radial heat pipes extending between the inner and outer radii. Such a configuration is well adapted to placement in or behind the turbine exhaust duct, permitting the axial flow of exhaust gas into and out of the regenerator core with minimum pressure loss. The addition of the regenerator will result in increased engine dimensions, but probably to a lesser extent than with other regenerator types.

An annular, radial-heat-pipe regenerator is best suited to gas turbines with a mass flow rate of 5 lb/sec or less and regenerator effectivenesses of 0.6 or less. The preferable core type is a two-zone core consisting of an array of 1/4-inch cesium-titanium heat pipes followed by an array of 1/8-inch cesium-Hastelloy X heat pipes. For a mass flow rate of 5 lb/sec, a regenerator effectiveness of 0.6, and staggered heat pipes, the outside core diameter is 31.4 inches, the annular thickness (normal to the flow direction) is 11.3 inches, and the core length (parallel to the flow direction) is 5.6 inches. If the heat pipes were arranged in an in-line rather than a staggered array, the outside core diameter could be reduced to 27 inches and the core length would increase to 7 inches. The core contains 2290 1/4-inch-diameter heat pipes and 5050 1/8-inch-diameter heat pipes. The core weight is 65 pounds, or 13 lb/lb/sec.

The weight of the heat pipe regenerator core is comparable to the estimated entire regenerator weight of other core types: hence, the total regenerator weight will exceed that of other core types. However, a precise weight comparison requires a detailed engine-regenerator integration study for a particular gas turbine. Because a heat pipe regenerator is characterized by short length, lack of gas-side headers, and counterflow design, the structural, ducting, and header weight should be considerably less for heat pipe regenerators than for other regenerator types. If regenerator weight comparisons are based on equal total cycle pressure losses resulting from regenerator installation rather than on core pressure losses only, the heat pipe regenerator weight should compare favorably with that of other regenerator types.

As with other advanced regenerator types, the heat pipe regenerator is expensive. Estimated costs for the heat pipes alone are $1700/lb/sec compared to a target cost for the entire regenerator of $700/lb/sec. As heat pipes of the type required have not yet been fabricated, extensive fabrication studies and testing of individual heat pipes as well as core modules will be required for development of a successful prototype.

RECOMMENDATIONS

The primary advantages of the heat pipe regenerator are: basic design simplicity, ease of integration with gas turbines, and reduced exhaust gas duct losses. The disadvantages are: the cost exceeds target objectives, weight is comparable to or in excess of that attainable with other regenerator types, and development costs of individual heat pipes as well as of core modules will be substantial.

Since neither experimental performance data nor firm cost data were available for the thin-wicked, small diameter heat pipes which were employed in the regenerator study, the study conclusions are subject to considerable uncertainty. Nevertheless, in view of the apparent disadvantages, the development of heat pipe regenerators in accordance with the design criteria of Table II does not appear to be justified at the present time.

Further consideration of the concept could be warranted, however, by the following circumstances:

1. The inability of advanced regenerator types currently under consideration to meet the design criteria, weight, or cost goals.

2. The development of gas turbines with compressor discharge temperatures of 850°F or higher. Minimum heat pipe temperatures in a regenerator would then approach 1000°F or higher, permitting the use of smaller diameter heat pipes and single-zone cores, which in turn would lead to significant reductions in specific core weight and, most probably, cost.

Should either of these eventualities come about or be anticipated, then it is recommended that consideration be given to the following areas of heat pipe regenerator development:

1. Fabrication studies and tests to determine optimum wick types and wick characteristics for the small diameter, thin-walled, thin-wicked heat pipes which have been considered in this study.

2. Fabrication studies to evaluate the problems of constructing small diameter heat pipes.

3. Testing of small diameter heat pipes to evaluate: heat transport capacity, transient thermal performance, lifetime in a turbine exhaust gas environment, and sensitivity to orientation and acceleration.

4. Study of techniques for mass production and qualification testing of small diameter heat pipes at minimum cost.

5. Study of fabrication techniques for assembling small diameter heat pipes into a regenerator core.

Should the results of these developmental programs prove to be favorable, then a firm basis will have been created for subsequent construction and testing of heat pipe regenerator modules and ultimately a complete heat pipe regenerator.

REFERENCES CITED

1. Grover, G.M., Cotter, T.P., and Erickson, G.F., STRUCTURES OF VERY HIGH THERMAL CONDUCTANCE, Journal of Applied Physics, Vol. 35, 1964, p. 1990.

2. Cotter, T.P., THEORY OF HEAT PIPES, LA-3246-MS, Los Alamos Scientific Laboratory, Los Alamos, New Mexico, March 1965.

3. Deverall, J.E., and Kemme, J.E., HIGH THERMAL CONDUCTANCE DEVICES UTILIZING THE BOILING OF LITHIUM OR SILVER, LA-3211, Los Alamos Scientific Laboratory, Los Alamos, New Mexico, April 1965.

4. Deverall, J.E., and Kemme, J.E., SATELLITE HEAT PIPE, LA-3278-MS, Los Alamos Scientific Laboratory, Los Alamos, New Mexico, April 1965.

5. Kemme, J.E., HEAT PIPE CAPABILITY EXPERIMENTS, LA-3585-MS, Los Alamos Scientific Laboratory, Los Alamos, New Mexico, October 1966.

6. PROCEEDINGS OF JOINT ATOMIC ENERGY COMMISSION/SANDIA LABORATORIES HEAT PIPE CONFERENCE-VOLUME 1, SC-M-66-623, Space Isotope Power Department, Sandia Laboratories, Albuquerque, New Mexico, October 1966.

7. THE HEAT PIPE-A UNIQUE AND VERSATILE DEVICE FOR HEAT TRANSFER APPLICATIONS, RCA Ref 994-619, Direct Energy Conversion Department, Radio Corporation of America, Lancaster, Pennsylvania (undated).

8. FIRST QUARTERLY REPORT: VAPOR-CHAMBER FIN STUDIES, Pratt and Whitney Aircraft; NASA CR-54832, NASA Lewis Research Center, Cleveland, Ohio, September 1965.

9. SECOND QUARTERLY REPORT: VAPOR-CHAMBER FIN STUDIES, Pratt and Whitney Aircraft; NASA CR-54922, NASA Lewis Research Center, Cleveland, Ohio, January 1966.

10. THIRD QUARTERLY REPORT: VAPOR-CHAMBER FIN STUDIES, Pratt and Whitney Aircraft; NASA CR-54989, NASA Lewis Research Center, Cleveland, Ohio, April 1966.

REFERENCES CITED (Continued)

11. Katzoff, S., HEAT PIPES AND VAPOR CHAMBERS FOR THERMAL CONTROL OF SPACECRAFT, Presented at AIAA Thermophysics Specialist Conference; New Orleans, Louisiana, April 1967; NASA Langley Research Center, Hampton, Virginia.

12. Deverall, J.E., Salmi, E.W., and Knapp, R.J., ORBITAL HEAT PIPE EXPERIMENT, LA-3714, Los Alamos Scientific Laboratory, Los Alamos, New Mexico, June 1967.

13. Wheeler, A.J., et al, SMALL GAS TURBINE ENGINE COMPONENT TECHNOLOGY REGENERATOR RESEARCH, The Boeing Company; USAAVLABS Technical Report 66-90, U.S. Army Aviation Materiel Laboratories, Fort Eustis, Virginia, January 1967.

14. HEAT REGENERATIVE SYSTEM FOR T53 SHAFT TURBINE ENGINES, Lycoming Division, Avco Corporation; USAAVLABS Technical Report 65-37, U.S. Army Aviation Materiel Laboratories, Fort Eustis, Virginia, July 1965.

15. Klueh, R.L., and Jansen, D.H., EFFECTS OF LIQUID AND VAPOR CESIUM ON STRUCTURAL MATERIALS, ORNL-TM-1813, Oak Ridge National Laboratory, Oak Ridge, Tennessee, June 1967.

16. Materials in Design Engineering, Vol. 62, No. 5, October 1965, pp. 35, 173.

17. METALS HANDBOOK, Eighth Edition, Metals Park, Ohio, American Society of Metals, 1964.

18. Kays, W.M., and London, A.L., COMPACT HEAT EXCHANGERS, Second Edition, New York, McGraw-Hill, 1964.

19. Kailos, N.C., INCREASED HELICOPTER CAPABILITY THROUGH ADVANCED POWER PLANT TECHNOLOGY, No. 119, American Helicopter Society, Inc., 23rd Annual National Forum Proceedings, Washington, D.C., May 1967.

20. Honig, R.E., VAPOR PRESSURE DATA FOR THE SOLID AND LIQUID ELEMENTS, RCA Review, December 1962, pp. 567-586.

21. Smithells, C.J., METALS REFERENCE BOOK-VOL. II, Third Edition, Washington, Butterworths, 1962, pp. 618-619; 698-699.

REFERENCES CITED (Continued)

22. Weatherford, W.D., Jr., et al, PROPERTIES OF INORGANIC ENERGY-CONVERSION AND HEAT-TRANSFER FLUIDS FOR SPACE APPLICATIONS, WADD TR 61-96, November 1961.

23. Burdi, G.F., SNAP TECHNOLOGY HANDBOOK-VOL. I, LIQUID METALS, NAA-SR-8617, August 1964.

24. Tepper, F., et al, THERMOPHYSICAL AND TRANSPORT PROPERTIES OF LIQUID METALS, AFML-TR-65, May 1965.

25. Eckert, E.R.G., and Drake, R.M., Jr., HEAT AND MASS TRANSFER, Second Edition, New York, McGraw-Hill, 1959, pp. 503-504.

26. Eshback, O.W., HANDBOOK OF ENGINEERING FUNDAMENTALS, First Edition, New York, Wiley, 1936, p. 6-28.

27. Roark, R.J., FORMULAS FOR STRESS AND STRAIN, Second Edition, New York, McGraw-Hill, 1964.

APPENDIX I
HEAT PIPE EQUATIONS

Equations which were used to determine heat pipe characteristics are derived below. Fluid property data required for calculations were obtained from References 18 and 20 through 25.

HEAT TRANSPORT CAPACITY

The vapor and liquid pressure variations with heat pipe length are shown in Figure 34 for zero, positive, and negative values of θ, where θ is the angle between the heat pipe and the horizontal with the condenser end at the apex (see Figure 13). When the heat pipe is horizontal ($\theta = 0$), the radius of curvature r of the liquid-vapor interface is assumed to be infinite at the common boundary between the evaporator and condenser sections, and the liquid and vapor pressures P_ℓ and P_V at that point are equal. In the evaporator section, liquid withdraws into the capillary pores, and

$$P_{ve(x)} = P_{\ell e(x)} + \frac{2\sigma}{r_{e(x)}} \qquad (1)$$

where $P_{ve(x)}$ = vapor pressure in evaporator section at distance x from end of condenser section
$P_{\ell e(x)}$ = liquid pressure in evaporator section at x
$r_{e(x)}$ = radius of curvature of liquid-vapor interface at x
σ = surface tension at liquid-vapor interface

In the condenser section, liquid bulges out of the capillary pores, and

$$P_{\ell c(x)} = P_{vc(x)} + \frac{2\sigma}{r_{c(x)}} \qquad (2)$$

The symbols in Equation (2) have the same meaning as those in Equation (1), except that the subscript c is used to denote conditions at a point x in the condenser section.

When θ is positive, the liquid pressure at any distance x from the end of the condenser section is reduced by

$$P_{h(x)} = (n + 1)\rho_\ell \times \sin\theta \qquad (3)$$

where $P_{h(x)}$ = effective liquid pressure head at x
ρ_ℓ = liquid density
n = vertical external acceleration (+ for upward acceleration, - for downward acceleration)

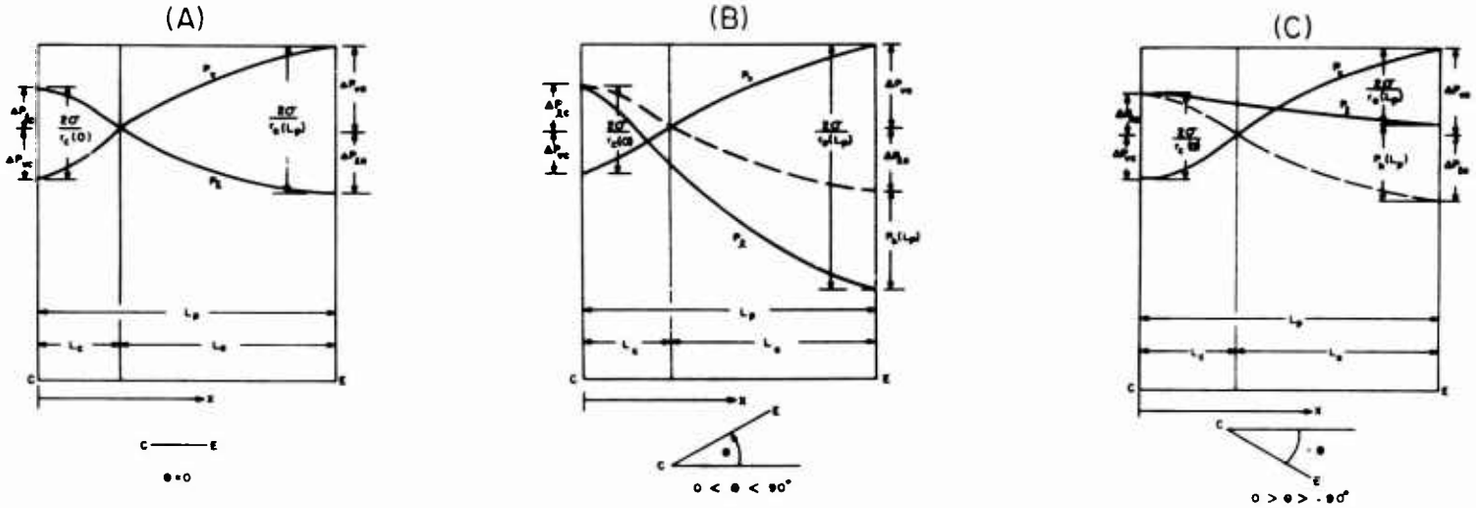

Figure 34. Pressure Variation in Vapor and Liquid With Heat Pipe Length and Orientation.

At $x = L_c$, $P_v > P_\ell$ and r is now finite. The point at which $P_v = P_\ell$ and r is infinite has shifted into the condenser section.

When θ is negative, the liquid pressure at x is increased by $- P_h(x)$. Now at $x = L_c$, r is finite and $P_\ell > P_v$, and the point at which r is infinite and $P_v = P_\ell$ has shifted into the evaporator section.

Now the following assumptions are made:

1. Both the liquid flow and the vapor flow are laminar.

2. The heat addition rate in the evaporator section is constant, and the heat removal rate in the condenser section is constant.

3. The liquid density and vapor density are constant. (For the vapor, this implies a negligible fractional pressure drop and, since the vapor is saturated, a negligible temperature variation along the heat pipe.)

4. The rate at which fluid enters or leaves the vapor or liquid stream at any point along the heat pipe is small compared to the axial-flow rate at that point.

With these assumptions, the liquid and vapor frictional pressure drops in the evaporator and condenser sections may be expressed as

$$\Delta P_{ve} = P_{ve}(L_p) - P_{ve}(L_c) = \frac{8\nu_v L_e Q}{2\pi\kappa r_v^4} \tag{4}$$

$$\Delta P_{vc} = P_{vc}(L_c) - P_{vc}(0) = \frac{L_c}{L_e}\,\Delta P_{ve} \tag{5}$$

$$\Delta P_{\ell e} = \left[P_{\ell e}(L_c) - P_{\ell e}(L_p)\right] - \left[P_h(L_p) - P_h(L_c)\right] = \frac{b\nu_\ell L_e Q}{2\pi\kappa\phi r_p^2 (r_w^2 - r_v^2)} \tag{6}$$

$$\Delta P_{\ell c} = \left[P_{\ell c}(0) - P_{\ell c}(L_c)\right] - \left[P_h(L_c) - P_h(0)\right] = \frac{L_c}{L_e}\,\Delta P_{\ell e} \tag{7}$$

where Q = heat input rate = heat output rate
ν_v = kinematic viscosity of vapor
ν_ℓ = kinematic viscosity of liquid
κ = heat of vaporization
r_v = inner wick radius

r_w = outer wick radius
ϕ = wick porosity
b = wick tortuosity
r_p = wick mean pore radius in axial direction

If Equations (1) through (7) are used, and if we note that

$$P_{\ell c}(L_c) = P_{vc}(L_c) - P_h(L_c) \tag{8}$$

$$P_{\ell e}(L_c) = P_{ve}(L_c) - P_h(L_c) \tag{8a}$$

then

$$Q = \frac{\frac{4\pi\kappa\sigma}{L_p r_c(0)} \left(1 + \frac{L_e}{L_c}\right)}{\frac{8\nu_v}{r_v^4} + \frac{b\nu_\ell}{\phi r_p^2(r_w^2 - r_v^2)}} \tag{9}$$

or

$$Q = \frac{\frac{4\pi\kappa\sigma}{L_p r_e(L_p)} (1-\alpha) \left(1 + \frac{L_c}{L_e}\right)}{\frac{8\nu_v}{r_v^4} + \frac{b\nu_\ell}{\phi r_p^2(r_w^2 - r_v^2)}} \tag{10}$$

where

$$\alpha = \frac{(1+n)\rho_\ell \, r_e(L_p) L_p \sin\phi}{2\sigma} \tag{11}$$

Q will take on a maximum value Q_m when either $r_c(0) = r_{pn}$ or $r_p(L_p) = r_{pn}$, where r_{pn} is the mean capillary pore radius in the radial direction. When $r_c(0) = r_e(L_p) = r_{pn}$, Q_m takes on its largest value. This will occur when L_e/L_c takes on an optimum value $(L_e/L_c)_o$. $(L_e/L_c)_o$ is obtained by equating Equations (10) and (11) when $r_c(0) = r_e(L_p) = r_{pn}$, and is found to be

$$(L_e/L_c)_o = 1 - \alpha \tag{12}$$

When $(L_e/L_c) < (L_e/L_c)_o$, $r_c(0)$ will reach its minimum value of r_{pn} first, and Equation (9) with $r_c(0) = r_{pn}$ is used to calculate Q_m. When $(L_e/L_c) > (L_e/L_c)_o$,

$r_e(L_p)$ will reach its minimum value of r_{pn} first, and Equation (10) with $r_e(L_p) = r_{pn}$ is used to calculate Q_m.

Now consider a horizontal heat pipe ($\alpha = 0$) with $L_e/L_c \gg 1$ (i.e., a very short condenser section). For this case, from Equation (12), $(L_e/L_c)_o = 1$ and $L_e/L_c > (L_e/L_c)_o$. Q_m is then calculated from Equation (10) with $r_e(L_p) = r_{pn}$, and takes the form

$$Q_m = \frac{\frac{4\pi\kappa\sigma}{L_p r_{pn}}}{\frac{8\nu_v}{r_v^4} + \frac{b\nu_\ell}{\phi r_p^2(r_w^2 - r_v^2)}} \tag{13}$$

Now, if the wick is uniform (i.e., $r_{pn} = r_p$), Q_m takes on its largest value Q_u for a given r_v when r_p has the optimum value

$$r_{pu} = \frac{r_v^2/r_w^2}{(1 - r_v^2/r_w^2)^{1/2}} \left(\frac{b}{8\phi}\frac{\nu_\ell}{\nu_v}\right)^{1/2} r_w \tag{14}$$

Q_u is then given by

$$Q_u = \left[\frac{\pi}{\sqrt{2}}\frac{r_v^2}{r_w^2}\left(1 - \frac{r_v^2}{r_w^2}\right)^{1/2}\left(\frac{\phi}{b}\right)^{1/2}\frac{r_w^3}{L_p}\right]\left[\frac{\kappa\sigma}{(\nu_\ell\nu_v)^{1/2}}\right] \tag{15}$$

If r_v now takes on the optimum value

$$r_{vo} = \left(\frac{2}{3}\right)^{1/2} r_w \tag{16}$$

then r_{pu} from Equation (14) becomes equal to r_{po}, where

$$r_{po} = \left(\frac{b\nu_\ell}{6\phi\nu_v}\right)^{1/2} r_w \tag{17}$$

and Q_u from Equation (15) assumes its largest value Q_o, where

$$Q_o = \left[\frac{\pi}{3}\left(\frac{2}{3}\right)^{1/2}\left(\frac{\phi}{b}\right)^{1/2}\frac{r_w^3}{L_p}\right]\left[\frac{\kappa\sigma}{(\nu_\ell\,\nu_v)^{1/2}}\right] \tag{18}$$

Now let

$$\left.\begin{aligned} r_{pn} &= p\,r_{pu} \\ r_p &= q\,r_{pu} \end{aligned}\right\} \tag{19}$$

If Equation (19) is substituted into Equations (9) and (10) with $r_c(0)$ and $r_e(L_p)$ equal to r_{pn}, and if Equation (15) is used,

$$Q_m = \frac{2q^2}{p(1+q^2)}\left(1 + \frac{L_e}{L_c}\right)Q_u \quad , \quad \frac{L_e}{L_c} < 1 - \alpha \tag{20}$$

$$Q_m = \frac{2q^2}{p(1+q^2)}(1-\alpha)\left(1 + \frac{L_c}{L_e}\right)Q_u \quad , \quad \frac{L_e}{L_c} > 1 - \alpha \tag{21}$$

Equations (20) and (21) express the heat transport capacity of heat pipes with nonuniform wicks in terms of Q_u. Note that Q_m can be increased by, at most, a factor of 2 by letting q be arbitrarily large, but it can be increased indefinitely by letting p be arbitrarily small. It is also evident that when $\alpha \geq 1$, Q_m drops to zero.

MINIMUM Q FOR NEGATIVE α

When α is negative (as, for example, when the evaporator is below the condenser and θ is negative), a minimum heat input Q_{min} is needed to keep the heat pipe full if $L_e/L_c > 1 - \alpha$. The critical condition for the pipe to remain just full is when the liquid in the wick at the bottom of the evaporator bulges into the vapor space with a radius of curvature r_{pn} which is now negative. When this critical condition exists, α is positive (because both θ and r_{pn} are negative) and p is negative. Q_{min} may then be found by letting p be negative in Equation (21). Then it is readily shown that

$$\frac{Q_{min}}{Q_m} = \frac{|\alpha| - 1}{|\alpha| + 1}, \qquad \alpha < 0 \tag{22}$$

When $|\alpha| \leq 1$, $Q_{min} = 0$, and the heat pipe will remain full at any heat input rate.

Now consider a horizontal heat pipe in which heat is transported at the rate $Q(\alpha = 0)$. If the heat pipe is now oriented with the evaporator end down (negative θ), it is necessary that $Q(\alpha = 0) \geq Q_{min}$ if the heat pipe is to continue functioning properly. From Equation (21), for negative θ,

$$\frac{Q_m(\alpha = 0)}{Q_m} = \frac{1}{1 - (-|\alpha|)} = \frac{1}{|\alpha| + 1} \tag{23}$$

By equating Equations (22) and (23), it is found that

$$Q_m\ (\alpha = 0) \geq Q_{min} \quad \text{when} \ |\alpha| \leq 2 \tag{24}$$

Thus, as long as $|\alpha|$ is less than the critical value of 2, a heat pipe in the evaporator-down position will function properly at a heat input rate Q_m $(\alpha = 0)$.

MAXIMUM HEAT TRANSPORT RATE FOR ISOTHERMAL OPERATION

In order for a heat pipe to operate isothermally, the pressure drop in the vapor must be a small fraction of the vapor pressure. For laminar vapor flow, the vapor pressure drop ΔP_v can be expressed as

$$\Delta P_v = \frac{4\nu_v L_p Q}{\pi g \kappa r_v^4} \tag{25}$$

where g is the acceleration of gravity. Equation (25) was derived from the basic pressure drop equation for laminar flow in smooth pipes[26] by substituting the average flow rate per unit area for the flow velocity and noting that the maximum mass flow rate of vapor in a heat pipe is equal to Q/κ. The factor g is necessary for dimensional consistency.

Dividing both sides of Equation (25) by P_v and solving for Q, we find that

$$Q = \frac{\pi}{4} g \left(\frac{\kappa P_v}{\nu_v}\right) \left(\frac{r_v^4}{L_p}\right)\left(\frac{\Delta P_v}{P_v}\right) = \frac{\pi}{4} g \beta^2 \left(\frac{r_v^4}{L_p}\right)\left(\frac{\Delta P_v}{P_v}\right) \tag{26}$$

Note that β^2 is a function of fluid properties only. It has been found from observation of vapor pressure - temperature curves for the fluids considered in this report that if $\Delta P_v/P_v \leq 0.1$, the temperature variation along a heat pipe is on the order of 10° F or less.

Now

$$r_w = \frac{d}{2}\left(1 - \frac{2t}{d}\right) \tag{27}$$

and

$$r_v = \sqrt{\frac{2}{3}}\, s\, r_w = \sqrt{\frac{2}{3}}\, s\, \frac{d}{2}\left(1 - \frac{2t}{d}\right) \tag{28}$$

where d = outer diameter of heat pipe
t = heat pipe wall thickness
$s = r_v/r_{vo}$
and r_{vo} is given by Equation (16).

Substituting Equation (28) into (26), we find that

$$Q = \frac{\pi}{144} g \beta^2 \frac{d^4}{L_p}\left(1 - \frac{2t}{d}\right)^4 s^4 \frac{\Delta P_v}{P_v} \tag{29}$$

The criterion for isothermal operation will now be established by letting $s^4 \Delta P_v/P_v = 0.1$. The maximum temperature variation along the heat pipe of about 10° F will then occur for heat pipes of optimum wick thickness, for which s = 1. The minimum temperature variation of about 4° F will occur for very thin wicks when $s \rightarrow \sqrt{3/2}$ and $s^4 \rightarrow 2.27$. Letting $Q \equiv Q_i$ for the isothermal case just defined, we obtain

$$Q_i = \frac{0.1\pi}{144} g \beta^2 \frac{d^4}{L_p}\left(1 - \frac{2t}{d}\right)^4 \tag{30}$$

It is convenient to express the maximum heat transport rate for isothermal operation Q_i in terms of Q_o. Using Equations (18), (27), and (30), we obtain

$$\frac{Q_i}{Q_o} = 0.0204\, g \left(\frac{b}{\phi}\right)^{1/2}\left(1 - \frac{2t}{d}\right) d \frac{\beta^2}{\gamma} \tag{31}$$

Note that Q_i/Q_o is independent of heat pipe length L_p. Now let $Q_m = Q_i$ in Equation (21) with $\alpha = 0$, $L_e/L_c \rightarrow \infty$, and using Equation (19),

$$r_{pn} = \frac{2\, r_{pu} \left(\frac{r_p}{r_{pu}} \right)^2}{1 + \left(\frac{r_p}{r_{pu}} \right)^2} \left(\frac{Q_u}{Q_i} \right) \tag{32}$$

Using Equations (14), (15), and (30) for any given geometry, we find that Equation (32) can be expressed as

$$r_{pn} \propto \frac{\left(\frac{r_p}{r_{pu}} \right)^2}{1 + \left(\frac{r_p}{r_{pu}} \right)^2} \left(\frac{\sigma}{P_v} \right) \tag{33}$$

Equation (33) is useful for comparing the relative radial pore radii for different heat pipe fluids which are needed to assure that $Q_u = Q_i$. For special cases, Equation (33) reduces to

$$r_{pn} \propto \frac{\sigma}{P_v} \quad , \quad \frac{r_p}{r_{pu}} = 1 \tag{34}$$

$$r_{pn} \propto \frac{\nu_v}{\nu_\ell} \frac{\sigma}{P_v} \quad , \quad \frac{r_p}{r_{pu}} << 1 \tag{35}$$

WALL STRENGTH AND STABILITY

The compressive stress σ_c in the heat pipe wall under a net external radial pressure ΔP and the net radial pressure for buckling ΔP_b were calculated from the formulas[27] .

$$\sigma_c = \frac{\Delta P \bar{r}}{t} \tag{36}$$

$$\Delta P_b = \frac{E}{4(1 - \omega^2)} \left(\frac{t}{\bar{r}} \right)^3 \tag{37}$$

where E = modulus of elasticity
ω = Poisson's ratio
$\overline{r}$ = mean radius of heat pipe wall

APPENDIX II
REGENERATOR EQUATIONS

BASIC RELATIONS

Basic relations and data used for regenerator calculations were obtained from Reference 18. The assumptions used in the calculations are presented in the "DESIGN STUDY - REGENERATOR CORE CHARACTERISTICS" section of this report.

The regenerator effectiveness ϵ is

$$\epsilon = \frac{T_{ao} - T_{ai}}{T_{gi} - T_{ai}} \tag{38}$$

The number of heat transfer units NTU is, for counterflow,

$$NTU = \frac{\epsilon}{1 - \epsilon} = \frac{AU}{WC} \tag{39}$$

where
- T_{ao} = outlet air temperature
- T_{ai} = inlet air temperature
- T_{gi} = inlet gas temperature
- W = gas or air mass flow rate
- C = gas or air specific heat at constant pressure
- AU = total core thermal conductance

The total core thermal conductance AU is given by

$$\frac{1}{UA} = \frac{1}{h_g A_g} + \frac{1}{h_a A_a} \tag{40}$$

where
- h_g = heat transfer coefficient between gas and heat pipe surface
- h_a = heat transfer coefficient between air and heat pipe surface
- A_g = gas-side heat pipe surface area
- A_a = air-side heat pipe surface area

The geometric relations for a bank of staggered heat pipes are

$$\frac{A_c}{A_f} = 1 - \frac{1}{X_t} \tag{41}$$

$$\frac{A}{V} = \frac{\pi}{X_\ell X_t d} \tag{42}$$

$$\frac{A_c}{A} = \frac{A_c/A_f}{(A/V)L} = \frac{(X_t - 1)X_\ell}{L}\frac{d}{\pi} \tag{43}$$

$$r_h = (X_t - 1)X_\ell \frac{d}{\pi} = L\frac{A_c}{A} \tag{44}$$

where
- X_t = transverse spacing /d
- X = longitudinal spacing /d
- A_c = core free flow area
- A_f = core frontal area
- A = core heat transfer surface area
- V = core volume
- r_h = hydraulic radius

The heat-transfer and pressure-drop parameters are given by

$$h = C_h \left(\frac{C^{1/3}k^{2/3}}{\mu^{4/15}}\right)\left(\frac{G^{3/5}}{d_h^{2/5}}\right) \tag{45}$$

$$f = C_f \left(\frac{\mu}{d_h G}\right)^{0.18} \tag{46}$$

$$\frac{\Delta P}{P_i} = f\frac{L}{r_h}\frac{\bar{v}}{P_i}\frac{G^2}{2g} \tag{47}$$

$$\bar{v} = \frac{R}{2}\left(\frac{T_i}{P_i} + \frac{T_o}{P_o}\right) \tag{48}$$

where h = heat transfer coefficient
C_h, C_f = dimensionless parameters from Fig. 7-5 of Reference 18
k = thermal conductivity
μ = viscosity
d_h = hydraulic diameter = 4r
G = mass flow rate
L = core length
f = coefficient of friction
ΔP = core pressure drop
P_i = inlet pressure
P_o = outlet pressure
T_i = inlet temperature
T_o = outlet temperature
R = gas constant, (lb - ft)/(lb - R)
$\bar{v}$ = mean specific volume

In Equations (41) through (44), the addition of subscript "g" or "a" identifies gas or air flow. All temperature-dependent properties are evaluated at the mean flow stream temperature.

The following additional relations may be noted:

$$\frac{A_g}{A_a} = \frac{L_g}{L_a} \tag{49}$$

$$\frac{h_g}{h_a} = \left(\frac{\mu_a}{\mu_g}\right)^{0.267}\left(\frac{G_g}{G_a}\right)^{0.6} = \left(\frac{\mu_a}{\mu_g}\right)^{0.267}\left(\frac{L_a}{L_g}\right)^{0.6} \tag{50}$$

where L_g = gas-side heat pipe length
L_a = air-side heat pipe length

Also,
$$G_g = \frac{W}{A_{cg}} \quad , \quad G_a = \frac{W}{A_{ca}} \tag{51}$$

Using Equations (40) and (51) and solving for A_g, we find that

$$A_g = \frac{WL}{r_h G_g} \tag{52}$$

Using Equations (39), (40), (50), and (52), we may show that

$$L = \left(\frac{C\epsilon}{1-\epsilon}\right)\left(\frac{r_h G_g}{h_g}\right)\left[1 + \left(\frac{\mu_a}{\mu_g}\right)^{0.267}\left(\frac{L_g}{L_a}\right)^{0.4}\right] \tag{53}$$

Substituting Equation (45) into Equation (53), and then Equations (46) and (53) into Equation (47), we obtain for the sum of the gas and air stream fractional pressure drops,

$$\left(\frac{\Delta P}{P_i}\right)_g + \left(\frac{\Delta P}{P_i}\right)_a = G_g^{2.22}\left[\left(\frac{\epsilon}{1-\epsilon}\right)\left(\frac{C_f}{C_h}\right)\left(\frac{C}{k}\right)^{2/3}\left(\frac{d_h^{0.22}}{2g}\right)\right]$$

$$\left[1 + \left(\frac{\mu_a}{\mu_g}\right)^{0.267}\left(\frac{L_g}{L_a}\right)^{0.4}\right]\left[\frac{\mu_g^{0.447}\bar{v}_g}{P_{ig}} + \frac{\mu_a^{0.447}\bar{v}_a}{P_{ia}}\left(\frac{L_g}{L_a}\right)^{1.82}\right] \tag{54}$$

For a specified total core fractional pressure drop, regenerator effectiveness, inlet and outlet temperatures and pressures, and core internal geometry, G_g can be solved explicitly from Equation (54).

EXTERNAL CORE GEOMETRY

Once G_g has been calculated from Equation (54), h_g can be calculated from Equation (45). The core length L is then calculable from Equation (53).

From Equations (41) and (51) and from the fact that $G_a/G_g = L_g/L_a$, it may be shown that

$$A_{fs} = \frac{A_f}{W} = \frac{X_t}{(X_t - 1)G_g}\left(1 + \frac{L_a}{L_g}\right) \tag{55}$$

where A_{fs} = specific core frontal area.

The specific heat transfer surface area A_s is, using Equation (42),

$$A_s = \frac{A}{V}\frac{V}{W} = \frac{A}{V} L A_{fs} = \frac{\pi L A_{fs}}{X_\ell X_{td}} \tag{56}$$

The heat pipe length L_p is found by equating the gas-side heat input rate Q_g of a heat pipe to the maximum isothermal heat transport capacity Q_i. Q_g is given by

$$Q_g = \pi d\left(\frac{L_g/L_a}{1 + L_g/L_a}\right)h_g \left(T_g - T_p\right) L_p \tag{57}$$

where T_p = heat pipe temperature

Since L_p decreases as the temperature T_p decreases, the calculation will be carried out at the air inlet end of the core, where T_p has a minimum value. T_p is found by equating the gas-side heat input rate to the air-side heat output rate of a heat pipe. Carrying out this operation and using Equations (49) and (50), we find that

$$T_p = \frac{T_{ai} + \left(\frac{\mu_a}{\mu_g}\right)^{0.267} \left(\frac{L_g}{L_a}\right)^{0.4} T_{go}}{1 + \left(\frac{\mu_a}{\mu_g}\right)^{0.267} \left(\frac{L_g}{L_a}\right)^{0.4}} \tag{58}$$

Equating Equations (30) and (57) and solving for L_p, we obtain

$$L_p = 0.0264\left[\frac{gd^3(1 + L_g/L_a)}{h_g(T_{go} - T_p)(L_g/L_a)}\right]^{1/2}\left(1 - \frac{2t}{d}\right)^2 \beta \tag{59}$$

CORE WEIGHT

The specific core weight W_{cs} can be expressed as

$$W_{cs} = \Omega A_s \tag{60}$$

where Ω is the heat pipe weight per unit of surface area. Ω is given by

$$\Omega = t\left(1 - \frac{t}{d}\right)\rho_w + t_w\left(1 - \frac{2t}{d} - \frac{t_w}{d}\right)\left[(1 - \phi)\rho_w + \phi\rho_\ell\right] \tag{61}$$

where ρ_w = density of heat pipe wall and wick material
ρ_ℓ = density of heat pipe liquid

APPENDIX III
PROPERTIES OF HEAT PIPE FLUIDS

The properties of heat pipe fluids which were used to evaluate heat pipe performance were obtained from Reference 18 and References 20 through 25. These properties are given in Table XIV as a function of temperature. The symbols used in Table XIV are defined in the List of Symbols on pages x through xiii.

TABLE XIV. PROPERTIES OF HEAT PIPE FLUIDS

Fluid	T (°F)	P_v (psi)	ρ_v (lb/ft^3)	ρ_ℓ (lb/ft^3)	μ_v (lb/hr-ft)	μ_ℓ (lb/hr-ft)	σ (lb/ft)	κ (Btu/lb)
Sodium	752	<0.01	1.3×10^{-5}	53.	0.0405	0.65	0.0111	1876.
	932	0.08	1.1×10^{-4}	52.	0.044	0.53	0.0104	1832.
	1112	0.39	6.5×10^{-4}	50.	0.047	0.48	0.00975	1788.
	1292	1.74	2.5×10^{-3}	48.5	0.050	0.43	0.00910	1744.
Potassium	752	0.08	2.1×10^{-4}	47.	0.0369	0.44	0.00515	914.
	932	0.58	1.6×10^{-3}	45.	0.0400	0.38	0.00495	898.
	1112	2.52	6.0×10^{-3}	43.	0.0429	0.36	0.00470	880.
	1292	8.70	1.8×10^{-2}	42.	0.0456	0.33	0.00450	862.
Cesium	752	0.35	3.50×10^{-3}	109.2	0.0544	0.60	0.00392	229.
	932	1.93	1.06×10^{-2}	107.6	0.0582	0.54	0.00357	223.
	1112	7.35	4.80×10^{-2}	106.0	0.0620	0.49	0.00320	217.
	1292	17.40	1.30×10^{-1}	104.5	0.0656	~0.46	0.00278	210.
Mercury	752	30.4	4.65×10^{-1}	770.	0.157	1.9	0.0275	125.
	932	117.	1.56	~750.	0.184	~1.7	0.0257	125.
	1112	337.	3.85		0.212			124.
	1292	760.	8.07		0.242			123.
Sulphur	752	7.35	1.2×10^{-1}	102.	0.0452	430.	0.00295	121.
	878	19.3	3.0×10^{-1}	98.0	0.0494	110.	0.00270	126.
	1112		1.0	87.7	0.0540	11.0		146.
	1292		3.5	75.0	0.0564	2.4		168.

Unclassified

Security Classification

DOCUMENT CONTROL DATA - R & D

(Security classification of title, body of abstract and indexing annotation must be entered when the overall report is classified)

1. ORIGINATING ACTIVITY (Corporate author) Calvin C. Silverstein, Engineering Consultant 2525 Farringdon Road Baltimore, Maryland 21209	2a. REPORT SECURITY CLASSIFICATION Unclassified 2b. GROUP

3. REPORT TITLE

Preliminary Evaluation of Gas Turbine Regenerators Employing Heat Pipes

4. DESCRIPTIVE NOTES (Type of report and inclusive dates)

Final Technical Report

5. AUTHOR(S) (First name, middle initial, last name)

Calvin C. Silverstein

6. REPORT DATE	7a. TOTAL NO. OF PAGES	7b. NO. OF REFS
April 1968	109	27

8a. CONTRACT OR GRANT NO. DAAJ02-67-C-0053 b. PROJECT NO. 1G121401D14413 c. d.	9a. ORIGINATOR'S REPORT NUMBER(S) USAAVLABS Technical Report 68-10 9b. OTHER REPORT NO(S) (Any other numbers that may be assigned this report)

10. DISTRIBUTION STATEMENT

This document has been approved for public release and sale; its distribution is unlimited.

11. SUPPLEMENTARY NOTES	12. SPONSORING MILITARY ACTIVITY
	U.S. Army Aviation Materiel Laboratories Fort Eustis, Virginia

13. ABSTRACT

A preliminary study of heat pipe gas turbine regenerators for future Army aircraft power plants was carried out, and a feasibility evaluation was made. Heat pipe regenerators appear to be technically feasible, and they can readily be integrated with gas turbines with a minimum of duct pressure losses and engine modification. Regenerator weight is comparable to or greater than that of other regenerator types. Considerable development can be anticipated for both individual heat pipes and regenerator core modules prior to completion of a successful prototype. Regenerator costs will be high.

DD FORM 1 NOV 68 1473 REPLACES DD FORM 1473, 1 JAN 64, WHICH IS OBSOLETE FOR ARMY USE.

Unclassified

Security Classification

14. KEY WORDS	LINK A		LINK B		LINK C	
	ROLE	WT	ROLE	WT	ROLE	WT
Heat Pipe Gas Turbine Regenerator						